Synthesis, Structures, and Reactions of (Silyl) (diarylboryl) benzenes Featuring Intramolecular Interaction

SHIMIZU, Tomomi / 清水, 智美

(開始ページ / Start Page)
1
(終了ページ / End Page)
200
(発行年 / Year)
2020-03-24
(学位授与番号 / Degree Number)
32675甲第486号
(学位授与年月日 / Date of Granted)
2020-03-24
(学位名 / Degree Name)
博士(理工学)
(学位授与機関 / Degree Grantor)
法政大学 (Hosei University)
(URL)
https://doi.org/10.15002/00022976

法政大学審査学位論文

Synthesis, Structures, and Reactions of (Silyl)(diarylboryl)benzenes Featuring Intramolecular Interaction

清水 智美

Table of contents

Chapter 1

General Introduction …… 5

Chapter 2

Intramolecular Activation of C–O Bond

by an *o*-Boryl Group in *o*-(Alkoxysilyl)(diarylboryl)benzenes …… 15

Chapter 3

Synthesis, Reactions, and Photophysical Properties

of *o*-(Alkoxysilyl)(borafluorenyl)benzenes …… 57

Chapter 4

1,2-Silyl Migration in 1-Halonaphthalenes Catalyzed by I_2 …… 127

Conclusion and Outlook …… 197

Acknowledgment …… 200

Chapter 1

General Introduction

General Introduction

Functionalized arylsilanes may be categorized into three types (A), (B), and (C) in terms of activation.

(A) Functionalized arylsilanes

Silicon-functionalized arylsilanes are one of the most versatile compounds in organosilicon chemistry because of their outstanding performances such as functional group transformations, behaviors as Lewis acids, and unique photophysical properties (Scheme 1).[1] Changing substituents on the aromatic ring of the functionalied arylsilanes may provide new reactivities and physical properties.

Scheme 1. Type A: Functionalized arylsilanes.

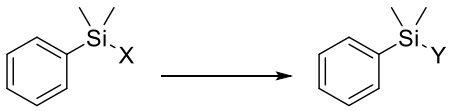

X = heteroatom

(B) Functionalized arylsilanes bearing a donor

The silicon atom in the arylsilanes can be penta- and hexacoordinated by coordination of a Lewis base (donor) to the Lewis acidic silicon center. The change in the coordination number of the silicon atom leads to change of the reactivity and physical properties (Scheme 2). Chuit et al. reported that nitrogen-coordinated silylnaphthalene **I** efficiently underwent the reaction with alcohols (Scheme 2 (1)).[2] Kano et al. reported that the coordination number in a fluorosilicate **II** could be controlled by photo irradiation (Scheme 2 (2)).[3]

Scheme 2. Type B: Functionalized arylsilanes bearing a donor.

(1) Nucleophilic activation of Si–X bond

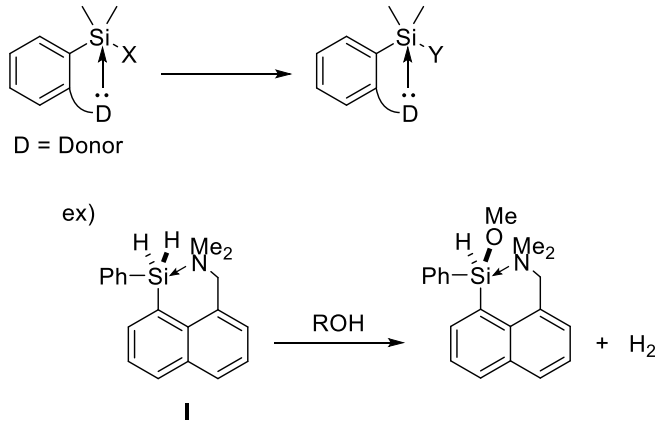

(2) Control of coordination number

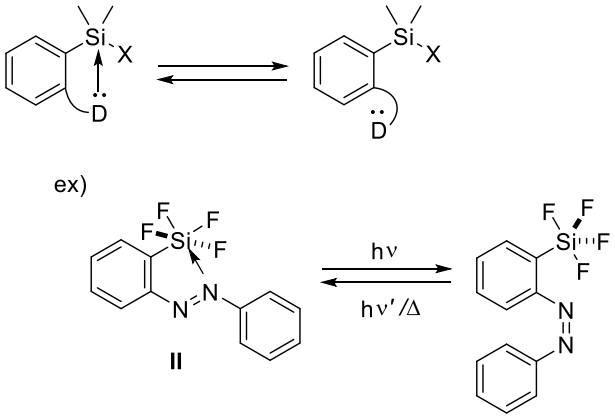

(C) Functionalized arylsilanes bearing an acceptor

(1) The Si−X bond in the arylsilane can be electrophilically activated (Scheme 3). Kawachi et al. reported a series of *o*-(hydrosilyl)(boryl)benzenes **III**, in which a hydrosilyl group and a dimesitylboryl group are linked through an ortho-phenylene skeleton (Scheme 3 (1)).[4] This skeleton may allow the boryl group to activate the Si−X bond via intramolecular electrophilic activation. Thus the Si−X (X = H) bond in **III** was efficiently activated by the *o*-boryl group and underwent various conversion reactions: (i) dehydrogenative condensation with alcohols,[5] (ii) nucleophilic displacement by a fluoride ion,[6] and (iii) H−Mes exchange between the hydrogen atom on the Si atom and mesityl (Mes) group on the boron atom.[7]

(2) Kawachi et al. also reported the facile preparation of new B/Si bidentate Lewis acids, *o*-(fluorosilyl)(boryl)benzenes **IV** (Scheme 3 (2)).[8] The functionalized arylsilanes as Lewis acids efficiently accept Lewis bases via a reversed chelation mode, thus **IV** formed a μ-fluoro bridge with fluoride ions.

(3) The X−Z bond in the arylsilane is also electrophilically activated (Scheme 3 (3)). The details are indicated below.

Scheme 3. Type (C): Functionalized arylsilanes bearing an acceptor.

(1) Electrophilic activation of Si−X bond

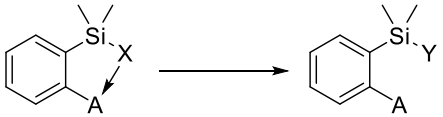

A = Acceptor

ex)

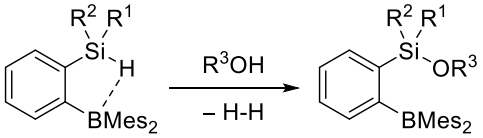

III

R^1, R^2 = Me, Me; Ph, Ph
Me, H; Ph, H

Mes = 2,4,6-trimethylphenyl

(2) Character of bidentate Lewis acids

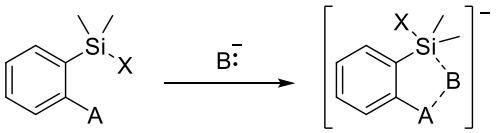

A = Acceptor

ex)

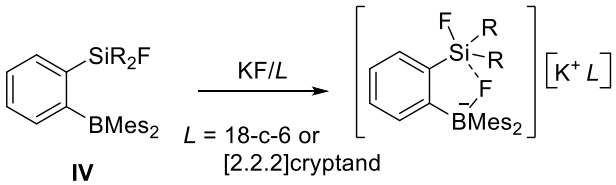

IV

R = Me, Ph

(3) Electrophilic activation of X−Z bond (this work)

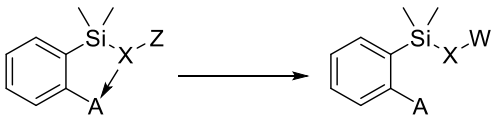

Survey of This Thesis

The author focussed her attention to (i) less-sterically demanding aryl groups other than mesityl groups on the silicon atom, (ii) construction of arene derivatives other than the *o*-phenylene framework, and (iii) alkoxysilanes as functionalized arylsilanes.

Chapter 2 describes the synthesis of noval *o*-(alkoxysilyl)(diarylboryl)benzenes **1** and **2** bearing less-sterically demanding aryl groups (Ar = *p*-tolyl, *p*-*t*-butylphenyl) on the boron atom. The C−O bonds in **1** and **2** are activated by intramolecular interaction between the oxygen atom and the boron atom. The interaction between the oxygen atom on the silicon atom and the boron atom is confirmed by NMR spectra, X-ray crystal structure analysis, and DFT calculation.

Chapter 3 describes the synthesis and photophysical properties of *o*-(alkoxysilyl)(borafluorenyl)benzenes **3**, in which a borafluorenyl group is introduced as a diarylboryl unit. The main focus in this study is to establish whether the planar borafluorenyl moiety increases the strength of the coordination of the oxygen atom to the boron atom and also how the photophysical properties change compared to those of the parent borafluorene. The C−O bond activation is demonstrated in the reactions of **3** with an amine and a fluoride. Compounds **3** shows emission with a large Stokes shifts attributed to the transition from the π orbitals of the borafluorenyl group to the vacant p orbital on the boron atom.

Chapter 2 **Chapter 3**

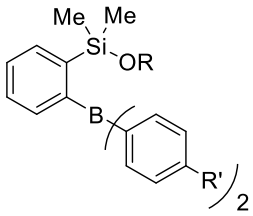

1 R' = CH_3
2 R' = *t*-Bu

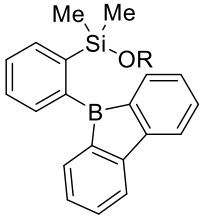

3

	R
a	Me
b	Et
c	*i*-Pr
d	*t*-Bu

Chapter 4 describes the synthetic studies of B/Si bidentate Lewis acids **4**, **5**, and **6** with a skeleton other than *o*-phenylene. In addition, this chapter describes the cationic 1,2-silyl migration in 1-halo-8-(hydrosilyl)naphthalenes **7**, during which a hydrosilyl group at the eight-position undergoes migration to the seven-position to form **8**. The driving force for the silyl migration may be relief of steric compression, which is supported by the NMR spectra and DFT calculations. A plausible reaction mechanism for this migration is discussed.

Chapter 4

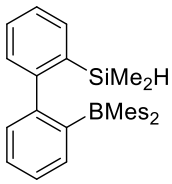

4

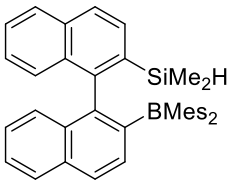

5

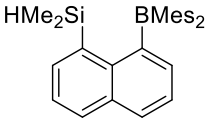

6

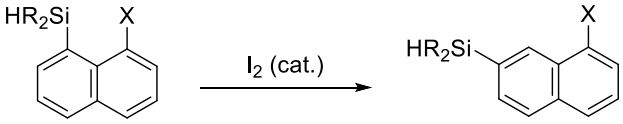

7 **8**

R = Me, Ph
X = Br, I

References

(1) "Arylsilanes", Colvin, E. W. In *Silicon in Organic Synthesis*; Butterworths; 1981; Chapter 10. Application examples of arylsilanes: (a) Bähr, S.; Oestreich, M. Electrophilic Aromatic Substitution with Silicon Electrophiles: Catalytic Friedel–Crafts C−H Silylation. *Angew. Chem. Int. Ed*. **2017**, *56*, 52–59. (b) Komiyama, T.; Minami, Y.; Hiyama, T. Recent Advances in Transition-Metal-Catalyzed Synthetic Transformations of Organosilicon Reagents. *ACS Catal.* **2017**, *7*, 631–651. (c) Dilman, A. D.; Ioffe, S. L. Carbon−Carbon Bond Forming Reactions Mediated by Silicon Lewis Acids. *Chem. Rev*. **2003**, *103*, 733–772. (d) Hong, Y.; Lama, J. W. Y.; Tang, B. Z. Aggregation-induced emission: phenomenon, mechanism and applications. *Chem. Commun*. **2009**, 4332–4353.

(2) Chuit, C.; Corriu, R, J, P.; Reye, C.; Young, J, C. Reactivity of penta- and hexacoordinate silicon compounds and their role as reaction intermediates. *Chem. Rev.* **1993**, *93*, 1371–1448.

(3) Kano, N.; Yamamura, M.; Kawashima, T. Reactivity Control of an Allylsilane Bearing a 2-(Phenylazo)phenyl Group by Photoswitching of the Coordination Number of Silicon. *J. Am. Chem. Soc.* **2004**, *126*, 6250–6251.

(4) Kawachi, A. Reactions of *o*-(Hydrosilyl)(boryl)benzenes: Intramolecular Activation of Si−H Bond by *o*-Boryl Group. *J. Synth. Org. Chem*. **2017**, *75*, 714–722.

(5) (a) Kawachi, A.; Zaima, M.; Tani, A.; Yamamoto, Y. Dehydrogenative Condensation of (*o*-Borylphenyl)hydrosilane with Alcohols and Amines. *Chem. Lett.* **2007**, *36*, 362–363. (b) Könczöl, L.; Kawachi, A.; Szieberth, D. Mechanism of Dehydrogenative Condensation of (*o*-

borylphenyl)hydrosilanes with Methanol. *Organometallics* **2012**, *31*, 120–125. (c) Kawachi, A.; Zaima, M.; Yamamoto, Y. Intramolecular Reaction of Silanol and Triarylborane: Boron-Aryl Bond Cleavage and Formation of a Si−O−B Heterocyle. *Organometallics* **2008**, *27*, 4691–4096.

(6) Kawachi, A.; Morisaki, H.; Tani, A.; Zaima, M.; Yamamoto, Y. Reaction of *o*-$(HSiR_2)(BMes_2)C_6H_4$ with a fluoride ion: Fluoride attack at silicon and hydride transfer from silicon to boron to form F−Si⋯H−B interaction. *Heteroatom Chem*. **2011**, *22*, 471–475.

(7) (a) Kawachi, A.; Morisaki, H.; Nishioka, N.; Yamamoto, Y. Intramolecular H-Ar Ligand Exchange between Silicon and Boron: Functionality Transfer of Si−H to B−H. *Chem. Asian. J.* **2012**, *7*, 546–553. (b) Kawachi, A.; Morisaki, H.; Hirofuji, T.; Yamamoto, Y. Synthesis of Silicon-Functionalized Dibenzosilaborins by Intramolecular B-H/C-H Dehydrogenative Cyclization and Their Tunable Photophysical and Chemical Properties by Silyl Groups. *Chem. Eur. J*. **2013**, *19*, 13294–13298. (c) Hirofuji, T.; Ikeda, T.; Haino, T.; Yamamoto, Y.; Kawachi, A. Synthesis of a Pentacene−Type Silaborin via Double Dehydrogenative Cyclization of 1,4-Diboryl-2,5-disilylbenzene. *Chem. Eur. J.* **2016**, *22*, 9734–9739.

(8) Kawachi, A.; Tani, A.; Shimada, J.; Yamamoto, Y. Synthesis of B/Si Bidentate Lewis Acids, *o*-(Fluorosilyl)(dimesitylboryl)benzenes, and Their Fluoride Ion Affinity. *J. Am. Chem. Soc.* **2008**, *130*, 4222–4223.

Chapter 2

Intramolecular Activation of C−O Bond

by an *o*-Boryl Group in *o*-(Alkoxysilyl)(diarylboryl)benzenes

Abstract

Halogen−lithium exchange reaction of *o*-(silyl)bromobenzene **5** with *tert*-BuLi afforded *o*-(silyl)lithiobenzene **6**, which was reacted with (alkoxy)diarylboranes **7** to form borate intermediates **8**. Treatment of **8** with chlorotrimethylsilane formed *o*-(alkoxysilyl)(diarylboryl)benzenes **4**. The C−O bond in **4** was activated by intramolecular interaction between the oxygen atom and the boron atom. **4a** readily reacted with MeOH and EtOH to afford corresponding alkoxysilanes **10** and **11**, respectively. Treatment of **10** with 1,4-diazabicyclo[2.2.2]octane (DABCO) afforded silyloxyborate complex **13**.

1. Introduction

Lewis acids have been recognized as useful catalysts in synthetic organic chemistry as well as main group chemistry. For example, Lewis acids such as BF_3, $AlCl_3$, and $SnCl_4$ activate the C−O bond in carbonyls, ethers, and epoxides by coordinating to the oxygen atom and lead to its cleavage.[1] In recent years, arylboranes have attracted much attention as Lewis acids. Piers and Oestreich reported that $B(C_6F_5)_3$ can activate the Si−H bond in the hydrosilylation of aromatic aldehydes, ketones, and esters.[2,3] In contrast to the well-studied Si−H bond activation, the silicon-heteroatom bond activation has been less investigated. Wrackmeyer reported that 2-boryl-1-(aminosilyl)alkene (**I**) readily reacted with nucleophiles to afford 2-boryl-1-(alkoxysilyl)alkene (**II**) owing to the intramolecular Si−N bond activation by the boryl group (Scheme 1).[4]

Scheme 1. Intramolecular Si–N bond activation.

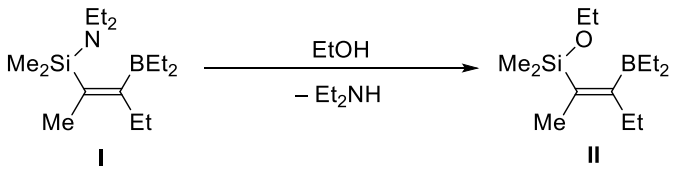

Recently, Kawachi et al. synthesized *o*-(hydrosilyl)(diarylboryl)benzene **1**, in which the dimesitylboryl and hydrosilyl groups were linked through an *o*-phenylene skeleton.[5] The Si−H bond was activated by the boryl group for several types of reactions (Scheme 2): (i) dehydrogenative condensation with alcohols to form **2** (R = Me (**a**); *i*-Pr (**b**)),[5a] (ii) nucleophilic displacement by a fluoride ion to form **3**,[5b] and (iii) H-Mes exchange between the hydrogen atom on the Si atom and mesityl (Mes) group on the boron atom.[5c]

Scheme 2. Si−H bond activation by an *o*-boryl group in **1**.

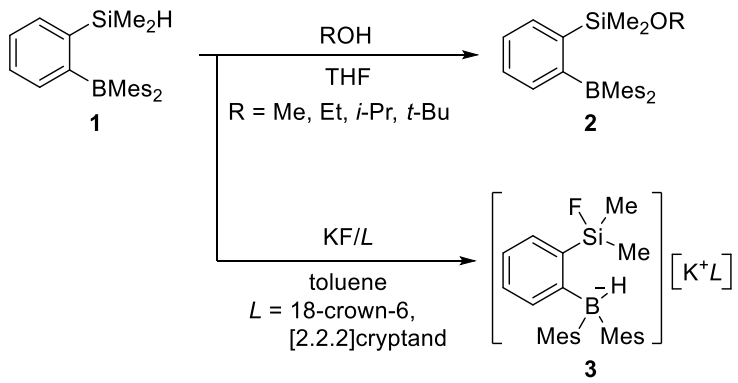

Herein, the author reports the preparation of *o*-(alkoxysilyl)(boryl)benzenes bearing less sterically demanding aryl groups (Ar = *p*-tolyl, *p*-*t*-butylphenyl) on the boron atom, and the activation of C−O bond by diarylboryl groups.

2. Results and discussion

2.1 Synthesis of *o*-[(alkoxy)silyl](diarylboryl)benzenes **4**

o-[(Isopropoxy)dimethylsilyl](diarylboryl)benzenes **4** were prepared as shown in Scheme 3. The Br-Li exchange reaction of *o*-(dimethylsilyl)bromobenzene (**5**) with *n*-BuLi produced *o*-silyl(lithio)benzene **6**,[5a] which reacted with diaryl(isopropoxy)borane **7** to form lithium [(isopropoxysilyl)phenyl]hydroborate **8** in 56% yield. The ^{11}B NMR spectrum of **8** showed a doublet at $\delta = -9.7$ because of the coupling of boron to one hydride ($^{1}J_{B\text{-}H} = 66$ Hz) in the typical region for tetracoordinate borates. The ^{29}Si NMR spectra of **8** was observed as a singlet at $\delta = 13.4$. It is plausible that the initially-formed lithium [(hydrosilyl)phenyl](isopropoxy)borate **9** underwent intramolecular hydride–isopropoxide exchange to form **8**. Treatment of **8** with chlorotrimethylsilane in situ afforded *o*-[(isopropoxy)silyl](diarylboryl)benzenes **4**.[6] Compound **4a** was isolated by distillation as a colorless oil in 70% yield whereas **4b** was isolated by recrystallization from toluene as colorless crystals in 58% yield. DFT calculations at B3PW91/6-31G(d) level of theory showed that anion part of **8** was more stable than that of **9** by 9.2–12.3 kcal/mol.[7]

Scheme 3. Preparations of **4** via hydride-isopropoxide exchange in **9**.

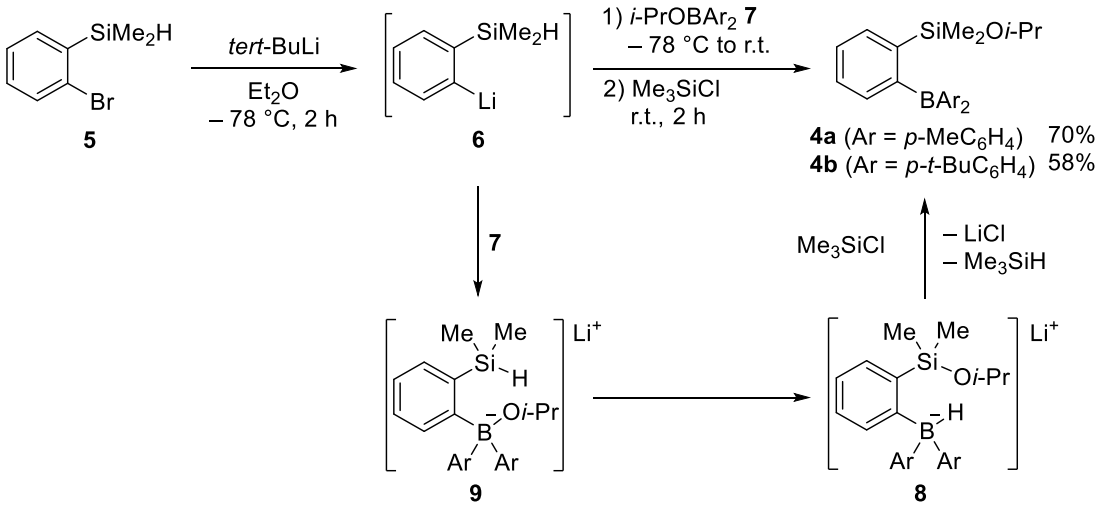

The reaction of **4a** with MeOH and EtOH in an NMR tube resulted in the formation of methoxysilane **10** and ethoxysilane **11** in 96% and 92% yield, respectively, as shown in Scheme 4. In contrast, **4a** did not react with *tert*-BuOH at all. When the same reaction was performed in a reaction flask, **10** and **11** were isolated as colorless crystals in 77% and 59% yield, respectively.

Scheme 4. Reactions of **4a** with alcohols. NMR yields are given in parentheses.

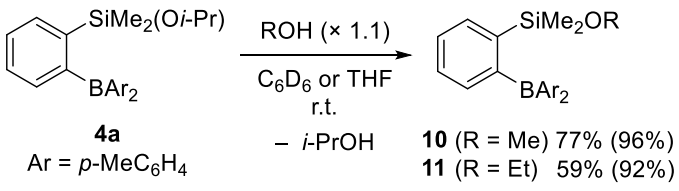

The ^{11}B NMR signal of **4a** (δ = 31) was shifted upfield whereas the ^{29}Si NMR signal of **4a** (δ = 20.0) was shifted downfield as compared to the corresponding values of **2b** (δ(^{11}B) = 73; δ(^{29}Si) =

4.6). With decreasing steric bulkiness of the alkoxy groups (**4a** > **11** > **10**), the ^{11}B NMR signal was shifted upfield and the ^{29}Si NMR signal was shifted downfield, as shown in Table 1. These chemical shifts were also compared to those of the corresponding dimethylphenyl(alkoxy)silanes **12** (R = Me, Et, *i*-Pr), showing that the electronic effect of the alkoxy groups are not significant. The intramolecular coordination of the oxygen atom to the boron atom increased the electron density on the boron atom and decreased that on the silicon atom.

Table 1. ^{11}B and ^{29}Si NMR shifts of *o*-(silyl)(diarylboryl)benzenes.

Compounds	R	δ(^{11}B)	δ(^{29}Si)
2b	*i*-Pr	73	4.6
4a	*i*-Pr	31	20.0
10	Me	17	33.1
11	Et	20	29.5
12	Me	-	8.5
12	Et	-	6.1
12	*i*-Pr	-	4.0

2.2 Structures of **10**

Molecular structure of **10** was finally determined by X-ray crystallographic analysis (Figure 1).[8] The B···O interatomic distance (1.652(2) Å) was much shorter than the sum of the van der Waals radii of the two elements (B: 1.85 Å; O: 1.52 Å)[9] and only 7–8% longer than the sum of their covalent bond radii (B: 0.84 Å; O: 0.66 Å).[9] The boron atom adopted an intermediate geometry between tetrahedral and trigonal planar with the sum of the bond angles around the boron atom (Σ(C−B−C) = 343°). The five-membered ring consisting of C1, Si1, O1, B1, and C2 atoms was almost planar and coplanar with the phenylene ring. The oxygen atom adopted a trigonal planar geometry (Σ(O) = 359°) and the tetrahedral geometry of the boron atom was distorted because of the small endocyclic bond angle (O1−B1−C2 = 99.78(9)°). The Si−O (1.714(1) Å) and C−O (1.448(1) Å) bonds were longer than the typical Si−O (1.51 Å) and C−O (1.43 Å) bonds,[9] respectively, but slightly shorter than those of silylated oxonium ions.[10] These structural parameters support the intramolecular coordination of the oxygen atom to the boron atom as mentioned above.

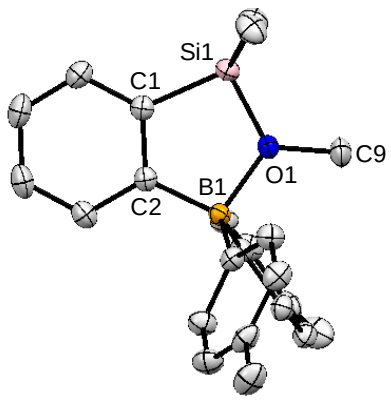

Figure 1. Crystal structure of **10** at 30% probability level. H atoms are omitted for clarity. Selected bond lengths (Å) and angles (deg): B1−O1, 1.652(2); Si1−O1, 1.714(1); B1−O1, 1.652(2), C9−O1; 1.448(1); C1−Si1−O1, 93.79(5); Si1−O1−B1, 116.68(6); O1−B1−C2, 99.78(9).

2.3 DFT calculations of **10**

To gain further insight into the electronic structure of the (alkoxysilyl)(boryl)benzenes, DFT calculations of **10** and **2** (R = Me) were performed at B3PW91/6-31++G(d,p) level of theory (Figure 2).[7] The lone pair electrons on the oxygen atom in **10** contributed to HOMO−1 (−6.27 eV). The HOMO (−6.46 eV) of **10** is the π orbital of the tolyl groups, and the LUMO (−0.59 eV) is mainly the π* orbital of the phenylene skeleton. The vacant 2p orbital on the boron atom in **10** was involved in LUMO+2 (−0.40 eV). The charge distribution was revealed by NBO analysis (Mulliken charge in parentheses), as shown in Figure 3.[11] Compared to **2** (R = Me), **10** exhibited more positive charges on the oxygen atom (−0.84 vs. −0.92) and the methyl carbon atoms (+0.39 vs. +0.31) bonded to it while the boron atom had lesser positive charges (+0.74 vs. +1.97).

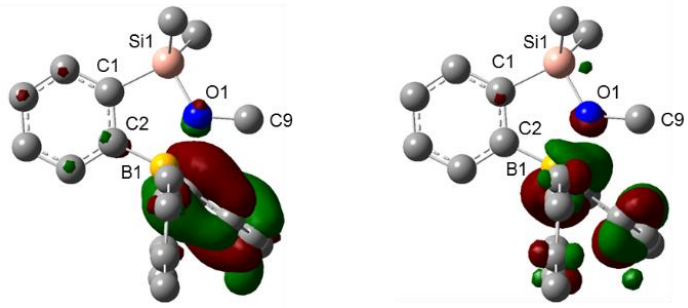

Figure 2. Optimized structure of **10** at the B3PW91/6-31++G(d,p) level of theory with overlay of HOMO−1 (left) and LUMO+2 (right) (isosurface value = 0.04).

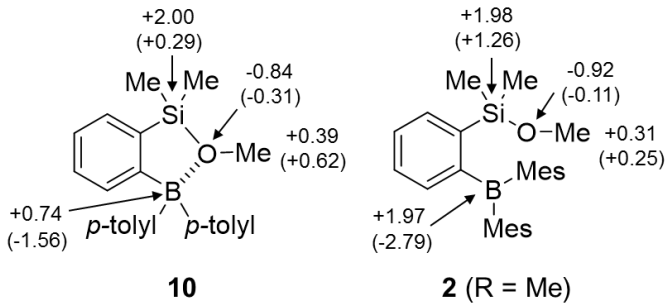

Figure 3. NBO charge and Mulliken charge (in parentheses) distributions in **10** (left) and **2** (R = Me) (right).

The perturbation theory energy analysis in NBO basis reveals delocalization from the donor LP_O to the acceptor LP^*_B with the occupancy of 0.306:[12] the stabilization energy $E(2)$ was calculated to be 16.2 kcal/mol.

2.4 C−O bond activation in *o*-[(methoxy)silyl](diarylboryl)benzenes **10**

The B···O interaction was expected to render the carbon atom more electropositive. Thus, treatment of **10** with 1,4-diazabicyclo[2.2.2]octane (DABCO) afforded silyloxyborate-(Me-DABCO)$^+$ complex **13**, as shown in Scheme 5. Compound **13** was isolated as colorless crystals by recrystallization from DMSO in 79% yield. The structure of **13** was characterized by its ^{11}B NMR (δ = 3.0) and ^{29}Si NMR (δ = 9.1) signals, which were consistent with those of oxasilaboratacyclopentene (δ(^{11}B) = 6.0; δ(^{29}Si) = 10.5)[5d] and benzosiloxaborole (δ(^{11}B) = 31.0; δ(^{29}Si) = 22.3).[13] The reaction of **10** with Et_3N in THF did not occur even after heating at 80 °C for a day. It is worth noting that compound **10** was regenerated upon treatment of **13** with MeI.[4a] The reaction of **10** with KF in the presence of 18-crown-6 led to Me−O bond cleavage to form **14** in 70% yield as a white precipitate from THF-hexane (Scheme 6). The reason why the fluoride ion attacks the methyl carbon rather than the boron atom may be that formation of the stable 5-membered ring is more favorable than formation of an acyclic fluoroborate.

Scheme 5. C−O bond cleavage in **10** with DABCO.

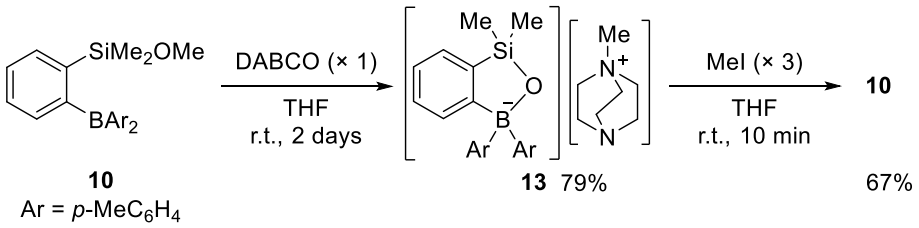

Scheme 6. C–O bond cleavage in **10** with KF/18-crown-6.

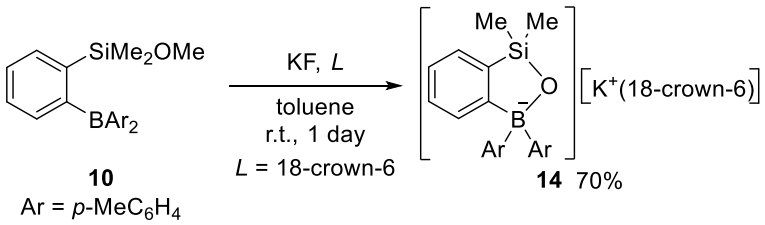

3. Conclusion

o-[Isopropoxy)silyl](diarylboryl)benzenes **4** bearing less sterically demanding aryl groups were prepared. The interaction between the oxygen atom and boron atom was confirmed by NMR spectra, X-ray crystal structure analysis, and DFT calculations. The B···O interaction led the C−O bond activation.

4. Experimental section

4.1 General considerations

^{1}H (400 MHz), ^{13}C (100 MHz), ^{11}B (128.3 MHz), and ^{29}Si (79.5 MHz) NMR spectra were recorded using a Bruker Avance III 400 spectrometer. ^{1}H and ^{13}C chemical shifts were referenced to the residual solvent signals $CDCl_3$ ($\delta(^{1}H) = 7.26$, $\delta(^{13}C) = 77.00$); C_6D_6 ($\delta(^{1}H) = 7.20$, $\delta(^{13}C) = 128.00$), and DMSO-d_6 ($\delta(^{1}H) = 2.50$; $\delta(^{13}C) = 39.52$). ^{11}B, and ^{29}Si chemical shifts were referenced to external standards $BF_3 \cdot OEt_2$ ($\delta = 0$), and tetramethylsilane ($\delta = 0$), respectively. The mass spectra (EI) were recorded 70 eV using a JEOL JMS-Q1000GC Mk II mass spectrometer and the elemental analyses were performed using the JSL MICRO CORDER JM10 elemental analyzer.

4.2 Materials

Triisopropyl borate (Tokyo Chemical Industry Co., Ltd.) was distilled under a nitrogen atmosphere over calcium hydride. Chlorotrimethylsilane (Tokyo Chemical Industry Co., Ltd.) was treated with small pieces of sodium under a nitrogen atmosphere to remove dissolved HCl, and the supernatant was used. *tert*-Butyllithium in pentane (Kanto Chemical Co., Inc.) and DABCO (Tokyo Chemical Industry Co., Ltd.) were used as received. KF (Wako Pure Chemical Industries, Ltd.) was dried in vacuo at 100 °C, 18-crown-6 (Wako Pure Chemical Industries, Ltd.) was recrystallized from CH_3CN, and *o*-(dimethylsilyl)bromobenzene (**5**) was prepared according to the literature methods.[5a]

THF and Et_2O were distilled under a nitrogen atmosphere over sodium benzophenone ketyl.

Hexane and toluene were distilled under a nitrogen atmosphere over sodium. All reactions were carried out under an inert gas atmosphere.

4.3 Experimental details

(Isopropoxy)di(*p*-tolyl)borane (7a). To a mixture of Mg turnings (972 mg, 40.0 mmol) and one crystal of I_2 in Et_2O (5 mL), a few drops of a solution of 4-bromotoluene (4.9 mL, 40.0 mmol) in Et_2O (15 mL) were added at room temperature. After the reaction started, Et_2O (20 mL) was added and the remaining solution was added dropwise at a rate that maintained a steady reflux. When the addition was complete, the reaction mixture was cooled to room temperature, added to triisopropyl borate (4.5 mL, 19.6 mmol) in Et_2O (20 mL) at 0 °C, and stirred overnight at room temperature. Chlorotrimethylsilane (5.3 mL, 40.0 mmol) was then added dropwise at room temperature and the reaction mixture was stirred for 6 h. Subsequently, the solvents were removed in vacuo and the residue was diluted with hexane (40 mL) and filtered. The filtrate was subjected to bulb-to-bulb distillation (90–110 °C/0.85 mmHg) to obtain **7a** (2.8 g, 56% yield) as a colorless viscous oil. ^{1}H NMR (C_6D_6, δ) 1.19 (d, J = 6 Hz, 6H), 2.20 (s, 6H), 4.66 (sept, J = 6 Hz, 1H), 7.15–7.17 (m, 4H), 7.74–7.76 (m, 4H). ^{13}C{^{1}H} NMR (C_6D_6, δ) 21.54, 24.88, 69.50, 128.69, 134.55, 135.32, 139.82. ^{11}B NMR (C_6D_6, δ) 44.95 (br). MS(EI) *m/z* 252 (M^+, 9), 160 (M^+−*p*-tolyl, 16), 119 ((M^+−*p*-tolyl−*i*-Pr, 100). Anal. Calcd for $C_{17}H_{21}BO$: C, 80.97; H, 8.39; Found: C, 80.61; H, 8.68.

(Isopropoxy)di(*p-tert*-butylphenyl)borane (7b). To a mixture of Mg turnings (972 mg, 40.0 mmol) and one crystal of I_2 in Et_2O (5 mL), a few drops of a solution of 1-bromo-4-*tert*-butylbenzene (6.8 mL, 40.0 mmol) in Et_2O (15 mL) were added at room temperature. After the reaction started, Et_2O (20 mL) was added and the remaining solution was added dropwise at a rate that maintained a steady reflux. When addition was complete, the reaction mixture was cooled to room temperature, added to triisopropyl borate (4.5 mL, 19.6 mmol) in Et_2O (20 mL) at 0 °C, and stirred overnight at room temperature. Next, chlorotrimethylsilane (5.3 mL, 40.0 mmol) was added dropwise at room temperature and the reaction mixture was stirred for 6 h. The solvents were subsequently removed in vacuo, and the residue was diluted with hexane (40 mL) and filtered. The filtrate was subjected to bulb-to-bulb distillation (150–170 °C/0.85 mmHg) to obtain **7b** (3.2 g, 48% yield) as a colorless viscous oil. ^{1}H NMR (C_6D_6, δ) 1.21 (d, J = 6 Hz, 6H), 1.29 (s, 18H), 4.68 (sept, J = 6 Hz, 1H), 7.42–7.45 (m, 4H), 7.81–7.83 (m, 4H). ^{13}C{^{1}H} NMR (C_6D_6, δ) 24.93, 31.33, 34.74, 69.58, 124.81, 126.02, 127.12, 134.51. ^{11}B NMR (C_6D_6, δ) 45.29 (br). MS(EI) *m/z* 266 (M^+−*i*-Pr−2Me, 31), 251 (M^+−*i*-Pr−3Me, 100). Anal. Calcd for $C_{23}H_{33}BO$: C, 82.14; H, 9.89; Found: C, 82.44; H, 9.78.

***o*-[(Isopropoxy)dimethylsilyl][di(*p*-tolyl)boryl]benzene (4a).** A solution of *tert*-BuLi in pentane (1.56 mol/L, 3.8 mL, 6.00 mmol) was added to a solution of **5** (645 mg, 3.00 mmol) in Et_2O (6 mL) at −78 °C over 4 min. After the reaction mixture was stirred at the same temperature for 2 h, **7a** (756 mg, 3.00 mmol) in Et_2O (3 mL) was added over 3 min. The reaction mixture was stirred at the same temperature for 30 min and then warmed to room temperature. Next, chlorotrimethylsilane (0.56 mL, 4.50 mmol) was added and the mixture was stirred for 2 h. After

the solvents were removed in vacuo, the residue was dissolved in hexane (20 mL) and filtered. The filtrate was subjected to bulb-to-bulb distillation (170–180 °C/0.90 mmHg) to obtain **4a** (811 mg, 70% yield) as a colorless oil. ^{1}H NMR (C_6D_6, δ) 0.30 (s, 6H), 0.77 (d, J = 6 Hz, 6H), 2.27 (s, 6H), 4.43 (sept, J = 6 Hz, 1H), 7.17–7.19 (m, 4H), 7.23 (dd, J = 7 Hz, J = 2 Hz, 1H), 7.26 (ddd, J = 7 Hz, J = 7 Hz, J = 2 Hz, 1H), 7.43–7.45 (m, 2H), 7.72–7.74 (m, 4H). ^{13}C{^{1}H} NMR (C_6D_6, δ) 2.75, 21.39, 24.14, 72.57, 125.69, 128.45, 128.67, 129.65, 130.07, 130.61, 136.01, 137.00 (signals corresponding to the *ipso* carbons in the two *p*-tolyl groups and the *ipso* carbon in the phenyl group were not observed). ^{11}B NMR (C_6D_6, δ) 30.94 (br). ^{29}Si{^{1}H} NMR (C_6D_6, δ) 19.99. Anal. Calcd for $C_{25}H_{31}BOSi$: C, 77.71; H, 8.09; Found: C, 77.50; H, 8.32.

***o*-[(Isopropoxy)dimethylsilyl][di(*p-tert*-butylphenyl)boryl]benzene (4b).** A solution of *tert*-BuLi in pentane (1.56 mol/L, 3.8 mL, 6.00 mmol) was added to a solution of **5** (645 mg, 3.00 mmol) in Et_2O (6 mL) at −78 °C over 4 min. After the reaction mixture was stirred at this temperature for 2 h, **7b** (1.01 g, 3.00 mmol) in Et_2O (3 mL) was added over 3 min. The reaction mixture was stirred at the same temperature for 30 min and then allowed to warm to room temperature. Next, chlorotrimethylsilane (0.56 mL, 4.50 mmol) was added and the mixture was stirred for 2 h. After the solvents were removed in vacuo, the residue was dissolved in hexane (20 mL) and filtered. The filtrate was concentrated in vacuo to give a white solid, which was recrystallized from toluene at −18 °C to obtain **4b** (821 mg, 58% yield) as a colorless crystal. ^{1}H NMR (C_6D_6, δ) 0.33 (s, 6H), 0.74 (d, J = 6 Hz, 6H), 1.35 (s, 18H), 4.48 (sept, J = 6 Hz, 1H), 7.23 (ddd, J = 7 Hz, J = 7 Hz, J = 2 Hz, 1H), 7.27 (ddd, J = 7 Hz, J = 7 Hz, J = 2 Hz, 1H), 7.42–7.47 (m, 6H), 7.76–7.78 (m, 4H).

$^{13}C\{^1H\}$ NMR (C_6D_6): δ 2.91, 24.00, 31.57, 34. 51, 73.14, 124.50, 125.64, 128.28, 129.81, 129.87, 130.67, 135.58, 149.95 (signals corresponding to the ipso carbons in the two *p-tert*-butylphenyl groups and the *ipso* carbon in the phenyl group were not observed). ^{11}B NMR (C_6D_6, δ) 27.96 (br). $^{29}Si\{^1H\}$ NMR (C_6D_6, δ) 21.31. MS(EI) *m/z* 294 (M^+−*i*-Pr−*p*-*t*-BuPh, 20), 279 (M^+−*i*-Pr−*p*-*t*-BuPh−Me, 100). Anal. Calcd for $C_{31}H_{43}BOSi$: C, 79.12; H, 9.21; Found: C, 78.81; H, 9.03.

Hydroborate 8b. A solution of *tert*-BuLi in pentane (1.56 mol/L, 3.8 mL, 6.00 mmol) was added to a solution of **5** (645 mg, 3.00 mmol) in Et_2O (6 mL) at −78 °C. After stirring at the same temperature for 2 h, **7b** (1.01 g, 3.00 mmol) in Et_2O (3 mL) was added. The reaction mixture was stirred at this temperature for 30 min and then allowed to warm to room temperature. The solvents were subsequently removed in vacuo, and the resulting white solid was dissolved in THF (5 mL). The solvent was removed in vacuo, and the residue was dissolved in hexane (10 mL) and filtered. The filtrate was concentrated in vacuo to obtain a white solid, which was recrystallized from hexane at −18 °C to obtain **8b** (1.1 g, 61% yield) as a colorless crystal. ^1H NMR (C_6D_6, δ) 0.66 (s, 6H), 0.68 (d, J = 6 Hz, 6H), 1.11 (m, 8H, THF), 1.35 (s, 18H), 3.06 (m, 8H, THF), 3.80 (sept, J = 6 Hz, 1H), 7.25 (ddd, J = 7 Hz, J = 7 Hz, J = 1 Hz, 1H), 7.37–7.39 (m, 5H), 7.65 (dd, J = 7 Hz, J = 1 Hz, 1H), 7.68 (d, J = 8 Hz, 4H), 8.10 (d, J = 8 Hz, 1H). $^{13}C\{^1H\}$ NMR (C_6D_6, δ) 1.50, 24.53, 25.09 (THF), 31.76, 34.25, 67.37 (THF), 68.10, 123.65, 124.58, 129.74, 133.08, 135.83, 137.40, 139.89, 146.67 (signals corresponding to the *ipso* carbons in the two *p-tert*-butylphenyl groups and the *ipso*

carbon in the phenyl group were not found). ^{11}B NMR (C_6D_6, δ) −9.66 (d, $^1J_{B-H}$ = 66 Hz). ^{29}Si{^{1}H} NMR (C_6D_6, δ) 13.43. Anal. Calcd for $C_{39}H_{60}BLiO_3Si$: C, 75.22; H, 9.71; Found: C, 75.02; H, 9.88.

***o*-[(Methoxy)dimethylsilyl][di(*p*-tolyl)boryl]benzene (10).** To a solution of **4a** (772 mg, 2.00 mmol) in THF (4.0 mL), MeOH (90 μL, 2.20 mmol) was added via a syringe at room temperature. The reaction mixture was stirred at the same temperature for 10 min and then concentrated in vacuo to afford a white solid. Recrystallization from toluene at −18 °C gave **10** (710 mg, 66% yield) as a colorless crystal. ^{1}H NMR (C_6D_6, δ) 0.08 (s, 6H), 2.26 (s, 6H), 2.93 (s, 3H), 7.13–7.19 (m, 5H), 7.24 (ddd, *J* = 8 Hz, *J* = 8 Hz, *J* = 1 Hz, 1H), 7.33 (ddd, *J* = 8 Hz, *J* = 1 Hz, *J* = 1 Hz, 1H), 7.50–7.53 (m, 5H). ^{13}C{^{1}H} NMR (C_6D_6, δ) −1.36, 21.35, 50.58, 125.45, 128.54, 129.76, 130.47, 131.05, 133.46, 134.74, 135.71 (signals corresponding to the *ipso* carbons in the two *p*-tolyl groups and the *ipso* carbon in the phenyl group were not observed). ^{11}B NMR (C_6D_6, δ) 17.35 (br). ^{29}Si{^{1}H} NMR (C_6D_6, δ) 33.12. MS(EI) *m/z* 252 (M^+−*p*-tolyl−Me, 36), 237 (M^+−*p*-tolyl−2Me, 100). Anal. Calcd for $C_{23}H_{27}BOSi$: C, 77.09; H, 7.59; Found: C, 76.82; H, 7.56.

***o*-[(Ethoxy)dimethylsilyl][di(*p*-tolyl)boryl]benzene (11).** To a solution of **4a** (772 mg, 2.00 mmol) in THF (4.0 mL), EtOH (0.13 mL, 2.20 mmol) was added via a syringe at room temperature. The reaction mixture was stirred at the same temperature for 10 min and then concentrated in vacuo to afford a white solid. Recrystallization from hexane at −18 °C gave **11** (439 mg, 59% yield) as a colorless crystal. ^{1}H NMR (C_6D_6, δ) 0.22 (s, 6H), 0.62 (t, *J* = 7 Hz, 3H), 2.29 (s, 6H), 3.64 (q, *J* = 7 Hz, 2H), 7.20–7.23 (m, 5H), 7.27 (ddd, *J* = 8 Hz, *J* = 8 Hz, *J* = 1 Hz, 1H), 7.37 (ddd, *J* = 7 Hz, *J* = 2 Hz, *J* = 1 Hz, 1H), 7.52 (ddd, *J* = 7 Hz, *J* = 2 Hz, *J* = 1 Hz, 1H), 7.63 (d, *J* = 8 Hz, 4H). ^{13}C{^{1}H}

NMR (C_6D_6, δ) 0.46, 16.14, 21.34, 63.29, 125.45, 128.48, 129.62, 130.31, 130.78, 134.11, 134.89, 135.81 (signals corresponding to the *ipso* carbons in the two *p*-tolyl groups and the *ipso* carbon in the phenyl group were not observed). ^{11}B NMR (C_6D_6, δ) 20.02 (br). ^{29}Si{^{1}H} NMR (C_6D_6, δ) 29.50. Anal. Calcd for $C_{24}H_{29}BOSi$: C, 77.41; H, 7.85; Found: C, 77.03; H, 7.94.

Silyloxyborate-[(Me-DABCO)$^+$] Complex 13. A solution of **10** (179 mg, 0.50 mmol) and DABCO (56 mg, 0.50 mmol) in THF (1 mL) was stirred at room temperature for 2 days. The solvent was removed in vacuo and the residue was recrystallized from DMSO at room temperature to obtain **13** (186 mg, 79% yield) as a colorless crystal. ^{1}H NMR (DMSO-d_6, δ) 0.13 (s, 6H), 2.12 (s, 6H), 2.75 (s, 3H), 2.87 (t, J = 8 Hz, 6H), 3.01 (t, J = 8 Hz, 6H) , 6.75 (d, J = 8 Hz, 4H), 6.81 (t, J = 7 Hz, 1H), 6.95 (dd, J = 7 Hz, J = 1 Hz, 1H), 7.18 (d, J = 7 Hz, 1H), 7.35 (d, J = 8 Hz, 4H), 7.39 (d, J = 7 Hz, 1H). ^{13}C{^{1}H} NMR (DMSO-d_6, δ) 2.82, 20.84, 44.61, 50.62 (t, J = 4 Hz), 53.14 (t, J = 3 Hz), 122.38, 126.30, 126.35, 128.49, 129.20, 130.10, 132.14, 144.31, 158.92 (br) (signals corresponding to the *ipso* carbons in the two *p*-tolyl groups were not observed). ^{11}B NMR (DMSO-d_6, δ) 2.54 (br). ^{29}Si{^{1}H} NMR (DMSO-d_6, δ) 9.12. Anal. Calcd for $C_{29}H_{39}BN_2OSi$: C, 74.03; H, 8.35; N, 5.95 Found: C, 73.82; H, 8.30; N, 6.12.

Silyloxyborate-[K(18-crown-6)$^+$] Complex 14. A solution of **10** (71 mg, 0.20 mmol), 18-crown-6 (53 mg, 0.20 mmol), and KF (12 mg, 0.20 mmol) in toluene (0.6 mL) was stirred at room temperature for 12 h. Subsequently, the solvent was removed in vacuo. The resulting white solid was dissolved in THF (0.5 mL) and toluene (1 mL) was slowly added to the solution. The resulting two-layer solution was allowed to stand at room temperature for a day to obtain **14** (108 mg, 70%

yield) as a colorless crystal. ^{1}H NMR ($CDCl_3$, δ) 0.35 (s, 6H), 2.22 (s, 6H), 3.40 (s, 24H, crown), 6.91 (d, J = 8 Hz, 4H), 6.96 (ddd, J = 8 Hz, J = 8 Hz, J = 1 Hz, 1H), 7.04 (ddd, J = 7 Hz, J = 7 Hz, J = 1 Hz, 1H), 7.34 (d, J = 8 Hz, 1H), 7.36 (d, J = 7 Hz, 1H), 7.50 (d, J = 8 Hz, 4H). ^{13}C{^{1}H} NMR ($CDCl_3$, δ). 2.93, 21.17, 69.51 (crown), 122.86, 127.11, 127.44, 128.37, 129.50, 131.31, 133.39, 142.99 (signals corresponding to the *ipso* carbons in the two *p*-tolyl groups and the *ipso* carbon in the phenyl group were not observed). ^{11}B NMR ($CDCl_3$, δ) 2.79 (br). ^{29}Si{^{1}H} NMR ($CDCl_3$, δ) 11.26. Anal. Calcd for $C_{42}H_{64}BKO_9Si$: C, 67.10; H, 8.58; Found: C, 66.76; H, 8.60.

Reaction of 13 with MeI: Formation of 10. To a solution of **13** (141 mg, 0.30 mmol) in THF (1 mL), MeI (56 μL, 0.90 mmol) was added dropwise via a syringe at room temperature and the reaction mixture was stirred at the same temperature for 10 min. After the solvents were removed in vacuo, the residue was dissolved in toluene (1 mL) and filtered. The filtrate was cooled to −18 °C to obtain colorless crystals of **10** (72 mg, 67% yield).

4.4 X-ray crystallographic data

X-ray crystallographic data for **2a** and **2b** were collected using a SMART APEX-II CCD diffractometer with graphite-monochromated Mo-K_α radiation (λ= 0.71073 Å) at 173 K at the Department of Chemistry, Graduate School of Science, Hiroshima University. The structures were solved by direct methods using SIR 97[12] and refined by a full-matrix least-squares procedure based on F^2 with SHELX-97[13]. All non-hydrogen atoms were refined anisotropically. Hydrogen atoms

were located at the expected positions by a geometrical calculation and refined isotropically or found on the difference Fourier map and refined isotropically.

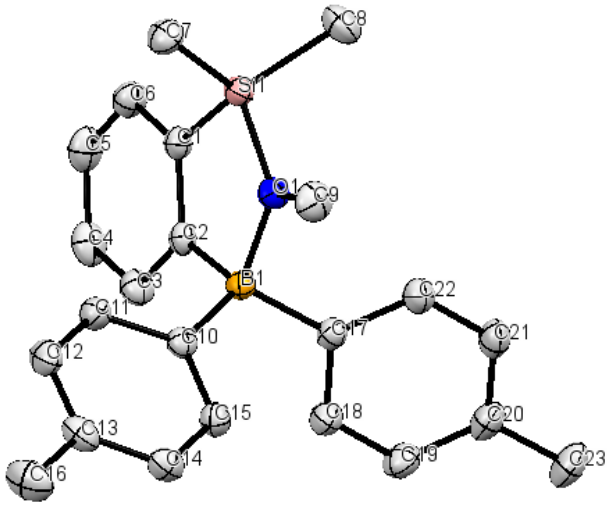

Figure 4. Crystal structure of **10** at the 30% probability level. H atoms are omitted for clarity.

Table 2. Crystal data and structure refinement for **10**.

Identification code	exp1262_0ma_a
Empirical formula	C23 H27 B O Si
Formula weight	358.34
Temperature	173(2) K
Wavelength	0.71073 Å
Crystal system	Orthorhombic
Space group	Pbca

Unit cell dimensions	a = 17.568(2) Å	α = 90°.
	b = 12.8876(16) Å	β = 90°.
	c = 18.107(2) Å	γ = 90°.
Volume	4099.6(9) Å3	
Z	8	
Density (calculated)	1.161 Mg/m3	
Absorption coefficient	0.123 mm-1	
F(000)	1536	
Crystal size	0.201 x 0.124 x 0.055 mm3	
Theta range for data collection	2.250 to 27.969°.	
Index ranges	-23<=h<=20, -17<=k<=9, -23<=l<=23	
Reflections collected	23523	
Independent reflections	4921 [R(int) = 0.0255]	
Completeness to theta = 25.242°	99.9 %	
Absorption correction	Semi-empirical from equivalents	
Max. and min. transmission	0.993 and 0.901	
Refinement method	Full-matrix least-squares on F2	
Data / restraints / parameters	4921 / 0 / 240	
Goodness-of-fit on F2	1.043	

Final R indices [I>2sigma(I)]	R1 = 0.0386, wR2 = 0.1085
R indices (all data)	R1 = 0.0466, wR2 = 0.1159
Extinction coefficient	n/a
Largest diff. peak and hole	0.366 and -0.242 e.Å-3

All hydrogen atoms were located at the expected positions by a geometrical calculation and refined isotropically.

Table 3. Atomic coordinates (x 10^4) and equivalent isotropic displacement parameters (Å^{2}x 10^3) for **10**. U(eq) is defined as one third of the trace of the orthogonalized U^{ij} tensor.

	x	y	z	U(eq)
Si(1)	3936(1)	5702(1)	8477(1)	22(1)
B(1)	3952(1)	4292(1)	7253(1)	20(1)
O(1)	3942(1)	5508(1)	7540(1)	23(1)
C(1)	3930(1)	4305(1)	8691(1)	22(1)
C(2)	3957(1)	3701(1)	8041(1)	21(1)
C(3)	3975(1)	2617(1)	8121(1)	28(1)
C(5)	3939(1)	2759(1)	9450(1)	33(1)

C(4)	3971(1)	2153(1)	8813(1)	32(1)
C(7)	4825(1)	6394(1)	8719(1)	31(1)
C(6)	3917(1)	3827(1)	9389(1)	29(1)
C(8)	3064(1)	6437(1)	8708(1)	36(1)
C(9)	4086(1)	6342(1)	7022(1)	32(1)
C(10)	4726(1)	4181(1)	6777(1)	22(1)
C(11)	5442(1)	4168(1)	7124(1)	27(1)
C(12)	6120(1)	4159(1)	6725(1)	31(1)
C(13)	6117(1)	4146(1)	5954(1)	29(1)
C(14)	5413(1)	4132(1)	5602(1)	28(1)
C(15)	4736(1)	4158(1)	6005(1)	25(1)
C(16)	6846(1)	4170(1)	5516(1)	43(1)
C(17)	3170(1)	4114(1)	6801(1)	23(1)
C(18)	3043(1)	3170(1)	6434(1)	29(1)
C(19)	2361(1)	2949(1)	6077(1)	32(1)
C(20)	1771(1)	3671(1)	6058(1)	30(1)
C(21)	1893(1)	4616(1)	6403(1)	31(1)
C(22)	2573(1)	4829(1)	6769(1)	28(1)
C(23)	1017(1)	3424(1)	5695(1)	39(1)

Table 4. Bond lengths [Å] and angles [°] for **10**.

Si(1)-O(1)	1.7147(10)	C(4)-H(4)	0.9500
Si(1)-C(1)	1.8412(13)	C(7)-H(7A)	0.9800
Si(1)-C(8)	1.8495(14)	C(7)-H(7B)	0.9800
Si(1)-C(7)	1.8509(14)	C(7)-H(7C)	0.9800
B(1)-C(17)	1.6154(17)	C(6)-H(6)	0.9500
B(1)-C(10)	1.6159(18)	C(8)-H(8A)	0.9800
B(1)-C(2)	1.6171(18)	C(8)-H(8B)	0.9800
B(1)-O(1)	1.6521(16)	C(8)-H(8C)	0.9800
O(1)-C(9)	1.4482(15)	C(9)-H(9A)	0.9800
C(1)-C(6)	1.4069(18)	C(9)-H(9B)	0.9800
C(1)-C(2)	1.4117(17)	C(9)-H(9C)	0.9800
C(2)-C(3)	1.4045(18)	C(10)-C(15)	1.3976(17)
C(3)-C(4)	1.388(2)	C(10)-C(11)	1.4056(17)
C(3)-H(3)	0.9500	C(11)-C(12)	1.3937(18)
C(5)-C(6)	1.381(2)	C(11)-H(11)	0.9500
C(5)-C(4)	1.394(2)	C(12)-C(13)	1.396(2)
C(5)-H(5)	0.9500	C(12)-H(12)	0.9500

C(13)-C(14)	1.3905(19)	C(23)-H(23B)	0.9800
C(13)-C(16)	1.5082(18)	C(23)-H(23C)	0.9800
C(14)-C(15)	1.3953(18)		
C(14)-H(14)	0.9500	O(1)-Si(1)-C(1)	93.79(5)
C(15)-H(15)	0.9500	O(1)-Si(1)-C(8)	107.65(6)
C(16)-H(16A)	0.9800	C(1)-Si(1)-C(8)	116.68(6)
C(16)-H(16B)	0.9800	O(1)-Si(1)-C(7)	107.43(5)
C(16)-H(16C)	0.9800	C(1)-Si(1)-C(7)	115.18(6)
C(17)-C(22)	1.3985(18)	C(8)-Si(1)-C(7)	113.48(7)
C(17)-C(18)	1.4046(18)	C(17)-B(1)-C(10)	115.63(10)
C(18)-C(19)	1.3919(18)	C(17)-B(1)-C(2)	112.59(10)
C(18)-H(18)	0.9500	C(10)-B(1)-C(2)	115.18(10)
C(19)-C(20)	1.394(2)	C(17)-B(1)-O(1)	106.48(9)
C(19)-H(19)	0.9500	C(10)-B(1)-O(1)	105.14(9)
C(20)-C(21)	1.386(2)	C(2)-B(1)-O(1)	99.78(9)
C(20)-C(23)	1.5115(18)	C(9)-O(1)-B(1)	119.89(9)
C(21)-C(22)	1.3927(18)	C(9)-O(1)-Si(1)	122.28(8)
C(21)-H(21)	0.9500	B(1)-O(1)-Si(1)	116.67(7)
C(22)-H(22)	0.9500	C(6)-C(1)-C(2)	120.51(12)
C(23)-H(23A)	0.9800	C(6)-C(1)-Si(1)	128.14(10)

C(2)-C(1)-Si(1)	111.34(9)	C(5)-C(6)-H(6)	119.7
C(3)-C(2)-C(1)	117.61(11)	C(1)-C(6)-H(6)	119.7
C(3)-C(2)-B(1)	124.01(11)	Si(1)-C(8)-H(8A)	109.5
C(1)-C(2)-B(1)	118.37(11)	Si(1)-C(8)-H(8B)	109.5
C(4)-C(3)-C(2)	121.42(13)	H(8A)-C(8)-H(8B)	109.5
C(4)-C(3)-H(3)	119.3	Si(1)-C(8)-H(8C)	109.5
C(2)-C(3)-H(3)	119.3	H(8A)-C(8)-H(8C)	109.5
C(6)-C(5)-C(4)	119.57(13)	H(8B)-C(8)-H(8C)	109.5
C(6)-C(5)-H(5)	120.2	O(1)-C(9)-H(9A)	109.5
C(4)-C(5)-H(5)	120.2	O(1)-C(9)-H(9B)	109.5
C(3)-C(4)-C(5)	120.37(13)	H(9A)-C(9)-H(9B)	109.5
C(3)-C(4)-H(4)	119.8	O(1)-C(9)-H(9C)	109.5
C(5)-C(4)-H(4)	119.8	H(9A)-C(9)-H(9C)	109.5
Si(1)-C(7)-H(7A)	109.5	H(9B)-C(9)-H(9C)	109.5
Si(1)-C(7)-H(7B)	109.5	C(15)-C(10)-C(11)	115.79(11)
H(7A)-C(7)-H(7B)	109.5	C(15)-C(10)-B(1)	123.12(11)
Si(1)-C(7)-H(7C)	109.5	C(11)-C(10)-B(1)	120.97(11)
H(7A)-C(7)-H(7C)	109.5	C(12)-C(11)-C(10)	122.20(12)
H(7B)-C(7)-H(7C)	109.5	C(12)-C(11)-H(11)	118.9
C(5)-C(6)-C(1)	120.51(13)	C(10)-C(11)-H(11)	118.9

C(11)-C(12)-C(13)	121.01(12)	C(18)-C(17)-B(1)	119.83(11)
C(11)-C(12)-H(12)	119.5	C(19)-C(18)-C(17)	122.28(13)
C(13)-C(12)-H(12)	119.5	C(19)-C(18)-H(18)	118.9
C(14)-C(13)-C(12)	117.50(12)	C(17)-C(18)-H(18)	118.9
C(14)-C(13)-C(16)	120.97(13)	C(18)-C(19)-C(20)	121.06(13)
C(12)-C(13)-C(16)	121.52(13)	C(18)-C(19)-H(19)	119.5
C(13)-C(14)-C(15)	121.17(12)	C(20)-C(19)-H(19)	119.5
C(13)-C(14)-H(14)	119.4	C(21)-C(20)-C(19)	117.38(12)
C(15)-C(14)-H(14)	119.4	C(21)-C(20)-C(23)	121.15(13)
C(14)-C(15)-C(10)	122.30(12)	C(19)-C(20)-C(23)	121.45(14)
C(14)-C(15)-H(15)	118.9	C(20)-C(21)-C(22)	121.44(13)
C(10)-C(15)-H(15)	118.9	C(20)-C(21)-H(21)	119.3
C(13)-C(16)-H(16A)	109.5	C(22)-C(21)-H(21)	119.3
C(13)-C(16)-H(16B)	109.5	C(21)-C(22)-C(17)	122.21(13)
H(16A)-C(16)-H(16B)	109.5	C(21)-C(22)-H(22)	118.9
C(13)-C(16)-H(16C)	109.5	C(17)-C(22)-H(22)	118.9
H(16A)-C(16)-H(16C)	109.5	C(20)-C(23)-H(23A)	109.5
H(16B)-C(16)-H(16C)	109.5	C(20)-C(23)-H(23B)	109.5
C(22)-C(17)-C(18)	115.61(11)	H(23A)-C(23)-H(23B)	109.5
C(22)-C(17)-B(1)	124.50(11)	C(20)-C(23)-H(23C)	109.5

H(23A)-C(23)-H(23C)	109.5
H(23B)-C(23)-H(23C)	109.

Symmetry transformations used to generate equivalent atoms: #1 -x+1,-y,-z+1

4.5 Computational methods

Computations were executed with the Gaussian 09 program package at the Research Center for Computing and Multimedia Studies, Hosei University.[7,11] The structures of **2**, anion part of **8** and **9**, and **10** were optimized at the B3PW91/6-31G(d) and B3PW91/6-31++G(d,p) level of theory.

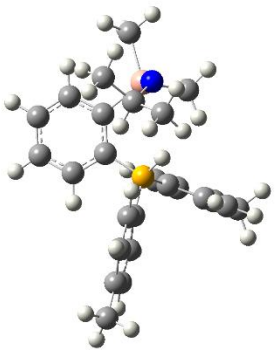

Total Energy (SCF Done) −1361.201444200 a.u.
Zero-point correction 0.504319 (Hartree/Particle)
Corrected Energy −1360.3028748 a.u.

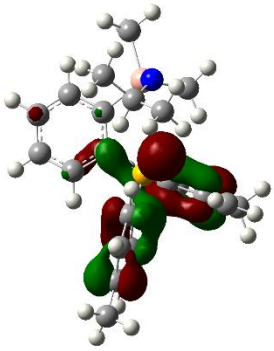

HOMO
−2.3753 eV

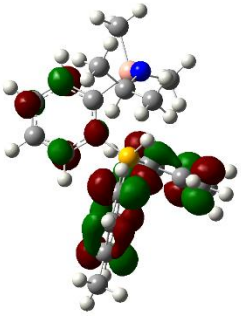

LUMO+2
3.3573 eV

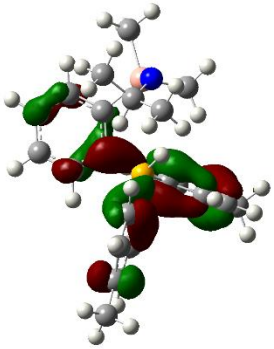

HOMO−1
−2.7862 eV

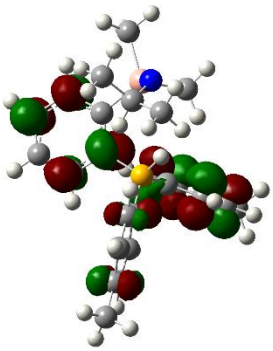

LUMO+1
3.3184 eV

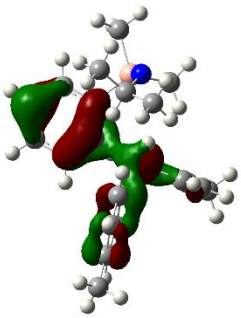

HOMO−2
−2.9179 eV

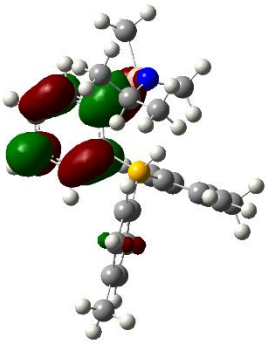

LUMO
2.9092 eV

Figure 5. Frontier molecular orbitals of anion part of **8**.

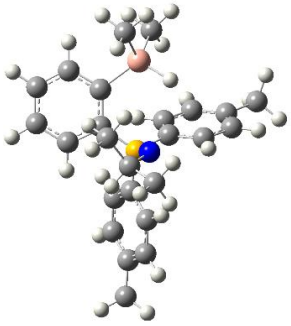

Total Energy (SCF Done) −1361.18097197 a.u.

Zero-point correction 0.503192 (Hartree/Particle)

Corrected Energy −1360.67777997 a.u.

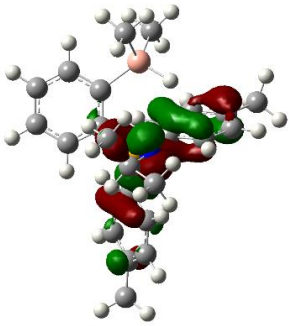

HOMO

−2.2106 eV

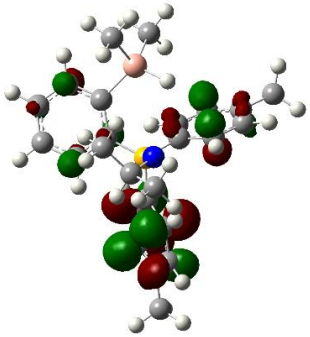

LUMO+2

3.3484 eV

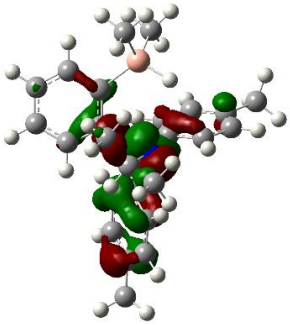

HOMO−1

−2.4610 eV

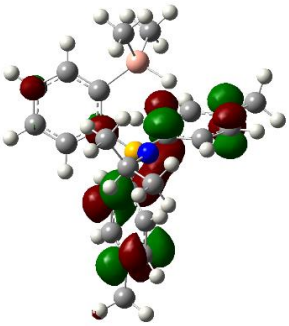

LUMO+1

3.2493 eV

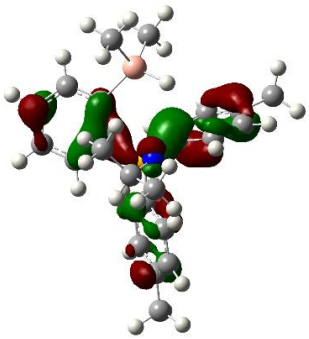

HOMO−2

−2.8139 eV

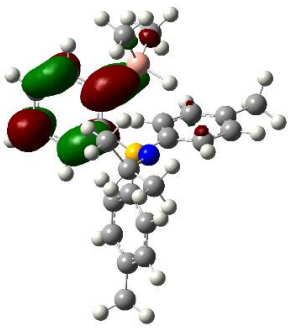

LUMO

2.9418 eV

Figure 6. Frontier molecular orbitals of anion part of **9**.

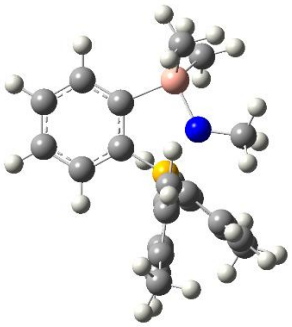

Total Energy (SCF Done) −1282.45555333 a.u.

Zero-point correction 0.439009 (Hartree/Particle)

Corrected Energy −1282.01654433 a.u.

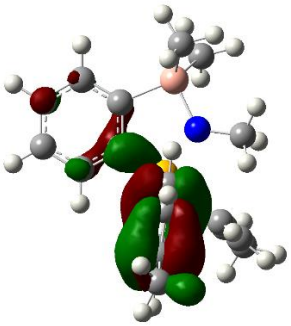

HOMO

−6.0276 eV

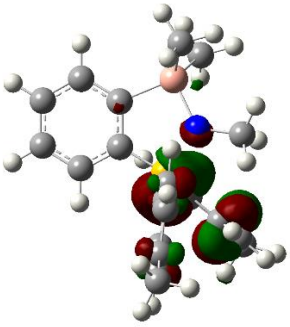

LUMO+2

−0.4030 eV

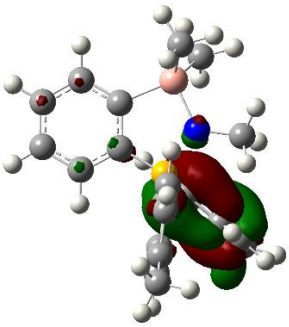

HOMO−1

−6.2673 eV

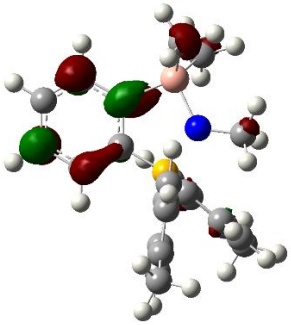

LUMO+1

−0.5752 eV

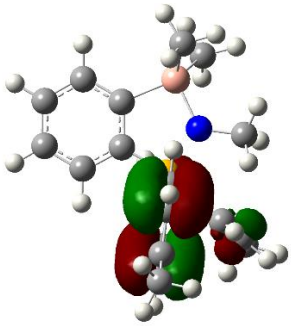

HOMO−2

−6.4589 eV

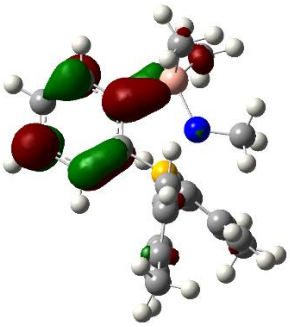

LUMO

−0.5946 eV

Figure 7. Frontier molecular orbitals of **10**.

Table 5. Selected second order perturbation theory analysis of fock matrix in NBO basis of **10**.[12]

Threshold for printing: 0.50 kcal/mol (Intermolecular threshold: 0.05 kcal/mol).

from unit 2 to unit 1		E(2)	E(j)-E(i)	F(i,j)
Donor NBO (i)	Acceptor NBO (j)	kcal/mol	a.u.	a.u.
95. LP (1) O 20	/ 98. LP*(1) B 25	1.54	0.44	0.025
95. LP (1) O 20	/320. RY*(3) B 25	0.22	1.14	0.014
95. LP (1) O 20	/326. RY*(9) B 25	0.09	1.69	0.011
95. LP (1) O 20	/327. RY*(10) B 25	0.08	1.98	0.012
95. LP (1) O 20	/320. RY*(3) B 25	0.22	1.14	0.014
95. LP (1) O 20	/326. RY*(9) B 25	0.09	1.69	0.011
95. LP (1) O 20	/327. RY*(10) B 25	0.08	1.98	0.012
95. LP (1) O 20	/625. BD*(1) B 25 - C 26	1.76	0.81	0.034
95. LP (1) O 20	/626. BD*(1) B 25 - C 36	1.60	0.81	0.032
95. LP (1) O 20	/ 98. LP*(1) B 25	16.20	0.50	0.082
95. LP (1) O 20	/319. RY*(2) B 25	0.91	1.22	0.032
96. LP (2) O 20	/320. RY*(3) B 25	0.13	1.20	0.012
96. LP (2) O 20	/321. RY*(4) B 25	0.27	1.55	0.019
96. LP (2) O 20	/322. RY*(5) B 25	0.07	0.95	0.008
96. LP (2) O 20	/324. RY*(7) B 25	0.20	1.93	0.019

96. LP (2) O 20	/325. RY*(8) B 25	0.09	2.00	0.013
96. LP (2) O 20	/326. RY*(9) B 25	0.06	1.75	0.010
96. LP (2) O 20	/327. RY*(10) B 25	0.18	2.04	0.018
96. LP (2) O 20	/328. RY*(11) B 25	0.08	1.67	0.011
96. LP (2) O 20	/329. RY*(12) B 25	0.08	2.05	0.012
96. LP (2) O 20	/330. RY*(13) B 25	0.08	3.27	0.015
96. LP (2) O 20	/331. RY*(14) B 25	0.07	2.50	0.013
96. LP (2) O 20	/625. BD*(1) B 25 - C 26	0.84	0.87	0.026
96. LP (2) O 20	/626. BD*(1) B 25 - C 36	0.43	0.87	0.018
97. LP (3) O 20	/318. RY*(1) B 25	0.16	1.59	0.015
97. LP (3) O 20	/319. RY*(2) B 25	0.57	1.54	0.029
97. LP (3) O 20	/320. RY*(3) B 25	0.10	1.53	0.012
97. LP (3) O 20	/323. RY*(6) B 25	0.06	1.25	0.008
97. LP (3) O 20	/324. RY*(7) B 25	0.07	2.25	0.012
97. LP (3) O 20	/325. RY*(8) B 25	0.12	2.32	0.016
97. LP (3) O 20	/327. RY*(10) B 25	0.08	2.37	0.013
97. LP (3) O 20	/330. RY*(13) B 25	0.07	3.59	0.015
97. LP (3) O 20	/625. BD*(1) B 25 - C 26	0.54	1.20	0.024
97. LP (3) O 20	/626. BD*(1) B 25 - C 36	0.52	1.19	0.024

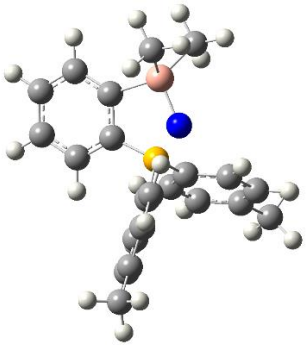

Total Energy (SCF Done) −1242.22003275 a.u.
Zero-point correction 0.397644 (Hartree/Particle)
Corrected Energy −1242.08749470 a.u.

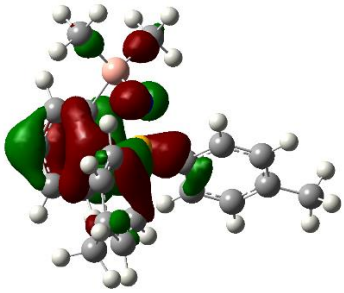

HOMO
−2.7630 eV

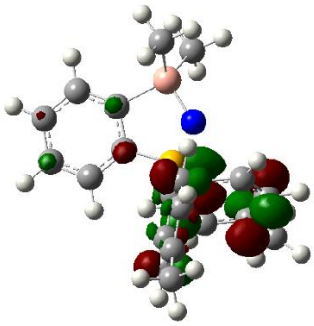

LUMO+2
−2.1581 eV

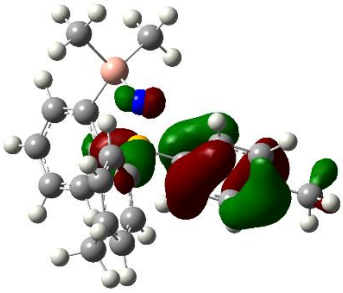

HOMO−1
−2.9081 eV

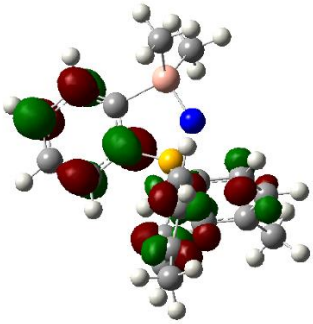

LUMO+1
−2.2234 eV

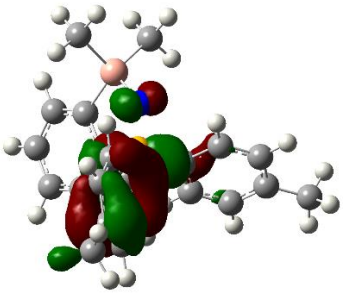

HOMO−2
−2.9516 eV

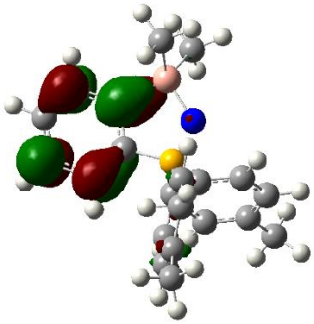

LUMO
−2.2645 eV

Figure 8. Frontier molecular orbitals of anion part of **13** and **14**.

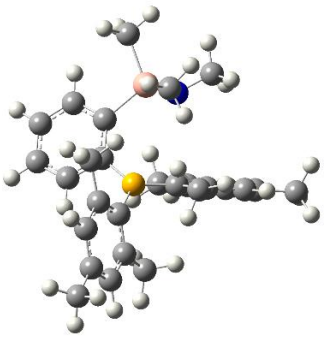

Total Energy (SCF Done) −1439.20881580 a.u.
Zero-point correction 0.548973 (Hartree/Particle)
Corrected Energy −1438.6598428 a.u.

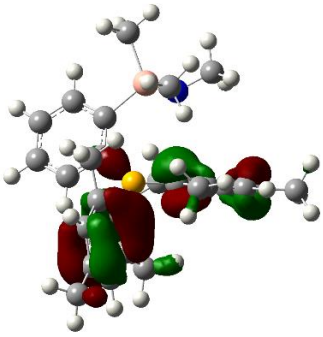

HOMO
−6.2210 eV

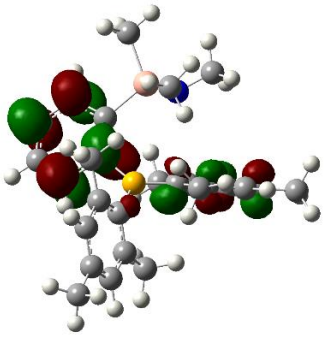

LUMO+2
−0.4090 eV

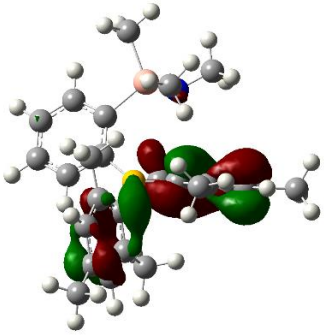

HOMO−1
−6.3160 eV

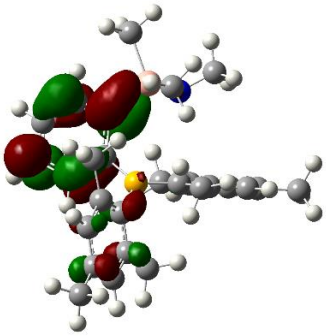

LUMO+1
−0.6313 eV

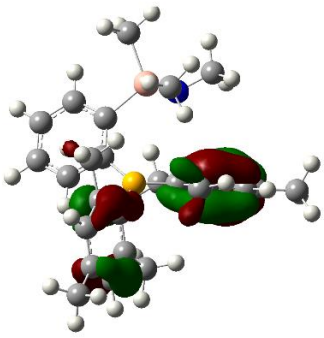

HOMO−2
−6.3787 eV

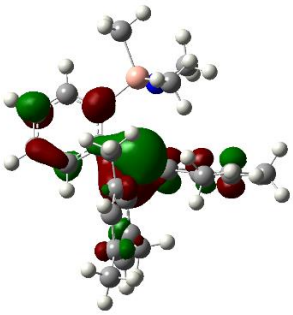

LUMO
−1.9222 eV

Figure 9. Frontier molecular orbitals of **2** (R = Me).

References

(1) As reviews: (a) Yamamoto, H. *Lewis Acid Reagents A Practical Approach;* Oxford University Press, New York, USA, 1999. (b) Ishihara, K.; Yamamoto, H. Arylboron Compounds as Acid Catalysts in Organic Synthetic Transformations. *Eur. J. Org. Chem.* **1999**, 527–538. (c) Chen, E. Y. -X.; Marks, T. J. Cocatalysts for Metal-Catalyzed Olefin Polymerization: Activators, Activation Processes, and Structure−Activity Relationships. *Chem. Rev.* **2000**, *100*, 1391–1434.

(2) (a) Parks, D. J.; Piers, W. E. Tris(pentafluorophenyl)boron-Catalyzed Hydrosilation of Aromatic Aldehydes, Ketones, and Esters. *J. Am. Chem. Soc.* **1996**, *118*, 9440–9441. (b) Parks, D. J.; Blackwell, J. M.; Piers, W. E. Studies on the Mechanism of $B(C_6F_5)_3$-Catalyzed Hydrosilation of Carbonyl Functions. *J. Org. Chem.* **2000**, *65*, 3090–3098. (c) Blackwell, J. M.; Morrison, D. J.; Piers, W. E. $B(C_6F_5)_3$ catalyzed hydrosilation of enones and silyl enol ethers. *Tetrahedron*, **2002**, *58*, 8247–8254.

(3) (a) Rendler, S.; Oestreich, M. Conclusive Evidence for an S_N2-Si Mechanism in the $B(C_6F_5)_3$-Catalyzed Hydrosilylation of Carbonyl Compounds: Implications for the Related Hydrogenation. *Angew. Chem. Int. Ed.* **2008**, *47*, 5997–6000. (b) Hog, D. T.; Oestreich, M. $B(C_6F_5)_3$-Catalyzed Reduction of Ketones and Imines Using Silicon-Stereogenic Silanes: Stereoinduction by Single-Point Binding. *Eur. J. Org. Chem.* **2009**, 5047–5056. (c) Mewald, M.; Oestreich, M. Illuminating the Mechanism of the Borane-Catalyzed Hydrosilylation of Imines with Both an Axially Chiral Borane and Silane. *Chem. Eur. J.* **2012**, *18*, 14079–14084.

(4) (a) Köster, R.; Seidel, G.; Wrackmeyer, B. Organosubstituierte 2,5-Dihydro-1,2,5-oxoniasilaboratole Charakterisierung und Reaktivität. *Chem. Ber*. **1991**, *124*, 1003–1016. (b) Wrackmeyer, B.; Suβ, J.; Milius, W. 2,5-Dihydro-1,2,5-azoniasilaboratole Derivatives-Useful Starting Materials in Heterocyclic Synthesis. *Chem. Ber.* **1996**, *129*, 147–153. (c) Wrackmeyer, B.; Milius, W.; Tok, O. L. Reaction of Alkyn-1-yl(diorganyl)silanes with 1-Boraadamantane: Si−H−B Bridges Confirmed by the Molecular Structure in the Solid State and in Solution. *Chem. Eur. J*. **2003**, *9*, 4732–4738.

(5) (a) Reaction with alcohols: Kawachi, A.; Zaima, M.; Tani, A.; Yamamoto, Y. Dehydrogenative Condensation of (*o*-Borylphenyl)hydrosilane with Alcohols and Amines. *Chem. Lett.* **2007**, *36*, 362–363. (b) Reaction with KF: Kawachi, A.; Morisaki, H.; Tani, A.; Zaima, M.; Yamamoto, Y. Reaction of *o*-$(HSiR_2)(BMes_2)C_6H_4$ with a fluoride ion: Fluoride attack at silicon and hydride transfer from silicon to boron to form F-Si⋯H-B interaction. *Heteroatom Chem*, **2011**, *22*, 471–475. (c) H-Ar Ligand Exchange: Kawachi, A.; Morisaki, H.; Nishioka, N.; Yamamoto, Y. Intramolecular H-Ar Ligand Exchange between Silicon and Boron: Functionality Transfer of Si-H to B-H. *Chem. Asian. J*. **2012**, *7*, 546–553. (d) Formation of Si−O−B linkage: Kawachi, A.; Zaima, M.; Yamamoto, Y. Intramolecular Reaction of Silanol and Triarylborane: Boron-Aryl Bond Cleavage and Formation of a Si−O−B Heterocyle. *Organometallics* **2008**, *27*, 4691–4096.

(6) Katz, H. E. Anion complexation and migration in (8-silyl-1-naphthyl)boranes. Participation of hypervalent silicon. *J. Am. Chem. Soc*. **1986**, *108*, 7640–7645.

(7) Gaussian 09, rev. B.01: Frisch, M. J.; Trucks, G. W.; Schlegel, H. B.; Scuseria, G. E.; Robb, M. A.; Cheeseman, J. R.; Scalmani, G.; Barone, V.; Mennucci, B.; Petersson, G. A.; Nakatsuji, H.; Caricato, M.; Hratchian, X.; Li, H. P.; Izmaylov, A. F.; Bloino, J.; Zheng, G.; Sonnenberg, J. L.; Hada, M.; Ehara, M.; Toyota, K.; Fukuda, R.; Hasegawa, J.; Ishida, M.; Nakajima, T.; Honda, Y.; Kitao, O.; Nakai, H.; Vreven, T.; Montgomery, Jr. J. A.; Peralta, J. E.; Ogliaro, F.; Bearpark, M.; Heyd, J. J.; Brothers, E.; Kudin, K. N.; Staroverov, V. N.; Kobayashi, R.; Normand, J.; Raghavachari, K.; Rendell, A.; Burant, J. C.; Iyengar, S. S.; Tomasi, J.; Cossi, M.; Rega, N.; Millam, J. M.; Klene, M.; Knox, J. E.; Cross, J. B.; Bakken, V.; Adamo, C.; Jaramillo, J.; Gomperts, R.; Stratmann, R. E.; Yazyev, O.; Austin, A. J.; Cammi, R.; Pomelli, C.; Ochterski, J. W.; Martin, R. L.; Morokuma, K.; Zakrzewski, V. G.; Voth, G. A.; Salvador, P.; Dannenberg, J. J.; Dapprich, S.; Daniels, A. D.; Farkas, Ö.; Foresman, J. B.; Ortiz, J. V.; Cioslowski, J.; and Fox, D. J. Gaussian, Inc., Wallingford CT, 2010.

(8) (a) SIR97: Altomare, A.; Burla, M. C.; Camalli, M.; Cascarano, G.; Giacovazzo, C.; Guagliardi, A.; Moliterni, A. G. G.; Polidori, G.; Spagna, R.; *J. Appl. Crystallogr.* **1999**, *32*, 115. (b) SHELX-97: Sheldrick, G. University of Göttingen, Göttingen, Germany, 1997.

(9) Emsley, J. *The Elements, 2nd Edition*; Clarendon, Oxford, UK, 1991.

(10) Silyloxonium ions: (a) Olah, G. A.; Li, X.-Y.; Wang, Q.-J.; Rusul, G.; Prakash, G. K. S. Trisilyloxonium Ions: Preparation, NMR Spectroscopy, Ab Initio/IGLO Studies, and Their Role in Cationic Polymerization of Cyclosiloxanes. *J. Am. Chem. Soc.* **1995**, *117*, 8962–8966. (b) Kira, M.; Hino, T.; Sakurai, H. Chemistry of organosilicon compounds. 292. An NMR study of

the formation of silyloxonium ions by using tetrakis[3,5-bis(trifluoromethyl)phenyl]borate as counteranion. *J. Am. Chem. Soc*. **1992**, *114*, 6697–6700. (c) Kira, M.; Hino, T.; Sakurai, H. Siloxycarbenium Tetrakis[3,5-bis(trifluoromethyl)phenyl]borates and Their Role in Reactions of Ketones with Nucleophiles. *Chem. Lett.* **1992**, 555–558. (d) Driess, M.; Barmeyer, R.; Monsé, C.; Merz, K. $E(SiMe_3)_4^+$ Ions (E = P, As): Persilylated Phosphonium and Arsonium Ions. *Angew. Chem. Int. Ed*. **2001**, *40*, 2308–2310. (e) Kordts, N.; Künzler, S.; Rathjen, S.; Sieling, T.; Großekappenberg, H.; Schmidtmann, M.; Müller, T. Silyl Chalconium Ions: Synthesis, Structure and Application in Hydrodefluorination Reactions. *Chem. Eur. J.* **2017**, *23*, 10068–10079. (f) Bläsing, K.; Labbow, R.; Michalik, D.; Reiß, F.; Schulz, A.; Villinger, A.; Walker, S. On Silylated Oxonium and Sulfonium Ions and Their Interaction with Weakly Coordinating Borate Anions. *Chem. Eur. J.* **2020**, *26*, 1–14.

(11) NBO Version 3.1; Glendening, E. D.; Reed, A. E.; Carpenter, J. E.; Weinhold, F.

(12) Second order perturbation theory analysis of fock matrix in NBO basis: LP_O = lone pair at oxygen atom; LP^*_B: vacant orbital at boron atom.

(13) Formation of Si−O−B linkage: Brzozowska, A.; Ćwik, P.; Durka, K.; Kliś, T.; Laudy, A. E.; Luliński, S.; Serwatowski, J.; Tyski, S.; Urban, M.; Wróblewski, W. Benzosiloxaboroles: Silicon Benzoxaborole Congeners with Improved Lewis Acidity, High Diol Affinity, and Potent Bioactivity. *Organometallics* **2015**, *34*, 2924–2932.

Chapter 3

Synthesis, Reactions, and Photophysical Properties

of *o*-(Alkoxysilyl)(borafluorenyl)benzenes

Abstract

The synthesis, reactions, and photophysical properties of *o*-(alkoxysilyl)(borafluorenyl)benzenes **4** are reported. Compounds **4** were prepared by the reaction of *o*-(silyl)(lithio)benzenes **6** with (alkoxy)borafluorenes **7**. The C−O bonds in **4** were activated by intramolecular coordination of the oxygen atom to the boron atom, as confirmed by reactions with nucleophiles and density functional theory (DFT) calculations. Compounds **4** exhibited absorption at 316 and 279 nm and emission at 536 and 496 nm with a large Stokes shift. DFT calculations were performed to elucidate the molecular orbitals and photophysical properties of **4**.

1. Introduction

Borafluorenes are the boron analogues of fluorenes in which the vacant p orbital on the boron is incorporated into the conjugated biphenyl π system.[1,2] Borafluorenes are more Lewis acidic and have higher electron-accepting abilities compared to the structurally similar, non-annulated boranes. Borafluorenes such as **I** (Chart 1) exhibit fluorescence, and thus the combination of their Lewis acidity and fluorescence properties allow the construction of sensors for Lewis bases and fluoride ions.[3,4]

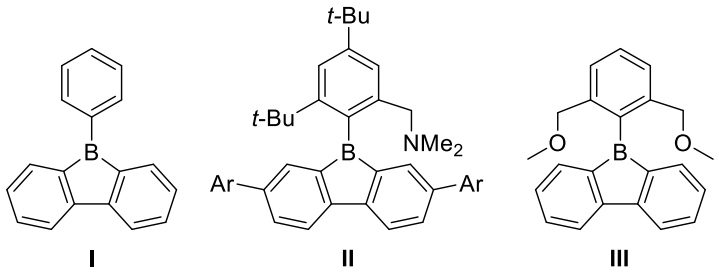

Chart 1. Phenyl-borafluorene **I** and coordinated borafluorenes **II** and **III**.

Coordination of a donor to the vacant p orbital on the boron atom is expected to cause significant changes in the photophysical properties of **I**. Chujo et al. prepared borafluorene **II** with intramolecular amine coordination.[5] Compound **II** exhibits dual emission due to its coordinated structure in the ground state and non-coordinated structure in the excited state. Rupar et al. also reported the photophysical properties of oxy-coordinated borafluorene **III** and its related species.[6]

Recently, the author prepared *o*-(alkoxysilyl)(diarylboryl)benzenes **1**–**3**, in which an alkoxysilyl group and a diarylboryl group are linked through an *o*-phenylene skeleton (Chart 2).[7,8] In contrast to (silyl)borylbenzene **1** bearing bulky mesityl groups on the boron atom, (silyl)borylbenzenes **2** and **3** bearing less sterically demanding groups (*p*-tolyl and *p*-*tert*-butylphenyl) on the boron atom exhibit C−O bond activation owing to the intramolecular interaction between the oxygen atom and the boron atom. The C−O bonds in **2** and **3** are cleaved with nucleophiles such as 1,4-diazabicyclo[2.2.2]octane (DABCO) and KF/18-crown-6.

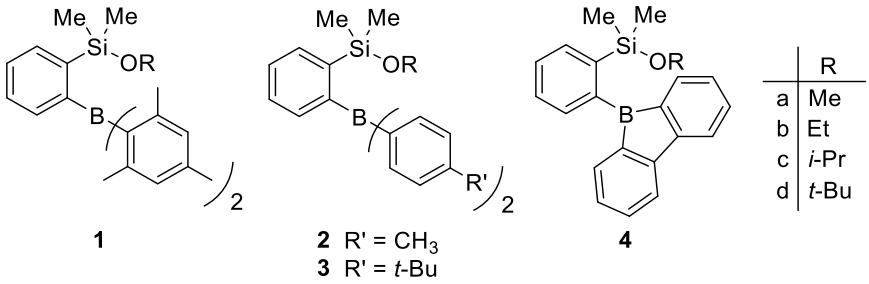

Chart 2. *o*-(Alkoxysilyl)(diarylboryl)benzenes **1**–**4**.

The author herein reports the preparation of *o*-(alkoxysilyl)(borafluorenyl)benzenes **4** (R = Me (**a**), Et (**b**), *i*-Pr (**c**), and *tert*-Bu (**d**)), in which a borafluorenyl group is introduced as a diarylboryl unit (Chart 2). My main focus in this study was to establish whether the planar borafluorenyl moiety increases the strength of the coordination of the oxygen atom to the boron atom and also how the photophysical properties of **4** change compared to those of the parent borafluorene **I**.

2. Results and discussion

2.1 Synthesis of *o*-[(alkoxy)silyl](borafluorenyl)benzenes **4**

o-[(Alkoxy)silyl](borafluorenyl)benzenes **4** were prepared in a manner similar to that presented in Chapter 3 (Scheme 1).[8] The reaction of *o*-(dimethylsilyl)bromobenzene (**5**) with *tert*-BuLi in Et_2O at −78 °C provided *o*-silyl(lithio)benzene **6**, which was reacted with 9-isopropoxy-9-borafluorene **7c** to form lithium [(isopropoxysilyl)phenyl]hydroborate **8c**.[9] It is plausible that the initially formed (isopropoxy)borate **9c** underwent intramolecular hydride-isopropoxide exchange to form **8c**. Treatment of **8c** with Me_3SiCl *in situ* afforded **4c**. *tert*-Butyloxysilyl derivative **4d** was prepared in a similar manner to **4c**.

The reactions of **4c** with MeOH and EtOH provided methoxysilane **4a** and ethoxysilane **4b**, respectively (Scheme 2). In contrast, **4a** did not react with bulky ROH (R = Et, *i*-Pr, *tert*-Bu) at all.

Scheme 1. Preparation of **4c** and **4d**.

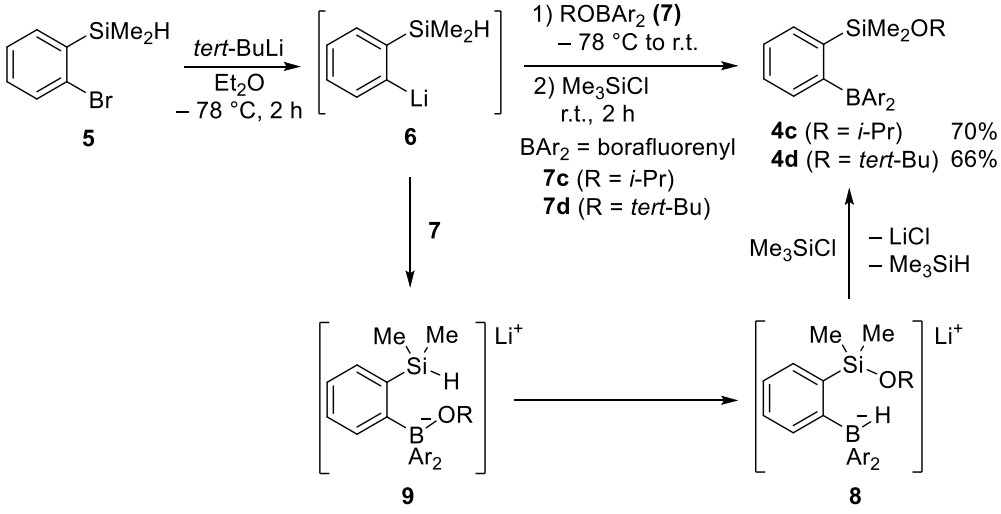

Scheme 2. Reactions of **4c** with alcohols to prepare **4a** and **4b**.

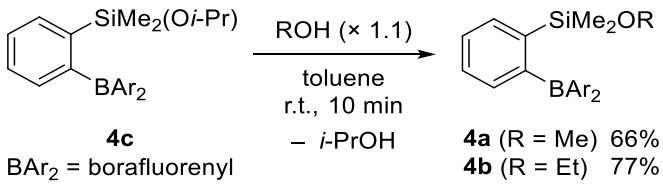

2.2 C−O bond activation in *o*-[(alkoxy)silyl](borafluorenyl)benzenes **4**

As previously observed in **2** and **3**,[10] C−O bond activation was observed in **4**. **4c** was refluxed with DABCO in THF for 12 h to form silyloxyborate-(*i*-Pr-DABCO)$^+$ complex **10** as a white precipitate, which was isolated by filtration and recrystallization from DMSO in 86% yield (Scheme 3). The ^{11}B NMR shift (δ = 4.6) and ^{29}Si NMR shift (δ = 12.2) of **10** are consistent with those of the DABCO complex derived from **2a** (δ(^{11}B) = 3.0; δ(^{29}Si) = 9.1).

Treatment of **4a** and **4c** with KF in the presence of 18-crown-6 led to C−O bond cleavage to form **11** (Scheme 4).

Scheme 3. C−O bond cleavage in **4c** with DABCO.

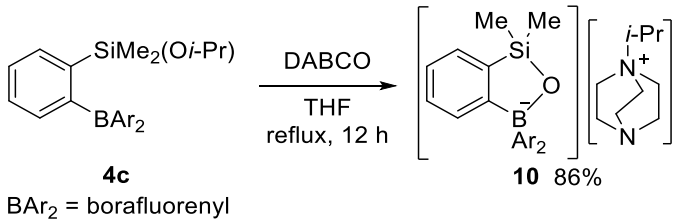

Scheme 4. C−O bond cleavage in **4a** and **4c** with KF/18-crown-6.

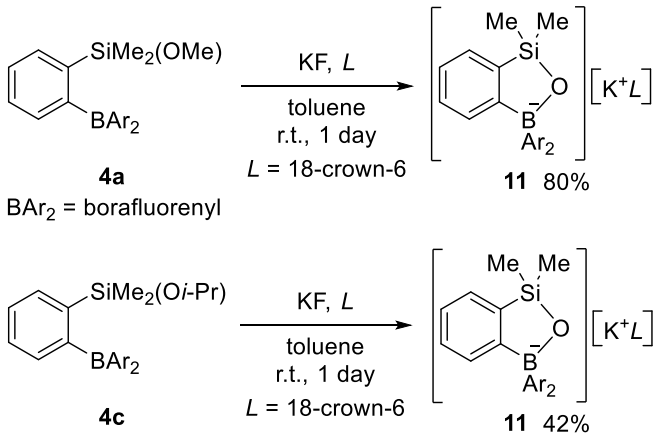

2.3 NMR spectra of **4**

The ^{11}B and ^{29}Si NMR shifts are good indicators of the coordination strength of the oxygen atom to the boron atom in **4** because the coordination increases the electron density on the boron atom and decreases that on the silicon atom.

The ^{11}B NMR signal of **4c** (δ = 14.8) is shifted upfield compared to that of the corresponding signal of **2c** (δ = 30.9), while the ^{29}Si NMR signal of **4c** (δ = 29.0) is shifted downfield compared to the corresponding signal of **2c** (δ = 20.0). With decreasing steric bulkiness of the alkoxy groups (**4d** > **4c** > **4b** > **4a**), the ^{11}B NMR signal is shifted upfield and the ^{29}Si NMR signal is shifted downfield, as shown in Table 1.

Table 1. ^{11}B and ^{29}Si NMR shifts of *o*-(silyl)(diarylboryl)benzenes **2** and **4**.

	4a	**4b**	**4c**	**4d**	**2a**	**2b**	**2c**
R	Me	Et	*i*-Pr	*tert*-Bu	Me	Et	*i*-Pr
δ(^{11}B)	12.7	14.2	14.8	23.6	17.4	20.0	30.9
δ(^{29}Si)	36.0	33.7	29.0	23.7	33.1	29.5	20.0

2.4 UV and fluorescence spectra of **4**

The UV-Vis absorption and fluorescence spectra of **4** were obtained, as shown in Figure 1 and Table 2. Absorption by **4a** in CH_2Cl_2 is observed at 279 nm (logε = 3.93) with a shoulder at 316 nm (logε = 0.71). **4b**, **4c**, and **4d** exhibit absorption and fluorescence spectra very similar to that of **4a**. As a reference, the absorption and fluorescence spectra of 9-phenyl-borafluorene (**I**) are also shown in Figure 2. The intense, short-wavelength absorption may be due to the biphenyl π to π* transition in the borafluorenyl moiety and the weak, long-wavelength absorption may be attributed to the transition from the biphenyl π to the vacant p orbital on the boron atom.[4a-c] The differences in absorption spectra between **4** and **I** can be explained by the fact that the oxygen atom is coordinated to the boron atom in **4** and the electron density is donated into the vacant p orbital on the boron atom.

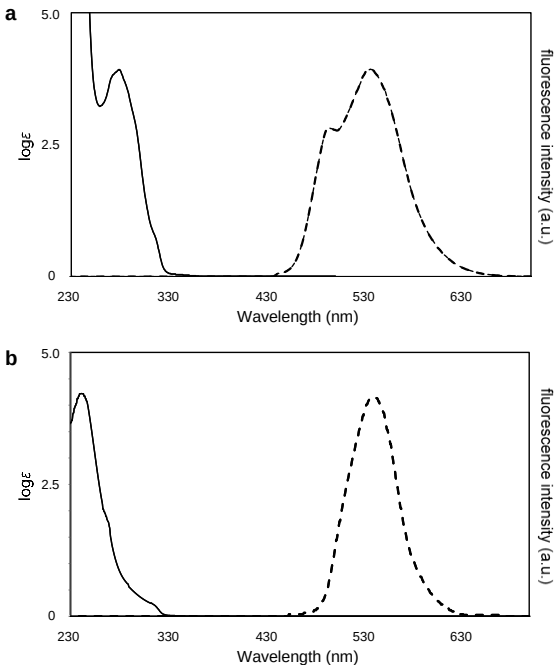

Figure 1. UV-Vis absorption (solid lines) and fluorescence spectra (dashed lines) for (a) **4a** and (b) **I** recorded in CH_2Cl_2 under an argon atmosphere.

Table 2. Experimental and calculated UV-Vis absorption and emission spectra of **4**.

	experimental			calculated	
compound	absorption λ_{max}, nm (log ε)	emission, nm [Φ_f]	Stokes shift, eV [cm^{-1}]	absorption λ_{max}, nm (oscillator strength)	emission, nm
4a	279 (3.93)	496	2.13 [17200]	290 (0.14)	548
	316 (0.71)	536 [0.02]		307 (0.02)	
4b	279 (3.91)	496	2.13 [17200]	290 (0.14)	
	316 (0.71)	536		307 (0.02)	
4c	279 (3.88)	496	2.13 [17200]	290 (0.14)	
	316 (0.71)	536		306 (0.02)	
4d	282 (3.83)	494	2.07 [16700]	258 (0.63)	548
	316 (0.71)	533 [0.02]		280 (0.07)	
				321 (0.01)	

Fluorescence in **4a** is observed at 536 nm with a shoulder at 496 nm (Figure 2 and Table 2). On the basis of the absorption at 279 nm and the emission at 536 nm, the fluorescence of **4a** has a large Stokes shift of 17,200 cm^{-1}. **4b**, **4c**, and **4d** exhibit similar fluorescence spectra to that of **4a**. The large Stokes shift in **4** may be attributed to the bond-cleavage-induced intramolecular charge transfer (BICT) due to the tetracoordinate ground state (coordination from O to C) and the tricoordinate (non-

coordination) excited state. BICT was recently proposed by Chujo et al. to explain the dual emission in **II**.[5] Rupar et al. also reported that BICT occurs in **III**.[6] The absorption and emission spectra of **4** closely resemble those of **II** and **III**, which indicates that **4** undergoes coordination of the oxygen atom to the boron center in the ground state and the dissociation of the oxygen atom in the excited state.[11,12] The quantum yield of **4** (Φ_f = 0.02) is similar to those **II** and **III** and low compared to that of **I** (Φ_f = 0.14),[13] which can be attribute to the inefficient process of the oxygen atom in the excited state.

2.5 DFT calculations of **4**

In order to gain further insight into **4**, density functional theory (DFT) calculations were carried out at the B3LYP/DGDZVP2 level of theory.[14] The optimized structure of **4a** is shown in Figure 2 and the molecular orbitals of **4a** and **I** as comparison are shown in Figure 3.

The plane of the borafluorenyl group is orthogonal to the *o*-phenylene skeleton. The O⋯B interatomic distances in **4a**–**4c** (1.689–1.705 Å) are slightly shorter than that of **2a** (1.751 Å), whereas that in **4d** is much longer (2.800 Å). The boron atom of **4a** adopts an intermediate geometry between tetrahedral and trigonal planar; the bond angles around the boron atom (Σ(C−B−C)) add up to 340°. The obtained geometries around the boron atom and interatomic distances between the boron atom and the oxygen atom in **4** are very close to those in **III**.

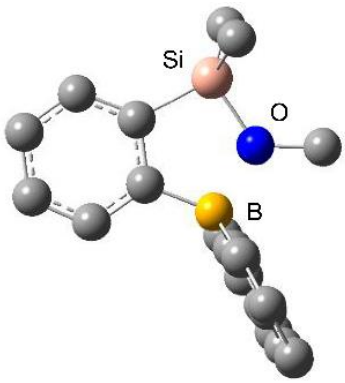

Figure 2. Optimized structure of **4a** at the B3LYP/DGDZVP2 level of theory.

The highest occupied molecular orbital (HOMO) in **4a** is delocalized over the carbon atoms of the borafluorene moiety and almost consistent with HOMO in **I** (Figure 3). The lowest unoccupied molecular orbital (LUMO) in **4a** is delocalized over the carbon atoms of the borafluorene moiety and looks similar to LUMO in **I**. However, LUMO in **4a** is deformed around the boron atom due to the contributions from the boron atom and the oxygen atom in the dative bond, which is quite similar to LUMO in **III**.[4c] The lone-pair electrons on the oxygen atom also contribute to HOMO−3.

The perturbation theory energy analysis in NBO basis reveals delocalization from the donor LP_O to the acceptor LP^*_B with the occupancy of 0.325:[15] the stabilization energy $E(2)$ was calculated to be 3.3 kcal/mol.

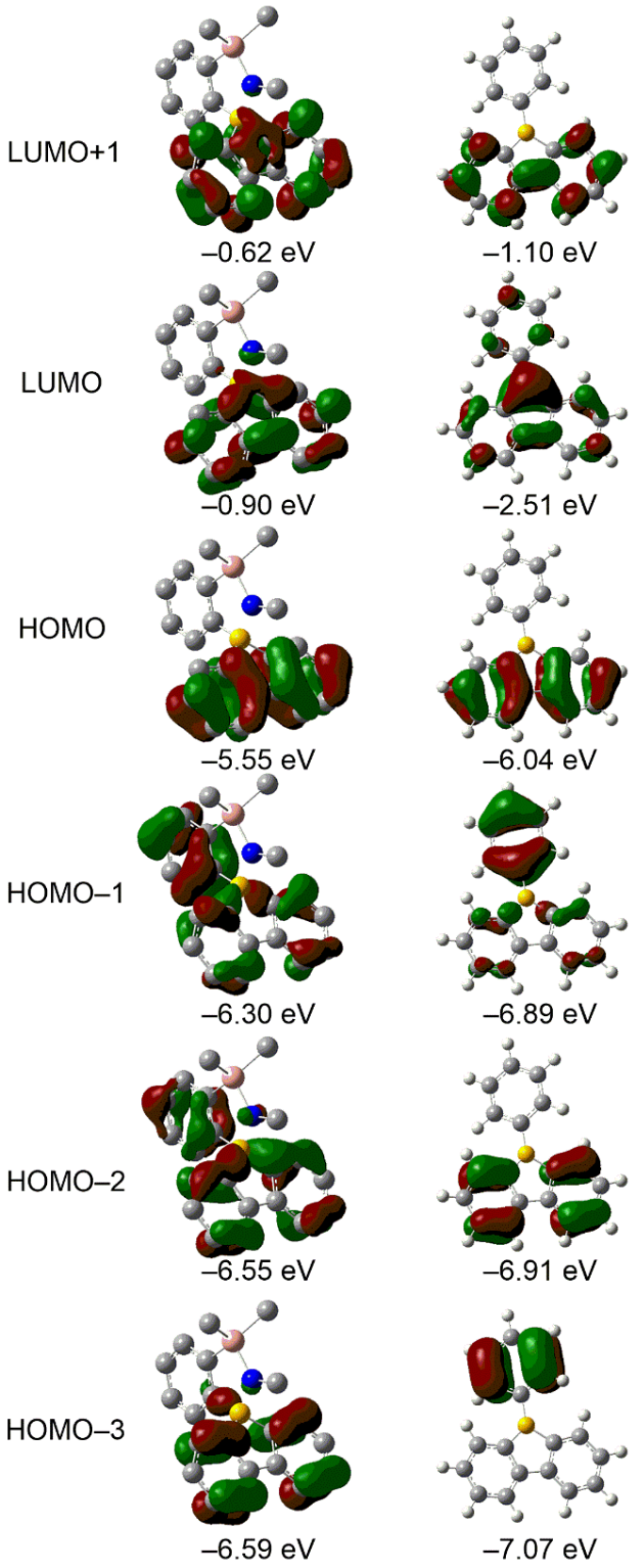

Figure 3. Frontier molecular orbitals of **4a** (left) and **I** (right) (isosurface value = 0.04).

Time dependent-DFT (TD-DFT) analysis was also performed. The calculated absorption wavelengths are in good agreement with those observed, as shown in Table 2. The calculated absorption at 290 nm ($f = 0.14$) (observed at 279 nm) in **4a** is attributable to transitions from HOMO−1 to LUMO and HOMO to LUMO+1 (π to π^* transition). The calculated absorption at 307 nm ($f = 0.02$) (observed at 316 nm) in **4a** is attributable to transitions from HOMO to LUMO and HOMO to LUMO+1. In the excited state, **4a** adopts a structure with a longer O⋯B distance (2.85 Å), which corresponds to the BICT mechanism.

3. Conclusions

o-[(Alkoxy)silyl](borafluorenyl)benzenes **4** bearing a borafluonenyl group were prepared. C−O bond activation was demonstrated in the reactions of **4** with an amine and fluoride. The coordination of the oxygen atom to the boron atom in **4** was indicated by the NMR, UV, and fluorescence spectra. The large Stokes shifts observed are ascribed to the BICT mechanism. The DFT calculation results for **4a** were in good agreement with the experimental data.

4. Experimental section

4.1 General considerations

^{1}H (400 MHz), ^{13}C (100 MHz), ^{11}B (128.3 MHz), and ^{29}Si (79.5 MHz) NMR spectra were recorded using a Bruker Avance III 400 spectrometer. ^{1}H and ^{13}C chemical shifts were referenced to the residual solvent signals in $CDCl_3$ ($\delta(^{1}H) = 7.26$, $\delta(^{13}C) = 77.00$), C_6D_6 ($\delta(^{1}H) = 7.20$, $\delta(^{13}C) = 128.00$), and DMSO-d_6 ($\delta(^{1}H) = 2.50$; $\delta(^{13}C) = 39.52$). ^{11}B and ^{29}Si chemical shifts were referenced to the external standards $BF_3{\cdot}OEt_2$ ($\delta = 0$), and tetramethylsilane ($\delta = 0$), respectively. Electron ionization mass spectra were recorded at 70 eV using a JEOL JMS-Q1000GC Mk II mass spectrometer, and elemental analyses were performed using a JSL MICRO CORDER JM10 elemental analyzer.

4.2 Materials

Chlorotrimethylsilane (Tokyo Chemical Industry Co., Ltd.) was treated with small pieces of sodium under a nitrogen atmosphere to remove dissolved HCl, and the supernatant was used. Potassium *tert*-butoxide in THF (Wako Pure Chemical Industries, Ltd.), *tert*-butyllithium in pentane (Kanto Chemical Co., Inc.) and DABCO (Tokyo Chemical Industry Co., Ltd.) were used as received. KF (Wako Pure Chemical Industries, Ltd.) was dried in vacuo at 100 °C, 18-crown-6 (Wako Pure Chemical Industries, Ltd.) was recrystallized from CH_3CN, and *o*-(dimethylsilyl)bromobenzene (**5**)[7] and 9-chloro-9-borafluorene[9] were prepared according to literature methods.

THF and Et_2O were distilled under a nitrogen atmosphere over sodium benzophenone ketyl.

Hexane and toluene were distilled under a nitrogen atmosphere over sodium. All reactions were carried out under an inert gas atmosphere.

4.3 Experimental details

9-Isopropoxy-9-borafluorene (7c). To a solution of 9-chloro-9-borafluorene (1.58 g, 8.00 mmol) in hexane (20 mL), *i*-PrOH (0.62 mL, 8.00 mmol) was added via a syringe at 0 °C. The reaction mixture was stirred at the same temperature for 1 h and then concentrated in vacuo to afford a pale yellow oil. Purification by bulb-to-bulb distillation (115–125 °C/0.75 mmHg) yielded **7c** (1.37 g, 77% yield) as a colorless oil. ^{1}H NMR (C_6D_6, δ) 1.23 (d, J = 6 Hz, 6H), 4.89 (sept, J = 6 Hz, 1H), 7.05 (dd, J = 7 Hz, J = 1 Hz, 2H), 7.17 (dd, J = 8 Hz, J = 1 Hz, 2H), 7.37 (d, J = 8 Hz, 2H), 7.61 (d, J = 7 Hz, 2H). ^{13}C{^{1}H} NMR (C_6D_6, δ) 24.70, 70.51, 119.93, 132.41, 132.64, 153.07 (signals corresponding to the *ipso* carbons in the borafluorenyl group and the *ipso* carbon in the phenyl group were not observed). ^{11}B NMR (C_6D_6, δ) 44.57 (br). Anal. Calcd for $C_{15}H_{15}BO$: C, 81.12; H, 6.81; Found: C, 80.92; H, 6.85.

9-(*tert*-Butoxy)-9-borafluorene (7d). To a solution of 9-chloro-9-borafluorene (1.58 g, 8.00 mmol) in hexane (40 mL), Potassium *tert*-butoxide in THF (1.0 mol/L, 7.5 mL, 7.50 mmol) was added at 0 °C and the reaction mixture was stirred at the same temperature for 1 h. After the solvents were removed in vacuo, the residue was dissolved in hexane (20 mL) and filtered. The filtrate was concentrated to approximately half the volume and the product was recrystallized at −18 °C to obtain **7d** (1.45 g, 82% yield) as colorless crystals. ^{1}H NMR (C_6D_6, δ) −1.44 (s, 9H), 7.07 (ddd, J = 7 Hz,

J = 7 Hz, J = 1 Hz, 2H), 7.17 (ddd, J = 8 Hz, J = 8 Hz, J = 1 Hz, 2H), 7.38 (d, J = 8 Hz, 2H), 7.74 (d, J = 7 Hz, 2H). $^{13}C\{^1H\}$ NMR (C_6D_6, δ) 30.60, 75.68, 119.83, 127.91, 132.46, 133.03, 153.25 (signals corresponding to the *ipso* carbons in the borafluorenyl group were not observed). ^{11}B NMR (C_6D_6, δ) 43.74 (br). Anal. Calcd for $C_{16}H_{17}BO$: C, 81.39; H, 7.26; Found: C, 81.11; H, 7.50.

***o*-[(Isopropoxy)dimethylsilyl](borafluorenyl)benzene (4c).** A solution of *tert*-BuLi in pentane (1.56 mol/L, 3.8 mL, 6.00 mmol) was added to a solution of **5** (645 mg, 3.00 mmol) in Et_2O (6 mL) at −78 °C over 4 min. After the reaction mixture was stirred at this temperature for 2 h, **7c** (666 mg, 3.00 mmol) in Et_2O (6 mL) was added over 5 min. The reaction mixture was stirred at the same temperature for 30 min and then allowed to warm to room temperature. Next, chlorotrimethylsilane (0.56 mL, 4.50 mmol) was added and the mixture was stirred for 2 h. After the solvents were removed in vacuo, the residue was dissolved in toluene (10 mL) and filtered. The filtrate was concentrated to approximately half the volume and the product was recrystallized at −18 °C to obtain **4c** (748 mg, 70% yield) as colorless crystals. ^1H NMR (C_6D_6, δ) 0.39 (s, 6H), 0.70 (d, J = 6 Hz, 6H), 4.08 (sept, J = 6 Hz, 1H), 7.10–7.20 (m, 3H), 7.22 (ddd, J = 8 Hz, J = 8 Hz, J = 1 Hz, 2H), 7.36–7.40 (m, 5H), 7.85 (d, J = 8 Hz, 2H). $^{13}C\{^1H\}$ NMR (C_6D_6, δ) 3.14, 23.54, 75.80, 119.96, 125.87, 127.05, 128.39, 129.30, 130.30, 130.37, 131.64, 135.15, 150.37 (signals corresponding to the *ipso* carbons in the borafluorenyl group and the *ipso* carbon in the phenyl group were not observed). ^{11}B NMR (C_6D_6, δ) 14.78 (br). $^{29}Si\{^1H\}$ NMR (C_6D_6, δ) 29.01. MS (EI) *m/z* 356 (M^+, 18), 313 (M^+−*i*-Pr, 61), 271 (M^+−*i*-Pr−2Me, 100). Anal. Calcd for $C_{23}H_{25}BOSi$: C, 77.52; H, 7.07; Found: C, 77.41; H, 7.27.

Hydroborate 8. A solution of *tert*-BuLi in pentane (1.56 mol/L, 3.8 mL, 6.00 mmol) was added to a solution of **5** (645 mg, 3.00 mmol) in Et_2O (6 mL) at −78 °C. After stirring at the same temperature for 2 h, **7c** (666 mg, 3.00 mmol) in Et_2O (6 mL) was added. The reaction mixture was stirred at this temperature for 30 min and then allowed to warm to room temperature. The solvent was removed in vacuo, and the residue was dissolved in toluene (20 mL) and filtered. The filtrate was concentrated to approximately half the volume and the product was recrystallized at −18 °C to obtain **8·Li(Et₂O)** (802 mg, 61% yield) as colorless crystals. ^{1}H NMR (C_6D_6, δ) 0.58 (t, J = 6 Hz, 6H, **Et₂O**), 0.67 (s, 6H), 0.88 (d, J = 6 Hz, 6H), 2.71 (q, J = 6 Hz, 4H, **Et₂O**), 3.98 (sept, J = 6 Hz, 1H), 7.17 (ddd, J = 8 Hz, J = 7 Hz, J = 1 Hz, 2H), 7.21–7.27 (m, 3H), 7.35–7.42 (m, 3H), 7.67–7.71 (m, 3H), 7.98 (d, J = 8 Hz, 2H). ^{13}C{^{1}H} NMR (C_6D_6, δ) 1.62, 14.08 (et₂o), 25.14, 65.28 (et₂o), 68.16, 119.92, 123.79, 126.04, 126.60, 129.77, 130.75, 132.79, 134.59, 140.92, 150.46 (signals corresponding to the *ipso* carbons in the borafluorenyl group and the *ipso* carbon in the phenyl group were not observed). ^{11}B NMR (C_6D_6, δ) −11.31 (d, $^1J_{B\text{-}H}$ = 67 Hz). ^{29}Si{^{1}H} NMR (C_6D_6, δ) 14.08. Anal. Calcd for $C_{27}H_{36}BLiO_2Si$: C, 73.97; H, 8.28; Found: C, 73.72; H, 8.48.

***o*-[(*tert*-Butoxy)dimethylsilyl](borafluorenyl)benzene (4d).** A solution of *tert*-BuLi in pentane (1.56 mol/L, 3.8 mL, 6.00 mmol) was added to a solution of **5** (645 mg, 3.00 mmol) in Et_2O (6 mL) at −78 °C over 4 min. After the reaction mixture was stirred at this temperature for 2 h, **7d** (708 mg, 3.00 mmol) in Et_2O (6 mL) was added over 3 min. The reaction mixture was stirred at the same temperature for 30 min and then allowed to warm to room temperature. Next, chlorotrimethylsilane (0.56 mL, 4.50 mmol) was added and the mixture was stirred for 2 h. After

the solvents were removed in vacuo, the residue was dissolved in toluene (20 mL) and filtered. The filtrate was concentrated to approximately half the volume and the product was recrystallized at −18 °C to obtain **4d** (733 mg, 66% yield) as colorless crystals. ^{1}H NMR (C_6D_6, δ) 0.50 (s, 6H), 1.03 (s, 9H), 6.93 (ddd, *J* = 8 Hz, *J* = 1 Hz, *J* = 1 Hz, 1H), 7.05 (ddd, *J* = 8 Hz, *J* = 8 Hz, *J* = 1 Hz, 1H), 7.12–7.20 (m, 3H), 7.31–7.36 (m, 3H), 7.42 (ddd, *J* = 8 Hz, *J* = 1 Hz, *J* = 1 Hz, 2H), 7.77 (ddd, *J* = 8 Hz, *J* = 1 Hz, *J* = 1 Hz, 2H). ^{13}C{^{1}H} NMR (C_6D_6, δ) 4.63, 30.68, 87.43, 119.94, 125.86, 127.17, 128.65, 129.29, 129.40, 130.01, 132.14, 135.56, 149.33 (signals corresponding to the *ipso* carbons in the borafluorenyl group and the *ipso* carbon in the phenyl group were not observed). ^{11}B NMR (C_6D_6, δ) 23.58 (br). ^{29}Si {^{1}H} NMR (C_6D_6, δ) 23.69. MS(EI) *m/z* 314 (M^+−*tert*-Bu, 100), 299 (M^+−*tert*-Bu−Me, 82), 257 (M^+−$SiMe_2$*tert*-Bu, 66). Anal. Calcd for $C_{24}H_{27}BOSi$: C, 77.83; H, 7.35; Found: C, 77.81; H, 7.52.

***o*-[(Methoxy)dimethylsilyl](borafluorenyl)benzene (4a).** To a solution of **4c** (713 mg, 2.00 mmol) in toluene (4.0 mL), MeOH (90 μL, 2.20 mmol) was added via a syringe at room temperature. The reaction mixture was stirred at the same temperature for 10 min and then concentrated in vacuo to afford a white solid. Recrystallization from toluene at −18 °C gave **4a** (431 mg, 66% yield) as colorless crystals. ^{1}H NMR (C_6D_6, δ) 0.17 (s, 6H), 2.65 (s, 3H), 7.16–7.19 (m, 3H), 7.23 (dd, *J* = 7 Hz, *J* = 1 Hz, 2H), 7.28 (ddd, *J* = 7 Hz, *J* = 2 Hz, *J* = 1 Hz, 2H), 7.37–7.41 (m, 3H), 7.85 (ddd, *J* = 7 Hz, *J* = 2 Hz, *J* = 1 Hz, 2H). ^{13}C{^{1}H} NMR (C_6D_6, δ) −1.19, 50.77, 119.59, 125.94, 127.20, 128.53, 129.81, 130.61, 130.82, 131.16, 134.30, 150.83(signals corresponding to the *ipso* carbons in the borafluorenyl group and the *ipso* carbon in the phenyl group were not observed). ^{11}B NMR (C_6D_6, δ)

12.74 (br). $^{29}Si\{^{1}H\}$ NMR (C_6D_6, δ) 36.02. MS(EI) *m/z* 328 (M^+, 100), 313 (M^+−Me, 31), 271 (M^+−OMe−2Me, 50). Anal. Calcd for $C_{21}H_{21}BOSi$: C, 76.83; H, 6.45; Found: C, 76.67; H, 6.60.

***o*-[(Ethoxy)dimethylsilyl](borafluorenyl)benzene (4b).** To a solution of **4c** (713 mg, 2.00 mmol) in toluene (4.0 mL), EtOH (0.13 mL, 2.20 mmol) was added via a syringe at room temperature. The reaction mixture was stirred at the same temperature for 10 min and then concentrated in vacuo to afford a white solid. Recrystallization from hexane at −18 °C gave **4b** (527 mg, 77% yield) as colorless crystals. ^{1}H NMR (C_6D_6, δ) 0.00 (s, 6H), 0.25 (t, *J* = 7 Hz, 2H), 3.06 (q, *J* = 7 Hz, 2H), 6.87–6.98 (m, 6H), 7.06 (d, *J* = 7 Hz, 2H), 7.10–7.15 (m, 3H), 7.59 (d, *J* = 8 Hz, 2H). $^{13}C\{^{1}H\}$ NMR (C_6D_6, δ) 0.34, 16.24, 63.76, 119.60, 125.92, 127.15, 128.44, 129.66, 130.56, 130.57, 131.38, 134.50, 150.52 (signals corresponding to the *ipso* carbons in the borafluorenyl group were not observed). ^{11}B NMR (C_6D_6, δ) 14.21 (br). $^{29}Si\{^{1}H\}$ NMR (C_6D_6, δ) 33.67. MS(EI) *m/z* 342 (M^+, 88), 313 (M^+−Et, 36), 271 (M^+−$SiMe_2OEt$, 100). Anal. Calcd for $C_{22}H_{23}BOSi$: C, 77.19; H, 6.77; Found: C, 77.01; H, 6.99.

Silyloxyborate-[(i-Pr-DABCO)$^+$] complex 10. A solution of **4c** (178 mg, 0.50 mmol) and DABCO (56 mg, 0.50 mmol) in THF (1 mL) was refluxed for 12 h. The solvent was removed in vacuo and the residue was recrystallized from DMSO at room temperature to obtain **10** (201 mg, 86% yield) as colorless crystals. ^{1}H NMR (DMSO-d_6, δ) 0.28 (s, 6H), 1.14 (d, *J* = 6 Hz, 6H), 2.87 (t, *J* = 7 Hz, 6H), 3.08 (t, *J* = 7 Hz, 6H), 3.34 (sept, *J* = 6 Hz, 1H), 6.32 (d, *J* = 7 Hz, 1H), 6.72 (dd, *J* = 7 Hz, *J* = 1 Hz, 1H), 6.71–6.74 (m, 3H), 6.94–6.97 (m, 4H), 7.33 (d, *J* = 7 Hz, 1H), 7.50 (d, *J* = 7 Hz, 2H). $^{13}C\{^{1}H\}$ NMR (DMSO-d_6, δ) 3.09, 15.56, 44.62, 48.40 (t, *J* = 3 Hz), 64.73 (t, *J* = 3 Hz), 117.64,

122.57, 124.06, 124.76, 126.17, 128.42, 128.76, 129.80, 145.02, 147.79 (signals corresponding to the *ipso* carbons in the borafluorenyl group and the *ipso* carbon in the phenyl group were not observed). ^{11}B NMR (DMSO-d_6, δ) 4.61 (br). ^{29}Si{^{1}H} NMR (DMSO-d_6, δ) 12.21. Anal. Calcd for $C_{29}H_{37}BN_2OSi$: C, 74.34; H, 7.96; N, 5.98 Found: C, 74.09; H, 8.20; N, 6.11.

Silyloxyborate-[K(18-crown-6)$^+$] complex 11. A solution of **4a** (164 mg, 0.20 mmol), 18-crown-6 (53 mg, 0.20 mmol), and KF (12 mg, 0.20 mmol) in toluene (0.6 mL) was stirred at room temperature for 12 h. Subsequently, the solvent was removed in vacuo. The resulting white solid was dissolved in THF (0.5 mL), and toluene (1 mL) was slowly added to the solution. The resulting two-layer solution was allowed to stand at room temperature for a day to obtain **11** (99 mg, 80% yield) as colorless crystals. ^{1}H NMR ($CDCl_3$, δ) 0.44 (s, 6H), 3.33 (s, 24H, crown), 6.54 (d, J = 7 Hz, 1H), 6.89 (ddd, J = 7 Hz, J = 7 Hz, J = 1 Hz, 1H), 6.94 (ddd, J = 7 Hz, J = 7 Hz, J = 1 Hz, 2H), 6.98 (ddd, J = 7 Hz, J = 7 Hz, J = 1 Hz, 1H), 7.03 (ddd, J = 7 Hz, J = 7 Hz, J = 1 Hz, 2H), 7.23 (d, J = 7 Hz, 2H), 7.46 (d, J = 7 Hz, 1H), 7.57 (d, J = 7 Hz, 2H). ^{13}C{^{1}H} NMR ($CDCl_3$, δ) 3.20, 69.60 (crown), 118.02, 123.29, 124.65, 125.60, 127.43, 128.69, 128.76, 130.49, 143.61, 148.24 (signals corresponding to the *ipso* carbons in the borafluorenyl group and the *ipso* carbon in the phenyl group were not observed). ^{11}B NMR ($CDCl_3$, δ) 4.50 (br). ^{29}Si{^{1}H} NMR ($CDCl_3$, δ) 13.88. Anal. Calcd for $C_{32}H_{42}BKO_7Si$: C, 62.33; H, 6.87; Found: C, 62.06; H, 6.98.

4.4 Computational methods

Computations were executed with the Gaussian 09 program package at the Research Center for Computing and Multimedia Studies, Hosei University.[19] The structures of **4** were optimized at the B3LYP/DGDZVP2 level of theory.

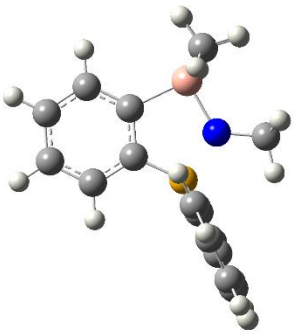

Total Energy (SCF Done) −1202.74380661 a.u.

Zero-point correction 0.362448 (Hartree/Particle)

Corrected Energy −1202.38135861 a.u.

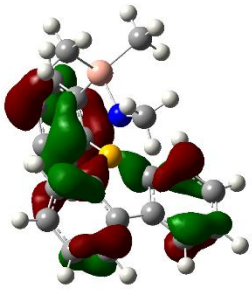

HOMO−1

−6.3019 eV

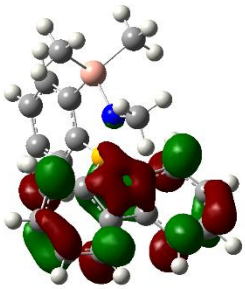

LUMO+1

−0.6172 eV

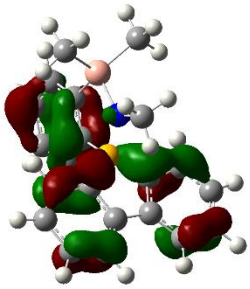

HOMO −2

−6.5473 eV

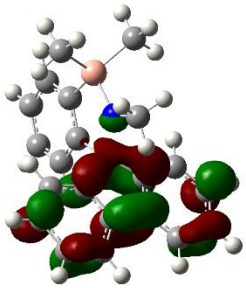

LUMO

−0.8969 eV

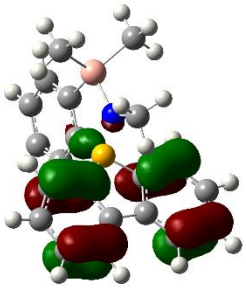

HOMO−3

−6.5860 eV

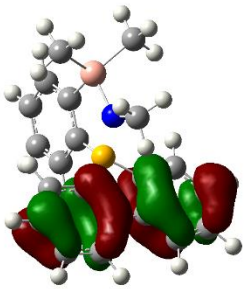

HOMO

−5.5547 eV

Figure 4. Frontier molecular orbitals of **4a**.

Table 3. Cartesian coordinates of optimized structure of **4a**.

	Coordinates (Angstroms)		
	X	Y	Z
H	1.100530	-4.537378	0.000000
C	1.485909	-3.519291	0.000000
C	2.506775	-0.911644	0.000000
C	0.610780	-2.416679	0.000000
C	2.868217	-3.317030	0.000000
C	3.374674	-2.006615	0.000000
C	1.110062	-1.089735	0.000000
H	3.547563	-4.164725	0.000000
H	4.449683	-1.846203	0.000000
H	2.918048	0.094874	0.000000
B	0.079925	0.138419	0.000000
C	0.073096	1.169837	1.240414
C	0.096455	3.373821	2.994529
C	0.089138	0.969875	2.622518
C	0.078017	2.498741	0.742679
C	0.092205	3.597282	1.609246

C	0.095232	2.066824	3.501766
H	0.108408	-0.038797	3.031064
H	0.103294	4.614261	1.226342
H	0.108157	1.906614	4.576575
H	0.107558	4.217589	3.679347
C	0.073096	1.169837	-1.240414
C	0.096455	3.373821	-2.994529
C	0.078017	2.498741	-0.742679
C	0.089138	0.969875	-2.622518
C	0.095232	2.066824	-3.501766
C	0.092205	3.597282	-1.609246
H	0.108408	-0.038797	-3.031064
H	0.108157	1.906614	-4.576575
H	0.103294	4.614261	-1.226342
H	0.107558	4.217589	-3.679347
Si	-1.238489	-2.441687	0.000000
C	-2.068813	-3.115216	1.542202
H	-1.664732	-2.642933	2.442467
H	-1.884187	-4.193090	1.619479

H	-3.154502	-2.970937	1.526855
C	-2.068813	-3.115216	-1.542202
H	-3.154502	-2.970937	-1.526855
H	-1.884187	-4.193090	-1.619479
H	-1.664732	-2.642933	-2.442467
O	-1.383141	-0.707046	0.000000
C	-2.638974	0.010171	0.000000
H	-2.412881	1.074930	0.000000
H	-3.207598	-0.244029	0.898344
H	-3.207598	-0.244029	-0.898344

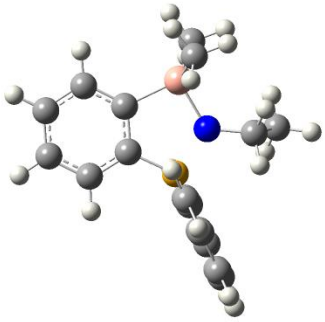

Total Energy (SCF Done) −1242.07126800 a.u.
Zero-point correction 0.391376 (Hartree/Particle)
Corrected Energy −1241.679892 a.u.

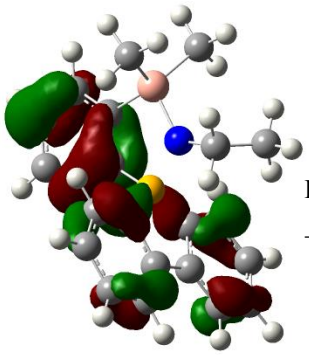

HOMO−1
−6.2896 eV

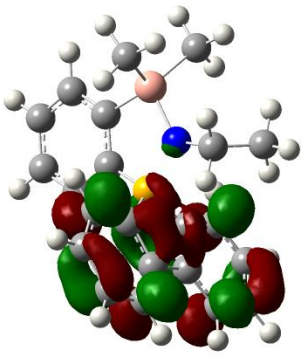

LUMO+1
−0.6278 eV

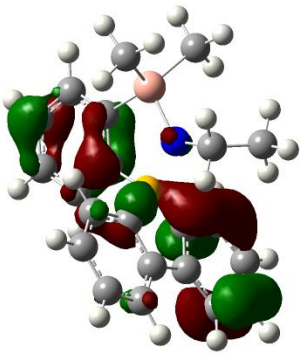

HOMO −2
−6.5386 eV

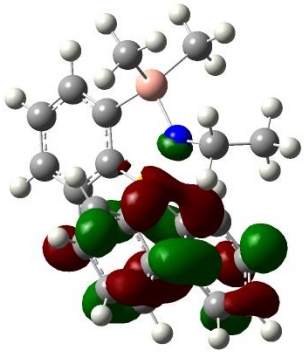

LUMO
−0.8934 eV

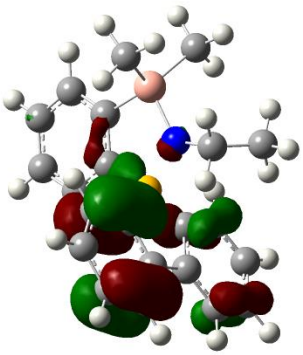

HOMO−3
−6.8579 eV

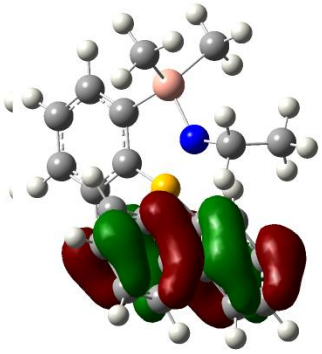

HOMO
−5.5593 eV

Figure 5. Frontier molecular orbitals of **4b**.

Table 4. Cartesian coordinates of optimized structure of **4b**.

	Coordinates (Angstroms)		
	X	Y	Z
H	4.543802	-0.366610	1.185030
C	3.525195	-0.463456	1.556764
C	0.916075	-0.709945	2.543261
C	2.423786	-0.215383	0.716023
C	3.320861	-0.837625	2.887074
C	2.009533	-0.958528	3.376721
C	1.097038	-0.337120	1.197526
H	4.167296	-1.031412	3.539846
H	1.847228	-1.246852	4.412077
H	-0.090826	-0.806160	2.942338
B	-0.126571	-0.065489	0.199145
C	-1.082432	-1.302373	-0.208536
C	-3.177650	-3.105363	-0.756371
C	-0.800678	-2.605511	-0.624451
C	-2.438694	-0.914190	-0.056110
C	-3.483158	-1.805654	-0.325100

C	-1.842639	-3.506836	-0.904571
H	0.230386	-2.940092	-0.724057
H	-4.520895	-1.507541	-0.201745
H	-1.617800	-4.519822	-1.227598
H	-3.978772	-3.808140	-0.969162
C	-1.232993	1.043520	0.586353
C	-3.540412	2.552199	1.168407
C	-2.528495	0.489453	0.420655
C	-1.118499	2.352691	1.060088
C	-2.266841	3.111311	1.345650
C	-3.678049	1.233695	0.709208
H	-0.136565	2.794503	1.218582
H	-2.172384	4.129795	1.712884
H	-4.669287	0.804970	0.588046
H	-4.424406	3.141744	1.396537
S	2.449900	0.295544	-1.060428
C	3.037064	-0.999326	-2.287373
H	2.478065	-1.932596	-2.172055
H	4.095134	-1.219520	-2.102990

H	2.951233	-0.665657	-3.327041
C	3.261655	1.947946	-1.424808
H	3.176391	2.232778	-2.478639
H	4.330801	1.885900	-1.188722
H	2.830727	2.742746	-0.809070
O	0.717033	0.438584	-1.183068
C	-0.009057	0.688149	-2.426582
H	-0.949914	0.144717	-2.336839
H	0.564909	0.235923	-3.241365
C	-0.244814	2.173440	-2.667884
H	-0.817781	2.609669	-1.848216
H	-0.815647	2.295152	-3.595028
H	0.695538	2.721092	-2.773666

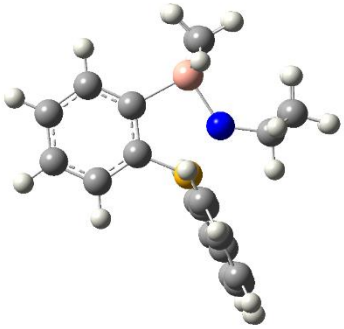

Total Energy (SCF Done) −1281.39595167 a.u.
Zero-point correction 0.419850 (Hartree/Particle)
Corrected Energy −1280.97610167 a.u.

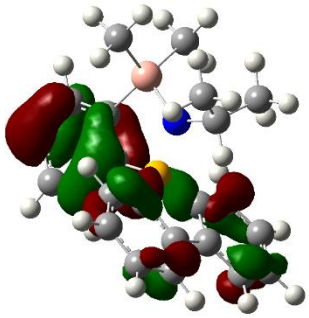

HOMO−1
−6.2673 eV

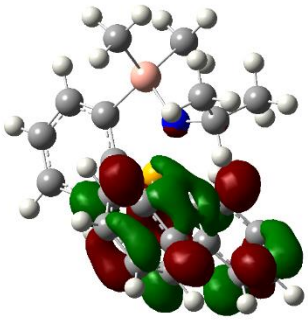

LUMO+1
−0.6351 eV

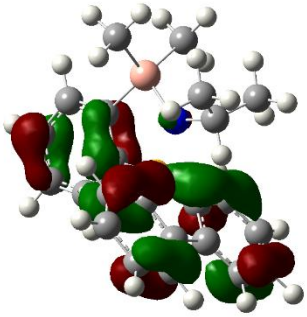

HOMO −2
−6.5397 eV

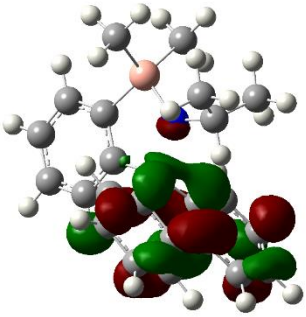

LUMO
−0.8936 eV

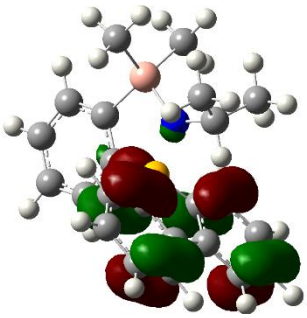

HOMO−3
−6.5803 eV

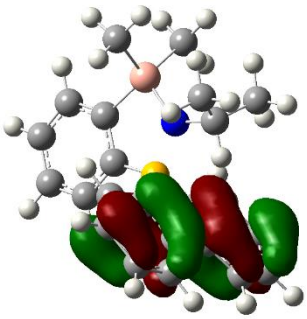

HOMO
−5.5707 eV

Figure 6. Frontier molecular orbitals of **4c**.

Table 5. Cartesian coordinates of optimized structure of **4c**.

	Coordinates (Angstroms)		
	X	Y	Z
H	-4.469962	-1.514697	-0.000329
C	-3.439453	-1.865894	-0.000300
C	-0.799664	-2.800252	-0.000161
C	-2.366112	-0.954706	-0.000148
C	-3.191442	-3.240658	-0.000388
C	-1.864834	-3.704048	-0.000321
C	-1.027293	-1.410506	-0.000082
H	-4.016241	-3.947718	-0.000495
H	-1.669320	-4.773261	-0.000388
H	0.220285	-3.177195	-0.000081
B	0.154558	-0.334183	0.000079
C	1.188039	-0.316091	-1.240607
C	3.393961	-0.347028	-2.993513
C	0.989795	-0.345462	-2.622894
C	2.516739	-0.316850	-0.742522
C	3.616007	-0.333989	-1.608364

C	2.087091	-0.354608	-3.501407
H	-0.018472	-0.374693	-3.031931
H	4.632654	-0.342164	-1.224514
H	1.927530	-0.377476	-4.576164
H	4.238191	-0.360548	-3.677670
C	2.516802	-0.317013	0.742491
C	2.087330	-0.355280	3.501404
C	3.616129	-0.334253	1.608260
C	1.188142	-0.316373	1.240672
C	0.989975	-0.345991	2.622968
C	3.394164	-0.347535	2.993418
H	4.632754	-0.342294	1.224353
H	-0.018273	-0.375311	3.032040
H	4.238441	-0.361133	3.677518
H	1.927859	-0.378363	4.576170
S	-2.463527	0.893467	0.000061
O	-0.731969	1.122562	0.000362
C	0.069143	2.367037	0.000463
H	1.094886	2.000137	0.001280

C	-0.164078	3.166098	-1.276977
H	-1.166560	3.601681	-1.313837
H	-0.011099	2.538303	-2.157230
H	0.557218	3.988879	-1.316095
C	-0.165656	3.166959	1.277070
H	-0.013570	2.539830	2.157962
H	-1.168236	3.602438	1.312530
H	0.555486	3.989860	1.316385
C	-3.256022	1.626234	1.537272
H	-3.330046	2.717352	1.507614
H	-2.715382	1.334090	2.441912
H	-4.275587	1.229946	1.619227
C	-3.255559	1.626903	-1.537071
H	-3.329049	2.718049	-1.507013
H	-4.275331	1.231182	-1.619169
H	-2.715042	1.334824	-2.441803

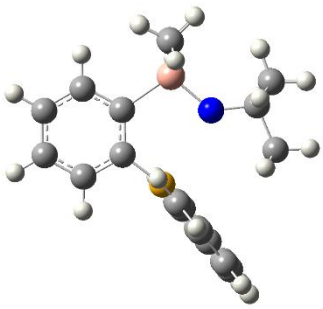

Total Energy (SCF Done) −1320.71004685 a.u.
Zero-point correction 0.445783 (Hartree/Particle)
Corrected Energy −1320.26426385 a.u.

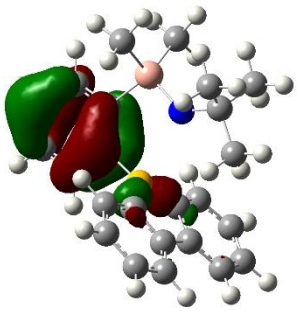

HOMO−1
−6.5098 eV

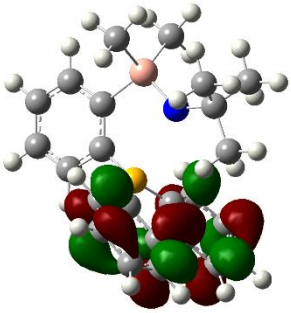

LUMO+1
−1.0112 eV

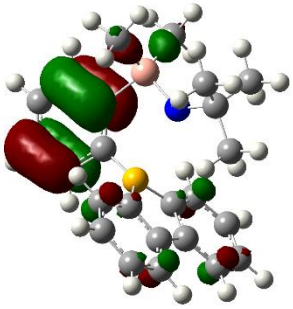

HOMO −2
−6.6929 eV

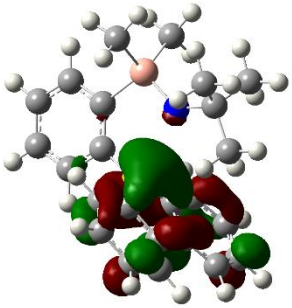

LUMO
−2.1377 eV

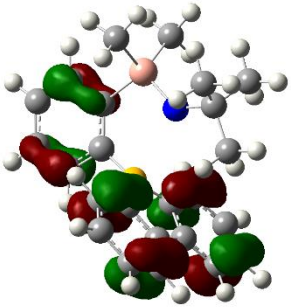

HOMO−3
−6.8507 eV

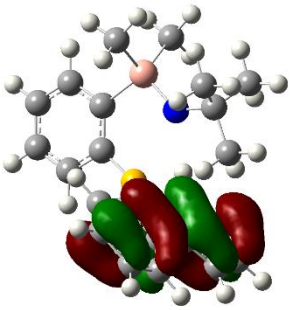

HOMO
−5.9252 eV

Figure 7. Frontier molecular orbitals of **4d**.

Table 6. Cartesian coordinates of optimized structure of **4d**.

	Coordinates (Angstroms)		
	X	Y	Z
H	1.715345	-4.264583	0.000000
C	2.105266	-3.247989	0.000000
C	3.154447	-0.682393	0.000000
C	1.215027	-2.152897	0.000000
C	3.491636	-3.076545	0.000000
C	4.019396	-1.779580	0.000000
C	1.749103	-0.840112	0.000000
H	4.152162	-3.939122	0.000000
H	5.094943	-1.624983	0.000000
H	3.582043	0.318283	0.000000
B	0.956200	0.511626	0.000000
C	0.668654	1.445191	1.235387
C	0.102389	3.546507	3.004622
C	0.744278	1.234428	2.612895
C	0.314436	2.732335	0.744891
C	0.033652	3.780788	1.617874

C	0.454906	2.286265	3.502206
H	1.027577	0.259692	3.002624
H	-0.233306	4.767612	1.249898
H	0.508251	2.126668	4.575411
H	-0.115797	4.354832	3.697464
C	0.668654	1.445191	-1.235387
C	0.102389	3.546507	-3.004622
C	0.314436	2.732335	-0.744891
C	0.744278	1.234428	-2.612895
C	0.454906	2.286265	-3.502206
C	0.033652	3.780788	-1.617874
H	1.027577	0.259692	-3.002624
H	0.508251	2.126668	-4.575411
H	-0.233306	4.767612	-1.249898
H	-0.115797	4.354832	-3.697464
Si	-0.626351	-2.545978	0.000000
C	-1.032459	-3.573141	1.532557
H	-0.926126	-2.978043	2.445187
H	-0.337880	-4.417716	1.606079

H	-2.046542	-3.984571	1.506825
C	-1.032459	-3.573141	-1.532557
H	-2.046542	-3.984571	-1.506825
H	-0.337880	-4.417716	-1.606079
H	-0.926126	-2.978043	-2.445187
O	-1.373578	-1.048033	0.000000
C	-2.769293	-0.635399	0.000000
C	-3.475490	-1.149739	-1.264751
H	-2.932484	-0.832220	-2.159347
H	-4.491107	-0.744209	-1.317448
H	-3.551457	-2.240229	-1.272142
C	-3.475490	-1.149739	1.264751
H	-2.932484	-0.832220	2.159347
H	-3.551457	-2.240229	1.272142
H	-4.491107	-0.744209	1.317448
C	-2.764861	0.896869	0.000000
H	-2.253191	1.279325	-0.885684
H	-2.253191	1.279325	0.885684
H	-3.792552	1.274617	0.000000

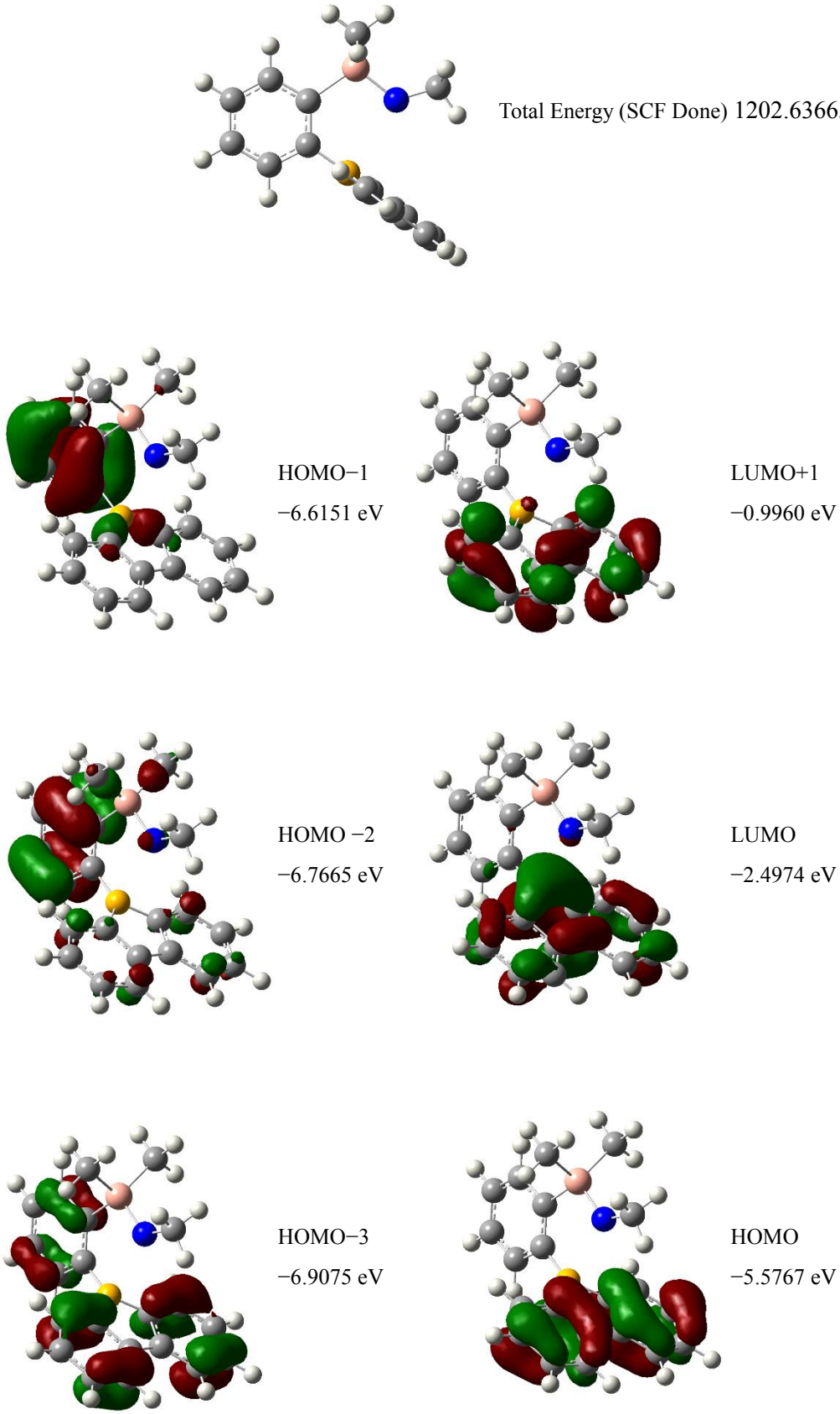

Figure 8. Frontier molecular orbitals of **4a** in the excited state.

Table 7. Cartesian coordinates of optimized structure of **4d**.

	Coordinates (Angstroms)		
	X	Y	Z
H	1.100530	-4.537000	0.000000
C	1.485909	-3.519000	0.000000
C	2.506775	-0.911000	0.000000
C	0.610780	-2.416000	0.000000
C	2.868217	-3.317000	0.000000
C	3.374674	-2.006000	0.000000
C	1.110062	-1.089000	0.000000
H	3.547563	-4.164000	0.000000
H	4.449683	-1.846000	0.000000
H	2.918048	0.094000	0.000000
B	0.079925	0.138000	0.000000
C	0.073096	1.169000	1.240414
C	0.096455	3.373000	2.994529
C	0.089138	0.969000	2.622518
C	0.078017	2.498000	0.742679
C	0.092205	3.597000	1.609246

C	0.095232	2.066000	3.501766
H	0.108408	-0.038000	3.031064
H	0.103294	4.614000	1.226342
H	0.108157	1.906000	4.576575
H	0.107558	4.217000	3.679347
C	0.073096	1.169000	-1.240414
C	0.096455	3.373000	-2.994529
C	0.078017	2.498000	-0.742679
C	0.089138	0.969000	-2.622518
C	0.095232	2.066000	-3.501766
C	0.092205	3.597000	-1.609246
H	0.108408	-0.038000	-3.031064
H	0.108157	1.906000	-4.576575
H	0.103294	4.614000	-1.226342
H	0.107558	4.217000	-3.679347
Si	-1.238489	-2.441000	0.000000
C	-2.068813	-3.115000	1.542202
H	-1.664732	-2.642000	2.442467
H	-1.884187	-4.193000	1.619479

H	-3.154502	-2.970000	1.526855
C	-2.068813	-3.115000	-1.542202
H	-3.154502	-2.970000	-1.526855
H	-1.884187	-4.193000	-1.619479
H	-1.664732	-2.642000	-2.442467
O	-1.383141	-0.707000	0.000000
C	-2.638974	0.010000	0.000000
H	-2.412881	1.074000	0.000000
H	-3.207598	-0.244000	0.898344
H	-3.207598	-0.244000	-0.898344

Table 8. Selected second order perturbation theory analysis of fock matrix in NBO basis of **4a**.[15]

Threshold for printing: 0.50 kcal/mol (Intermolecular threshold: 0.05 kcal/mol).

from unit 2 to unit 1		E(2)	E(j)-E(i)	F(i,j)
Donor NBO (i)	Acceptor NBO (j)	kcal/mol	a.u.	a.u.
87. LP (1) O 41	/168. RY*(4) C 7	0.10	1.59	0.012
87. LP (1) O 41	/195. RY*(2) B 11	0.29	1.08	0.016
87. LP (1) O 41	/200. RY*(7) B 11	0.17	1.84	0.016
87. LP (1) O 41	/201. RY*(8) B 11	0.15	1.66	0.014
87. LP (1) O 41	/211. RY*(4) C 12	0.09	1.40	0.01
87. LP (1) O 41	/212. RY*(5) C 12	0.07	1.37	0.009
87. LP (1) O 41	/237. RY*(2) C 14	0.07	1.16	0.008
87. LP (1) O 41	/315. RY*(4) C 22	0.10	1.46	0.011
87. LP (1) O 41	/316. RY*(5) C 22	0.05	1.31	0.007
87. LP (1) O 41	/354. RY*(2) C 25	0.08	1.17	0.009
87. LP (1) O 41	/414. RY*(1) Si 32	1.38	1.26	0.038
87. LP (1) O 41	/416. RY*(3) Si 32	0.96	1.22	0.031
87. LP (1) O 41	/419. RY*(6) Si 32	0.16	0.96	0.011
87. LP (1) O 41	/544. BD*(1) B 11 - C 12	2.45	0.81	0.04
87. LP (1) O 41	/545. BD*(1) B 11 - C 22	2.45	0.81	0.04

87. LP (1) O 41	/547. BD*(2) C 12 - C 14	0.18	0.42	0.008
87. LP (1) O 41	/562. BD*(2) C 22 - C 25	0.20	0.44	0.009
87. LP (1) O 41	/573. BD*(1) Si 32 - C 33	3.66	0.60	0.042
87. LP (1) O 41	/574. BD*(1) Si 32 - C 37	3.66	0.60	0.042
87. LP (1) O 41	/576. BD*(1) C 33 - H 35	0.09	0.79	0.008
87. LP (1) O 41	/579. BD*(1) C 37 - H 39	0.10	0.79	0.008
87. LP (2) O 41	/ 85. LP*(1) B 11	3.34	0.57	0.04
87. LP (2) O 41	/ 86. LP*(1) Si 32	127.39	0.54	0.236
87. LP (2) O 41	/101. RY*(7) C 2	0.05	1.34	0.008
87. LP (2) O 41	/196. RY*(3) B 11	1.30	1.23	0.038
87. LP (2) O 41	/197. RY*(4) B 11	0.44	1.75	0.026
87. LP (2) O 41	/199. RY*(6) B 11	0.31	2.39	0.026
87. LP (2) O 41	/201. RY*(8) B 11	0.09	1.78	0.012
87. LP (2) O 41	/202. RY*(9) B 11	0.09	1.96	0.013
87. LP (2) O 41	/205. RY*(12) B 11	0.09	2.05	0.013
87. LP (2) O 41	/206. RY*(13) B 11	0.11	2.58	0.016
87. LP (2) O 41	/207. RY*(14) B 11	0.07	2.42	0.012
87. LP (2) O 41	/209. RY*(2) C 12	0.13	1.72	0.014
87. LP (2) O 41	/211. RY*(4) C 12	0.07	1.52	0.01

87. LP (2) O 41	/212. RY*(5) C 12	0.07	1.49	0.01
87. LP (2) O 41	/313. RY*(2) C 22	0.10	1.72	0.013
87. LP (2) O 41	/315. RY*(4) C 22	0.08	1.58	0.011
87. LP (2) O 41	/316. RY*(5) C 22	0.05	1.43	0.008
87. LP (2) O 41	/415. RY*(2) Si 32	2.00	1.57	0.053
87. LP (2) O 41	/417. RY*(4) Si 32	0.32	1.43	0.02
87. LP (2) O 41	/418. RY*(5) Si 32	1.45	1.51	0.044
87. LP (2) O 41	/420. RY*(7) Si 32	0.72	1.14	0.027
87. LP (2) O 41	/422. RY*(9) Si 32	1.54	1.20	0.041
87. LP (2) O 41	/424. RY*(11) Si 32	0.08	1.08	0.009

Table 9. List of first 20 calculated singlet excited states at B3LYP/DZVP2 level for **4a**–**4d**.

(1) **4a**

Excited State	1:	Singlet-A"	4.0331 eV	307.42 nm	f=0.0228	<S**2>=0.000
87 -> 88		0.58683				
87 -> 89		0.36585				
Excited State	2:	Singlet-A"	4.2742 eV	290.08 nm	f=0.1354	<S**2>=0.000
85 -> 88		-0.16709				
86 -> 88		0.29710				

87 -> 88 -0.35909

87 -> 89 0.49491

Excited State 3: Singlet-A' 4.4580 eV 278.12 nm f=0.0096 <S**2>=0.000

87 -> 90 0.70135

Excited State 4: Singlet-A' 4.7246 eV 262.42 nm f=0.0016 <S**2>=0.000

84 -> 88 -0.22792

87 -> 91 0.64922

87 -> 92 0.12764

Excited State 5: Singlet-A" 4.7496 eV 261.04 nm f=0.0413 <S**2>=0.000

81 -> 88 0.11199

85 -> 88 0.42328

86 -> 88 0.52390

87 -> 89 -0.12868

Excited State 6: Singlet-A' 4.8550 eV 255.37 nm f=0.0374 <S**2>=0.000

82 -> 89 0.10292

84 -> 88 0.51543

87 -> 91 0.27022

87 -> 92 -0.36582

Excited State 7: Singlet-A' 4.9974 eV 248.10 nm f=0.0274 <S**2>=0.000

83 -> 91 0.33060

85 -> 90 0.22824

86 -> 90 0.56732

Excited State 8: Singlet-A" 5.0636 eV 244.85 nm f=0.0212 <S**2>=0.000

85 -> 88 -0.14823

85 -> 89 0.32330

86 -> 89 0.59659

Excited State 9: Singlet-A" 5.1506 eV 240.72 nm f=0.3177 <S**2>=0.000

85 -> 88 0.48954

86 -> 88 -0.34016

86 -> 89 0.15104

87 -> 89 0.29743

Excited State 10: Singlet-A" 5.3448 eV 231.97 nm f=0.0038 <S**2>=0.000

83 -> 88 0.69629

Excited State 11: Singlet-A' 5.3543 eV 231.56 nm f=0.0099 <S**2>=0.000

83 -> 91 0.11071

84 -> 88 0.13572

84 -> 89 0.29497

85 -> 90 0.53167

86 -> 90 -0.27277

87 -> 92 0.10548

Excited State 12: Singlet-A" 5.3951 eV 229.81 nm f=0.0283 <S**2>=0.000

84 -> 90 0.49719

85 -> 89 0.41748

86 -> 89 -0.22409

Excited State 13: Singlet-A' 5.4248 eV 228.55 nm f=0.0352 <S**2>=0.000

82 -> 88 -0.11443

84 -> 88 0.15739

84 -> 89 0.54347

85 -> 90 -0.29534

86 -> 90 0.17492

87 -> 92 0.10454

Excited State 14: Singlet-A" 5.4508 eV 227.46 nm f=0.1451 <S**2>=0.000

84 -> 90 0.48564

85 -> 89 -0.41387

86 -> 89 0.21980

Excited State 15: Singlet-A' 5.5144 eV 224.84 nm f=0.0838 <S**2>=0.000

83 -> 90 -0.25559

86 -> 91 0.62705

87 -> 92 -0.12452

Excited State 16: Singlet-A' 5.6114 eV 220.95 nm f=0.1228 <S**2>=0.000

82 -> 88 0.18586

82 -> 89 0.23124

84 -> 88 0.24181

84 -> 89 -0.19230

85 -> 91 -0.24368

86 -> 91 0.14440

87 -> 92 0.46564

Excited State 17: Singlet-A" 5.6623 eV 218.96 nm f=0.0018 <S**2>=0.000

83 -> 89 -0.20089

87 -> 93 0.67229

Excited State 18: Singlet-A" 5.6683 eV 218.73 nm f=0.0024 <S**2>=0.000

83 -> 89 0.65988

84 -> 91 0.10391

87 -> 93 0.20279

Excited State 19: Singlet-A" 5.7126 eV 217.04 nm f=0.0458 <S**2>=0.000

83 -> 89 -0.10285

84 -> 91 0.68030

Excited State 20: Singlet-A' 5.7240 eV 216.61 nm f=0.0063 <S**2>=0.000

82 -> 88 0.10533

82 -> 89 0.12207

83 -> 90	-0.30626
85 -> 91	0.55716
87 -> 92	0.17101
87 -> 95	-0.10313

(2) **4b**

Excited State	1:	Singlet-A	4.0385 eV	307.00 nm	f=0.0206	<S**2>=0.000
91 -> 92		0.58215				
91 -> 93		0.36866				
Excited State	2:	Singlet-A	4.2738 eV	290.10 nm	f=0.1354	<S**2>=0.000
89 -> 92		0.16106				
90 -> 92		-0.28993				
91 -> 92		-0.36698				
91 -> 93		0.48806				
Excited State	3:	Singlet-A	4.4866 eV	276.34 nm	f=0.0106	<S**2>=0.000
91 -> 93		-0.10147				
91 -> 94		0.69208				
Excited State	4:	Singlet-A	4.7331 eV	261.95 nm	f=0.0300	<S**2>=0.000

89 -> 92	0.37972					
90 -> 92	0.46795					
91 -> 93	0.11141					
91 -> 95	-0.29860					
Excited State	5:	Singlet-A	4.7500 eV	261.02 nm	f=0.0181	<S**2>=0.000
88 -> 92	0.28609					
89 -> 92	0.10240					
90 -> 92	0.27153					
91 -> 95	0.53859					
91 -> 96	0.13398					
Excited State	6:	Singlet-A	4.8616 eV	255.03 nm	f=0.0389	<S**2>=0.000
88 -> 92	0.45714					
89 -> 92	-0.16416					
91 -> 95	-0.33797					
91 -> 96	0.34938					
Excited State	7:	Singlet-A	4.9948 eV	248.23 nm	f=0.0234	<S**2>=0.000
87 -> 95	0.30593					
89 -> 93	-0.11921					
89 -> 94	0.16531					
90 -> 93	-0.30933					

90 -> 94 0.48798

Excited State 8: Singlet-A 5.0450 eV 245.76 nm f=0.0165 <S**2>=0.000

87 -> 95 0.11896

89 -> 92 -0.11298

89 -> 93 0.24664

89 -> 94 0.11437

90 -> 93 0.52746

90 -> 94 0.29758

Excited State 9: Singlet-A 5.1546 eV 240.53 nm f=0.3141 <S**2>=0.000

88 -> 92 0.17492

89 -> 92 0.47780

90 -> 92 -0.31663

90 -> 93 0.13799

91 -> 93 -0.28660

Excited State 10: Singlet-A 5.3220 eV 232.97 nm f=0.0077 <S**2>=0.000

87 -> 92 0.68158

Excited State 11: Singlet-A 5.3512 eV 231.69 nm f=0.0172 <S**2>=0.000

87 -> 92 0.11866

88 -> 92 -0.15175

88 -> 93 -0.28566

89 -> 93 0.42455

89 -> 94 -0.33854

90 -> 93 -0.15315

90 -> 94 0.12435

91 -> 96 0.10820

Excited State 12: Singlet-A 5.4169 eV 228.89 nm f=0.0569 <S**2>=0.000

88 -> 93 0.30616

88 -> 94 0.43134

89 -> 93 0.31591

89 -> 94 0.12162

90 -> 93 -0.19012

90 -> 94 -0.12475

Excited State 13: Singlet-A 5.4285 eV 228.39 nm f=0.0222 <S**2>=0.000

88 -> 93 0.44240

88 -> 94 -0.20615

89 -> 94 -0.39206

90 -> 94 0.22624

Excited State 14: Singlet-A 5.4615 eV 227.02 nm f=0.1045 <S**2>=0.000

88 -> 94 0.48715

89 -> 93 -0.29280

89 -> 94 -0.32195

90 -> 93 0.14569

Excited State 15: Singlet-A 5.5236 eV 224.46 nm f=0.0995 <S**2>=0.000

87 -> 93 0.10630

87 -> 94 -0.25402

90 -> 95 0.60051

91 -> 96 0.16443

Excited State 16: Singlet-A 5.6097 eV 221.02 nm f=0.1021 <S**2>=0.000

86 -> 92 -0.16417

86 -> 93 -0.22749

88 -> 92 -0.23556

88 -> 93 0.15810

89 -> 95 0.22069

90 -> 95 -0.19055

91 -> 96 0.46551

Excited State 17: Singlet-A 5.6332 eV 220.10 nm f=0.0100 <S**2>=0.000

87 -> 93 0.67889

87 -> 94 0.12292

Excited State 18: Singlet-A 5.7275 eV 216.47 nm f=0.0400 <S**2>=0.000

87 -> 94 0.10904

88 -> 95	0.49338					
89 -> 95	-0.42538					
91 -> 96	0.10174					
Excited State 19:	Singlet-A	5.7433 eV	215.88 nm	f=0.0142	<S**2>=0.000	
87 -> 94	-0.26265					
88 -> 95	0.45604					
89 -> 95	0.36765					
91 -> 96	-0.10405					
91 -> 97	0.18060					
Excited State 20:	Singlet-A	5.7586 eV	215.30 nm	f=0.0011	<S**2>=0.000	
89 -> 95	-0.12172					
91 -> 97	0.67010					

(3) **4c**

Excited State 1:	Singlet-A	4.0556 eV	305.71 nm	f=0.0194	<S**2>=0.000	
95 -> 96	0.56284					
95 -> 97	0.39880					
Excited State 2:	Singlet-A	4.2736 eV	290.12 nm	f=0.1369	<S**2>=0.000	

93 -> 96 0.17919

94 -> 96 -0.28006

95 -> 96 -0.39281

95 -> 97 0.47294

Excited State 3: Singlet-A 4.5461 eV 272.72 nm f=0.0100 <S**2>=0.000

95 -> 98 0.69709

Excited State 4: Singlet-A 4.7086 eV 263.31 nm f=0.0459 <S**2>=0.000

89 -> 96 -0.10554

93 -> 96 0.36076

94 -> 96 0.56314

95 -> 97 0.13684

Excited State 5: Singlet-A 4.7671 eV 260.08 nm f=0.0016 <S**2>=0.000

92 -> 96 0.37644

95 -> 99 0.53587

95 ->100 0.22433

Excited State 6: Singlet-A 4.8830 eV 253.91 nm f=0.0441 <S**2>=0.000

92 -> 96 -0.41988

95 -> 99 0.45260

95 ->100 -0.31199

Excited State 7: Singlet-A 4.9959 eV 248.17 nm f=0.0110 <S**2>=0.000

93 -> 96 -0.13407

93 -> 97 0.25674

94 -> 97 0.63141

Excited State 8: Singlet-A 5.0145 eV 247.25 nm f=0.0199 <S**2>=0.000

91 -> 99 0.33351

93 -> 98 0.18129

94 -> 98 0.57668

Excited State 9: Singlet-A 5.1522 eV 240.64 nm f=0.2925 <S**2>=0.000

93 -> 96 0.53434

94 -> 96 -0.28428

94 -> 97 0.11764

95 -> 97 -0.28478

Excited State 10: Singlet-A 5.2790 eV 234.86 nm f=0.0146 <S**2>=0.000

91 -> 96 0.69061

91 -> 97 0.10148

Excited State 11: Singlet-A 5.3748 eV 230.68 nm f=0.0283 <S**2>=0.000

90 -> 96 -0.11119

92 -> 96 0.18215

92 -> 97 0.58334

93 -> 98 0.23422

95 ->100 -0.13129

Excited State 12: Singlet-A 5.3997 eV 229.61 nm f=0.0950 <S**2>=0.000

92 -> 98 0.21784

93 -> 97 0.59103

94 -> 97 -0.24352

Excited State 13: Singlet-A 5.4683 eV 226.73 nm f=0.0020 <S**2>=0.000

92 -> 97 -0.25755

93 -> 98 0.58073

94 -> 98 -0.25206

Excited State 14: Singlet-A 5.4925 eV 225.73 nm f=0.0549 <S**2>=0.000

92 -> 98 0.65666

93 -> 97 -0.18279

Excited State 15: Singlet-A 5.5351 eV 224.00 nm f=0.1284 <S**2>=0.000

91 -> 98 -0.27989

94 -> 99 0.57564

95 ->100 0.20454

Excited State 16: Singlet-A 5.5768 eV 222.32 nm f=0.0162 <S**2>=0.000

91 -> 96 -0.10078

91 -> 97 0.68898

Excited State 17: Singlet-A 5.6154 eV 220.79 nm f=0.0867 <S**2>=0.000

90 -> 96 -0.13967

90 -> 97 -0.23645

91 -> 98 0.10083

92 -> 96 -0.25751

92 -> 97 0.14307

93 -> 99 0.18709

94 -> 99 -0.23157

95 ->100 0.46317

Excited State 18: Singlet-A 5.7566 eV 215.38 nm f=0.0511 <S**2>=0.000

92 -> 99 0.68183

Excited State 19: Singlet-A 5.7687 eV 214.93 nm f=0.0087 <S**2>=0.000

90 -> 96 0.14561

90 -> 97 0.10507

91 -> 98 -0.26044

93 -> 99 0.57143

95 ->100 -0.11522

95 ->102 0.17659

Excited State 20: Singlet-A 5.7909 eV 214.10 nm f=0.0166 <S**2>=0.000

88 -> 96 0.13510

90 -> 96 0.47819

91 -> 98	0.12007
93 -> 99	-0.17339
95 ->102	0.42738

(4) **4d**

Excited State	1:	Singlet-A"	3.0045 eV	412.67 nm	f=0.0016	<S**2>=0.000
99 ->100	0.70309					
Excited State	2:	Singlet-A"	3.5560 eV	348.66 nm	f=0.0007	<S**2>=0.000
98 ->100	0.69887					
Excited State	3:	Singlet-A"	3.8685 eV	320.50 nm	f=0.0095	<S**2>=0.000
96 ->100	-0.22988					
97 ->100	0.59785					
99 ->101	0.28986					
Excited State	4:	Singlet-A"	3.9712 eV	312.21 nm	f=0.0011	<S**2>=0.000
96 ->100	0.56605					
97 ->100	0.34088					
99 ->101	-0.24270					
Excited State	5:	Singlet-A'	4.4269 eV	280.07 nm	f=0.0603	<S**2>=0.000

95 ->100 0.65846

99 ->104 -0.18839

Excited State 6: Singlet-A" 4.5720 eV 271.18 nm f=0.0150 <S**2>=0.000

94 ->100 0.69179

99 ->101 0.10654

Excited State 7: Singlet-A' 4.7545 eV 260.77 nm f=0.0132 <S**2>=0.000

89 ->100 0.14199

91 ->100 -0.17142

92 ->100 0.21587

93 ->100 0.62157

Excited State 8: Singlet-A" 4.8145 eV 257.52 nm f=0.6343 <S**2>=0.000

94 ->100 -0.12493

96 ->100 0.31646

97 ->100 -0.13800

98 ->101 0.25945

99 ->101 0.53303

Excited State 9: Singlet-A" 4.8952 eV 253.27 nm f=0.1312 <S**2>=0.000

96 ->100 -0.12278

98 ->101 0.64940

99 ->101 -0.21307

Excited State 10: Singlet-A' 4.9209 eV 251.96 nm f=0.0009 <S**2>=0.000

92 ->100 0.25555

98 ->102 0.11079

99 ->102 0.62253

Excited State 11: Singlet-A' 4.9941 eV 248.26 nm f=0.0448 <S**2>=0.000

89 ->100 0.11779

91 ->100 -0.24447

92 ->100 0.47452

93 ->100 -0.25532

95 ->101 -0.14106

99 ->102 -0.27921

99 ->103 0.10076

Excited State 12: Singlet-A' 5.0810 eV 244.01 nm f=0.0059 <S**2>=0.000

96 ->102 0.10783

96 ->103 -0.12339

97 ->102 0.11832

97 ->103 -0.34672

98 ->102 0.50779

98 ->103 0.15585

99 ->102 -0.14057

99 ->103 -0.11146

Excited State 13: Singlet-A' 5.1257 eV 241.89 nm f=0.0006 <S**2>=0.000

92 ->100 -0.10090

99 ->103 0.68442

Excited State 14: Singlet-A" 5.1716 eV 239.74 nm f=0.0009 <S**2>=0.000

90 ->100 0.69678

Excited State 15: Singlet-A" 5.1892 eV 238.93 nm f=0.0061 <S**2>=0.000

97 ->101 0.69802

Excited State 16: Singlet-A' 5.2135 eV 237.81 nm f=0.0063 <S**2>=0.000

89 ->100 -0.15146

91 ->100 0.47305

92 ->100 0.24016

95 ->101 0.10319

99 ->104 -0.38138

Excited State 17: Singlet-A' 5.3547 eV 231.54 nm f=0.0413 <S**2>=0.000

91 ->100 -0.29219

92 ->100 -0.13572

93 ->100 -0.13056

95 ->100 -0.16589

95 ->101 0.40562

99 ->104	-0.35968					
Excited State 18:	Singlet-A"	5.3580 eV	231.40 nm	f=0.0044	<S**2>=0.000	
96 ->101	0.68120					
Excited State 19:	Singlet-A'	5.5546 eV	223.21 nm	f=0.0100	<S**2>=0.000	
89 ->100	0.64574					
91 ->100	0.25175					
Excited State 20:	Singlet-A'	5.6548 eV	219.25 nm	f=0.0714	<S**2>=0.000	
95 ->101	0.13975					
97 ->102	0.45055					
98 ->102	-0.20617					
98 ->103	0.44673					

4.5 UV−vis Absorption and Fluorescence Data

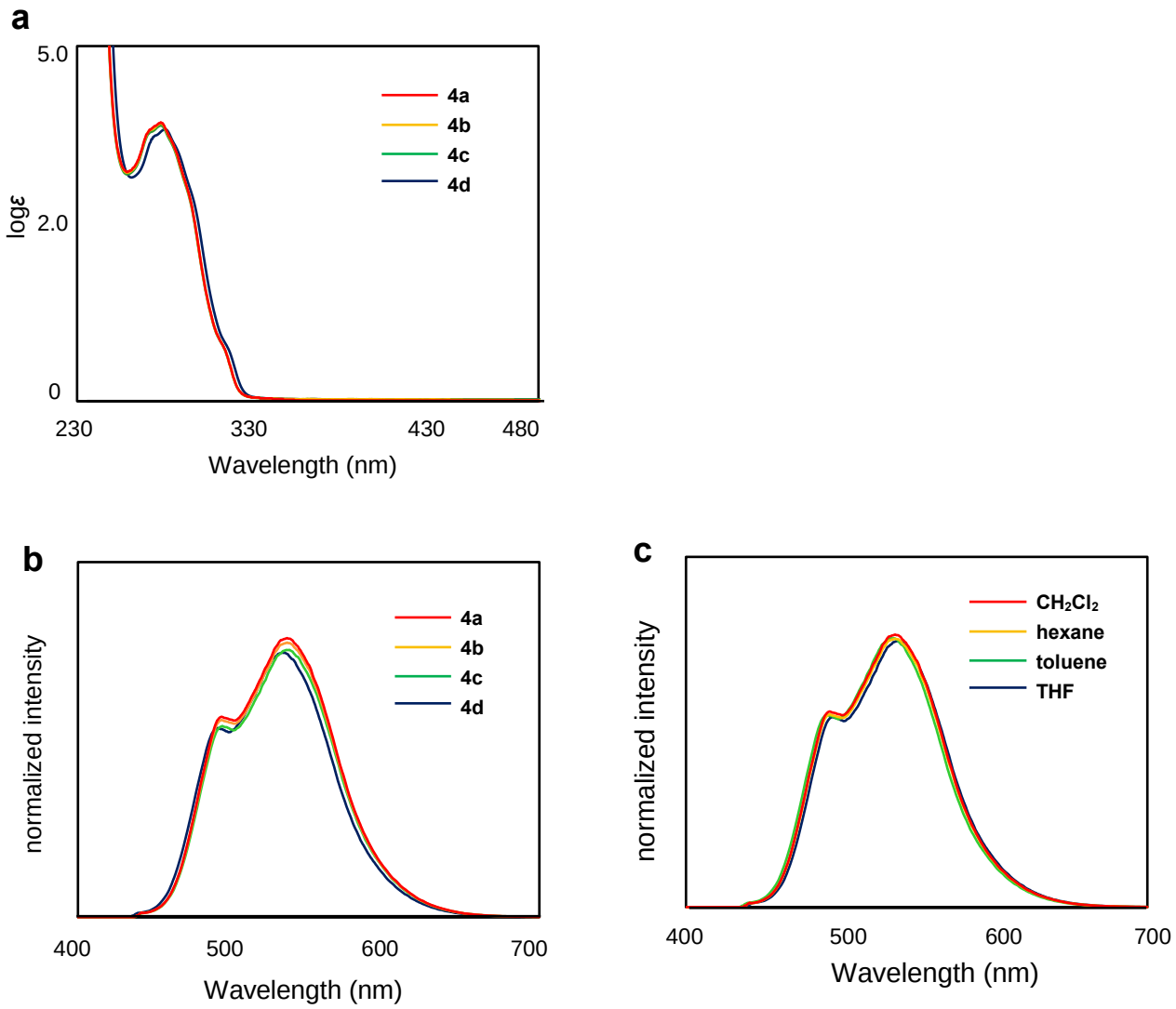

Figure 9. UV−vis absorption and fluorescence spectra for **4**. (a): absorption spectra of **4a**–**4d** in CH_2Cl_2 (1.0×10^{-5} mol/L) under an argon atmosphere. (b): Fluorescence spectra of **4a**–**4d** in CH_2Cl_2 (1.0×10^{-5} mol/L) under an argon atmosphere. (c): Fluorescence spectra of **4a** in different solvents (excitation at 280 nm) under an argon atmosphere.

References

(1) As review: Wade, C. R.; Broomsgrove, A. E.; Aldridge, S.; Gabbaï, F. P. Fluoride Ion Complexation and Sensing Using Organoboron Compounds. *Chem. Rev.* **2010**, *110*, 3958–3984.

(2) (a) Chase, P. A.; Piers, W. E.; Patrick, B. O. New Fluorinated 9-Borafluorene Lewis Acids. *J. Am. Chem. Soc*. **2000**, *122*, 12911–12912. (b) Chase, P. A.; Romero, P. E.; Piers, W. E.; Parvez, M.; Patrick, B. O. Fluorinated 9-borafluorenes vs. conventional perfluoroaryl boranes Comparative Lewis acidity. *Can. J. Chem*. **2005**, *83*, 2098–2105. (c) Wakamiya, A.; Mishima, K.; Ekawa, K.; Yamaguchi, S. Kinetically stabilized dibenzoborole as an electron-accepting building unit. *Chem. Commun*. **2008**, 579–581. (d) Smith, M. F.; Cassidy, S. J.; Adams, I. A.; Vasiliu, M.; Gerlach, D. L.; Dixon, D. A.; Rupar, P. A. Substituent Effects on the Properties of Borafluorenes. *Organometallics* **2016**, *35*, 3182–3191.

(3) (a) Bluer, K. R.; Laperriere, L. E.; Pujol, A.; Yruegas, S.; Adiraju, V. A. K.; Martin, C. D. Coordination and Ring Expansion of 1,2-Dipolar Molecules with 9-Phenyl-9-borafluorene. *Organometallics* **2018**, *37*, 2917−2927. (b) Laperriere, L. E.; Yruegas, S.; Martin, C. D. Investigating the reactivity of 9-phenyl-9-borafluorene with N−H, O−H, P−H, and S−H bonds. *Tetrahedron* **2019**, *75*, 937–943.

(4) (a) Yamaguchi, S.; Shirasaka, T.; Akiyama, S.; Tamao, K. Dibenzoborole-Containing π-Electron Systems: Remarkable Fluorescence Change Based on the "On/Off" Control of the pπ−π* Conjugation. *J. Am. Chem. Soc.* **2002**, *124*, 8816–8817. (b) Thanthiriwatte, K. S.; Gwaltney, S. R. Excitation Spectra of Dibenzoborole Containing π-Electron Systems:

Controlling the Electronic Spectra by Changing the pπ−π* Conjugation. *J. Phys. Chem. A.* **2006**, *110*, 2434–2439. (c) Berger, C. J.; He, G.; Merten, C.; McDonald, R.; Ferguson, M. J.; Rivard, E. Synthesis and Luminescent Properties of Lewis Base-Appended Borafluorenes. *Inorg. Chem.* **2014**, *53*, 1475–1486. (d) Adams, I. A.; Rupar, P. A. A Poly(9-Borafluorene) Homopolymer: An Electron-Deficient Polyfluorene with "Turn-On" Fluorescence Sensing of NH_3 Vapor. *Macromol. Rapid Commun*. **2015**, *36*, 1336–1340. (e) Bontemps, S.; Devillard, M.; Mallet-Ladeira, S.; Bouhadir, G.; Miqueu, K.; Bourissou, D. Phosphino-Boryl-Naphthalenes: Geometrically Enforced, Yet Lewis Acid Responsive P→B Interactions. *Inorg. Chem.* **2013**, *52*, 4714–4720.

(5) Matsumoto, T.; Takamine, H.; Tanaka, K.; Chujo, Y. Design of bond-cleavage-induced intramolecular charge transfer emission with dibenzoboroles and their application to ratiometric sensors for discriminating chain lengths of alkanes. *Mater. Chem. Front.* **2017**, *1*, 2368–2375.

(6) Cassidy, S. J.; Brettell-Adams, I.; McNamara, L. E.; Smith, M. F.; Bautista, M.; Cao, H.; Vasiliu, M.; Gerlach, D. L.; Qu, F.; Hammer, N. I.; Dixon, D. A.; Rupar, P. A. Boranes with Ultra-High Stokes Shift Fluorescence. *Organometallics* **2018**, *37*, 3732–3741.

(7) (a) Reaction with alcohols: Kawachi, A.; Zaima, M.; Tani, A.; Yamamoto, Y. Dehydrogenative Condensation of (*o*-Borylphenyl)hydrosilane with Alcohols and Amines. *Chem. Lett.* **2007**, *36*, 362–363. (b) Formation of Si-O-B linkage: Kawachi, A.; Zaima, M.; Yamamoto, Y. Intramolecular Reaction of Silanol and Triarylborane: Boron-Aryl Bond Cleavage and Formation of a Si−O−B Heterocyle. *Organometallics* **2008**, *27*, 4691−4096.

(8) Shimizu, T.; Morisako, S.; Yamamoto, Y.; Kawachi, A. Intramolecular Activation of C–O Bond by an *o*-Boryl Group in *o*-(Alkoxysilyl)(diarylboryl)benzenes. *ACS Omega* **2020**, *5*, 871–876.

(9) Biswas, S.; Oppel, I. M.; Bettinger, H. F. Synthesis and Structural Characterization of 9-Azido-9-Borafluorene: Monomer and Cyclotrimer of a Borole Azide. *Inorg. Chem*. **2010**, *49*, 4499–4506.

(10) As reviews for C−O bond activation: (a) Yamamoto, H. Lewis Acid Reagents A Practical Approach; Oxford University Press, New York, USA, 1999. (b) Ishihara, K.; Yamamoto, H. Arylboron Compounds as Acid Catalysts in Organic Synthetic Transformations. *Eur. J. Org. Chem*. **1999**, 527–538. (c) Chen, E. Y. -X.; Marks, T. J.; Cocatalysts for Metal-Catalyzed Olefin Polymerization: Activators, Activation Processes, and Structure−Activity Relationship. *Chem. Rev.* **2000**, *100*, 1391–1434.

(11) Matsuo, K.; Saito, S.; Yamaguchi, S. Photodissociation of B−N Lewis Adducts: A Partially Fused Trinaphthylborane with Dual Fluorescence. *J. Am. Chem. Soc.* **2014**, *136*, 12580–12583.

(12) Hou, Q.; Liu, L.; Mellerup, S. K.; Wang, N.; Peng, T.; Chen, P.; Wang, S. Stimuli-Responsive B/N Lewis Pairs Based on the Modulation of B–N Bond Strength. *Org. Lett.* **2018**, *20*, 6467–6470.

(13) The fluorescence quantum yields of compounds **4a**, **4d**, and **I** were estimated relative to that of 9,10-diphenylanthracene (Φ = 0.90): S. Fery-Forgues, D. Lavabre, Are Fluorescence Quantum Yields So Tricky to Measure? A Demonstration Using Familiar Stationery Products. *J. Chem. Educ.* **1999**, *9*, 1260–1264.

(14) Gaussian 09, rev. B.01: Frisch, M. J.; Trucks, G. W.; Schlegel, H. B.; Scuseria, G. E.; Robb, M. A.; Cheeseman, J. R.; Scalmani, G.; Barone, V.; Mennucci, B.; Petersson, G. A.; Nakatsuji, H.; Caricato, M.; Hratchian, X.; Li, H. P.; Izmaylov, A. F.; Bloino, J.; Zheng, G.; Sonnenberg, J. L.; Hada, M.; Ehara, M.; Toyota, K.; Fukuda, R.; Hasegawa, J.; Ishida, M.; Nakajima, T.; Honda, Y.; Kitao, O.; Nakai, H.; Vreven, T.; Montgomery, Jr. J. A.; Peralta, J. E.; Ogliaro, F.; Bearpark, M.; Heyd, J. J.; Brothers, E.; Kudin, K. N.; Staroverov, V. N.; Kobayashi, R.; Normand, J.; Raghavachari, K.; Rendell, A.; Burant, J. C.; Iyengar, S. S.; Tomasi, J.; Cossi, M.; Rega, N.; Millam, J. M.; Klene, M.; Knox, J. E.; Cross, J. B.; Bakken, V.; Adamo, C.; Jaramillo, J.; Gomperts, R.; Stratmann, R. E.; Yazyev, O.; Austin, A. J.; Cammi, R.; Pomelli, C.; Ochterski, J. W.; Martin, R. L.; Morokuma, K.; Zakrzewski, V. G.; Voth, G. A.; Salvador, P.; Dannenberg, J. J.; Dapprich, S.; Daniels, A. D.; Farkas, Ö.; Foresman, J. B.; Ortiz, J. V.; Cioslowski, J.; and Fox, D. J. Gaussian, Inc., Wallingford CT, 2010.

(15) Second order perturbation theory analysis of fock matrix in NBO basis: LP_O = lone pair at oxygen atom; LP^*_B: vacant orbital at boron atom.

Chapter 4

1,2-Silyl Migration in 1-Halonaphthalenes Catalyzed by I_2

Abstract

1-Halo-8-hydrosilylnaphthalenes undergo 1,2-silyl migration to form 1-halo-7-silylnaphthalenes. The influence of the substituents on the silicon atom, the solvent effect, and the D-labeling experiments are investigated. The migration process may include four steps: (i) generation of acid (HI) by the reaction of the hydrosilane with I_2, (ii) protonation of the naphthalene ring, (iii) silyl group migration in the protonated intermediate, and (iv) deprotonation of the naphthalene ring.

1. Introduction

1.1 Construction studies of arene derivatives other than *o*-phenylene framework.

The synthesis of B/Si bidentate Lewis acids biphenyl derivatives **5**, binaphthyl derivatives **6**, and naphthyl derivatives **7** with a framework other than *o*-phenylene was studied.

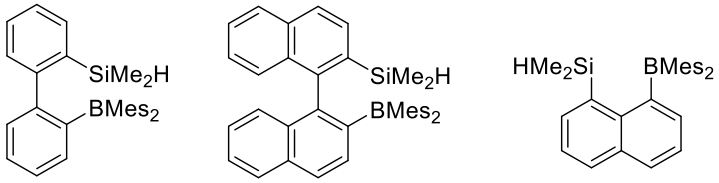

5 **6** **7**

Chart 1. B/Si bidentate Lewis acids **5**, **6**, and **7**.

1.2 Silyl migrations

Silyl migrations have received much attention in terms of mechanistic considerations as well as synthetic utilities because the migratory aptitudes of silyl groups are higher than those of organyl groups.[1] Silyl migrations can be classified as neutral, cationic, anionic, and radical migrations. Although anionic migrations have been well studied, cationic migrations have been less thoroughly explored. As a typical example of the cationic migration, 1,2-bis(trimethylsilyl)benzene **I** underwent 1,2-rearrangement to its 1,3-disilyl isomer **II** in an acid-catalyzed manner (Scheme 1).[2] 1,8-Bis(trimethylsilyl)naphthalene **III** similarly afforded 1,7-disilyl isomer **IV**. 1-Silylnaphthalene **V** also underwent 1,2-rearrangement to its 2-silyl isomer **VI** (Scheme 1).[3] The main driving force for these migrations was discussed to be relief of steric compression.

Scheme 1. Silyl migration in 1,2-disilylbenzene **I**, 1,8-disilylnaphthalene **III**, and 1-silylnaphthalene **V**.

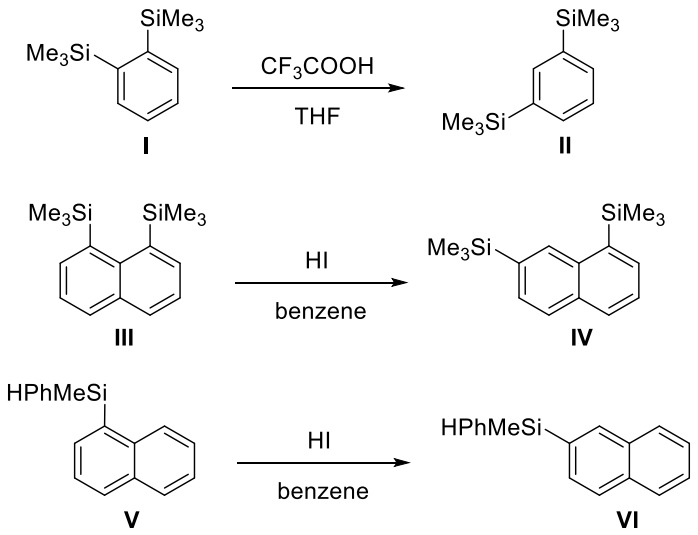

Here the author reports cationic 1,2-silyl migration in 1-halo-8-(hydrosilyl)naphthalenes **1** and **2**, during which a hydrosilyl group at the eight-position undergoes migration to the seven-position to form **3** and **4**, respectively, upon standing, on silica gel, or in the presence of catalytic amounts of I_2 (Scheme 2).

Scheme 2. 1,2-Silyl migration in 1-halo-8-silylnaphthalenes **1** and **2**.

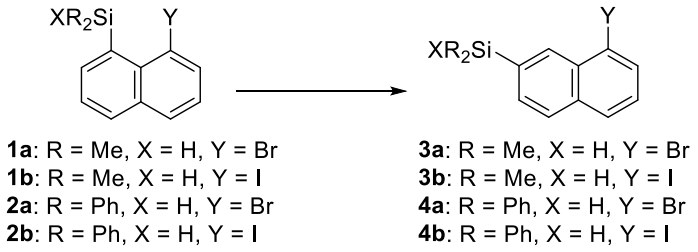

2. Results and discussion

2.1 Preparation of biphenyl, binaphthyl, and naphthalene ring compounds

The Br-Li exchange reaction of 2,2'-dibromobiphenyl (**8**) with *n*-BuLi produced lithiated product **9**, which reacted with chlorosilanes **10** to form 2-bromo-2'-silylbiphenyl **11** in 51–81% yields. The lithiation of **11** again with *tert*-BuLi followed by the treatment with Mes_2BF gave silafluorene **12** in 90–98% yields (Scheme 3). It is plausible that the intramolecular cyclization reaction proceeded to produce **12** faster than the reaction of **13** with Mes_2BF. The lithiation of 2-bromo-2'-silylbinaphthyl **14** and subsequent treatment with Mes_2BF produced dinaphthosilole **15** in 78–91% yields (Scheme 4).

Scheme 3. Preparation of 2-bromo-2'-silylnaphthalene **11** and generation of silafluorene **12**.

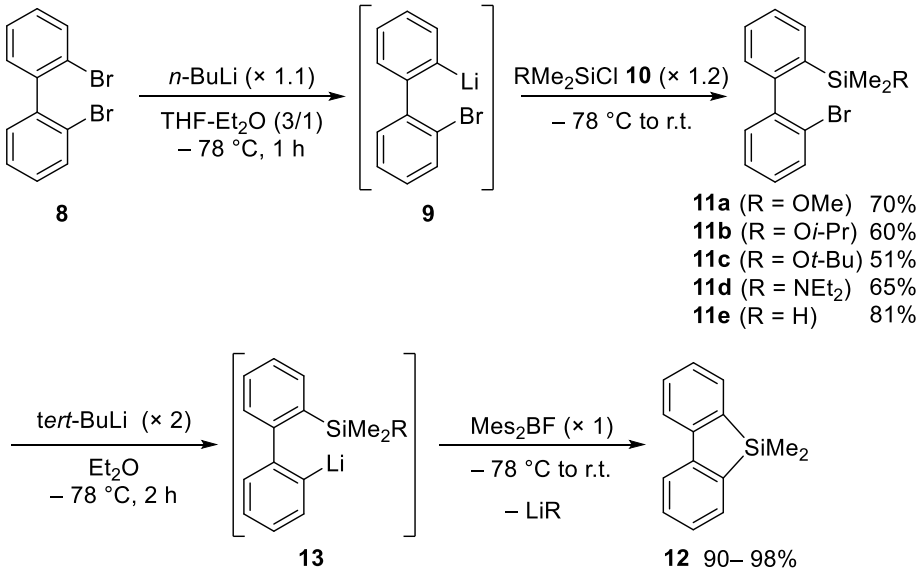

Scheme 4. Generation of dinaphthosilole **15**.

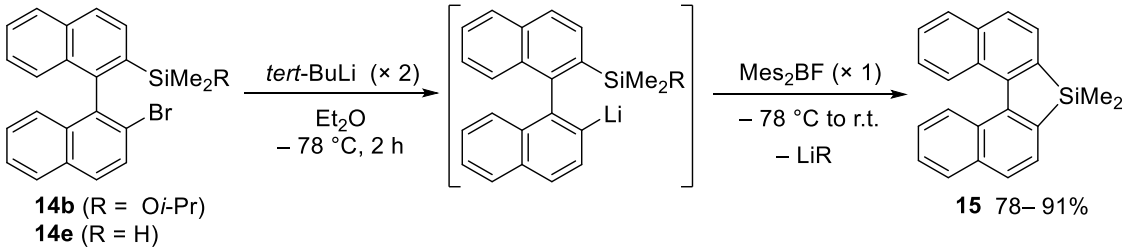

1,8-Disubstituted naphthalene was selected as a rigid framework to avoid the intramolecular cyclization. 1-Bromo-8-silylnaphthalene **1b** was prepared by Br-Li exchange of 1,8-diiodonaphthalene **16b** with *n*-BuLi and the subsequent treatment with chlorodimethylsilane (Scheme 5). When applied to column chromatography on silica gel eluted with hexane, 1-iodo-8-silylnaphthalene **1b** underwent 1,2-silyl migration to afford 1-iodo-7-silylnaphthalene **3b**. The lithiation of **3b** again with BuLi followed by the treatment with Mes_2BF gave 1-(boryl)-7-silylnaphthalene **17** in 54% (Scheme 5).

Scheme 5. Preparation of 1-iodo-8-silylnaphthalene **1b** and 1-(boryl)-7-silylnaphthalene **17**.

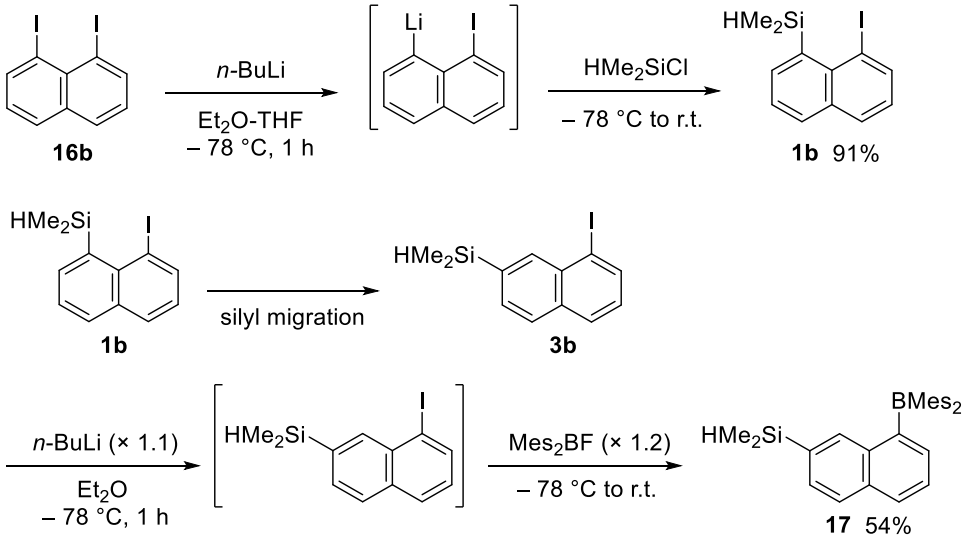

1-Boryl-7-silylnaphthalene **17** was characterized by NMR spectroscopy and X-ray crystallographic analysis (Figure 1). The ^{29}Si NMR was observed at δ = −17.43 with the $^{1}J_{\text{Si-H}}$ coupling constant of 194 Hz. The ^{11}B NMR spectra showed a broad signal at δ = 74 ppm in a typical range of triaryl boranes. The Si−H bond length (1.40 Å) in the crystal structure are within normal values of tetracoordinate Si−H bond, and the boron atom adopted a trigonal planar geometry (Σ(B) = 360°). The interatomic distance between boron and the hydrogen on silicon was 5.36 Å, which was larger than the sum of the van der Waals radii (B: 1.85 Å; H: 1.43 Å).[4] There seems to be no noticeable intramolecular Si−H···B interaction.

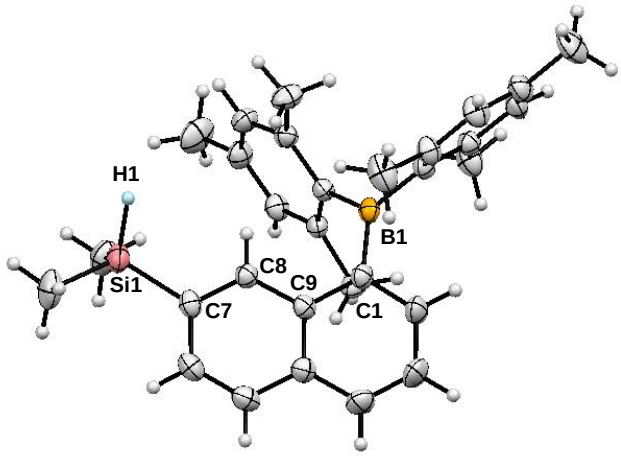

Figure 1. Crystal structure of **17** at 30% probability level. Selected bond lengths (Å) and angles (deg): Si1−H1, 1.402(1); Si1−C8, 1.867(7); B1−C1, 1.588(8), B1–H1, 5.356, Si1−C8−C9, 117.8(8); B1−C1−C9, 124.5(5).

2.2 Preparation of silylnaphthalene derivatives

1-Halo-8-silylnaphthalenes **1**, **2**, **18**, **19**, and **20** were prepared in good yields by lithium-halogen exchange of 1,8-dihalonaphthalenes **16** with *n*-BuLi and the subsequent treatment with chlorosilanes (XR_2SiCl) (Scheme 6).[5-8] 1-Silylnaphthalenes **21** and **22** was prepared by lithium-halogen exchange of 1-halonahutarenes **23** and **24** with *n*-BuLi and the subsequent treatment with chlorosilane (Scheme 7). Methoxysilane **20a** was also obtained by chlorination of **1a** with trichloroisocyanuric acid (TCCA) and alcoholysis of **25** (Scheme 8).[9,10] Reduction of **20a** with $LiAlD_4$ afforded deuterated silane **1a-D** (Scheme 9).[11] The structures were characterized by NMR spectroscopy.

Scheme 6. Preparation of 1-halo-8-silylnaphthalene **1**, **2**, **18**, and **19**.

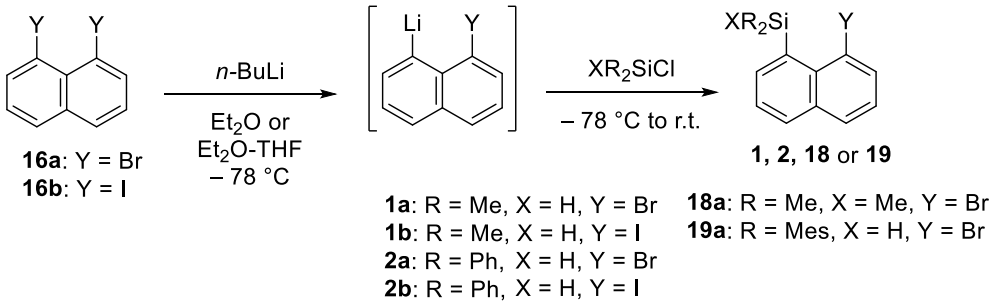

Scheme 7. Preparation of silylnaphthalene **21** and **22**.

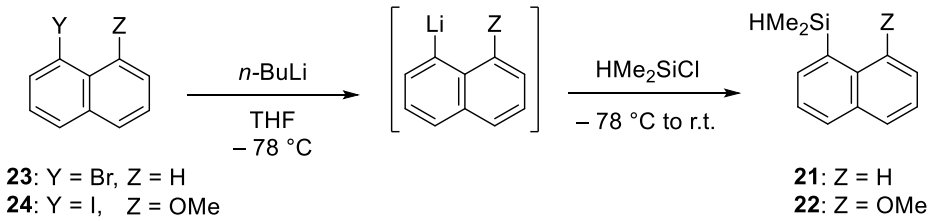

Scheme 8. Preparation of 1-halo-8-(methoxy)silylnaphthalene **20a**.

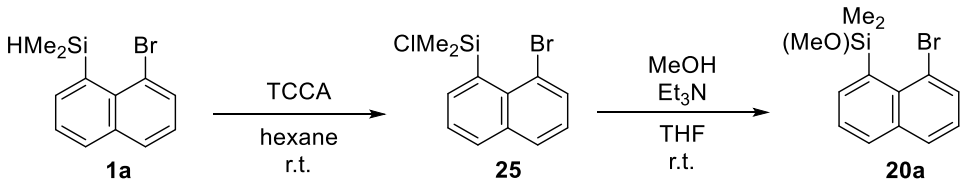

Scheme 9. Preparation of 1-halo-8-deuteriosilylnaphthalene **1a-D**.

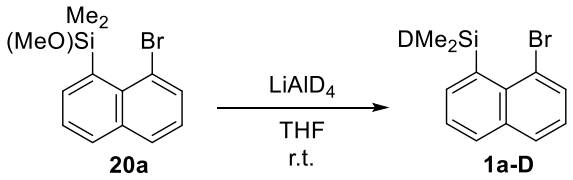

2.3 Silyl migration in 1-halo-8-silylnaphthalenes

Upon standing in air for 3 days, 1-iodo-8-silylnaphthalene **1b** underwent 1,2-silyl migration to afford 1-iodo-7-silylnaphthalene **3b**.[1] No other product was observed in the ^{1}H NMR spectra as shown in Figure 2. The silyl migration also occurred when **1b** was subjected to column chromatography on silica gel eluted with hexane. The ^{1}H resonance of the proton bonded to the silicon atom was shifted upfield from $\delta = 5.66$ ppm in **1b** to $\delta = 4.59$ ppm in **3b**. Compound **1a** was

airstable in the solid state and in solution over the course of several months and can be purified by column chromatography.

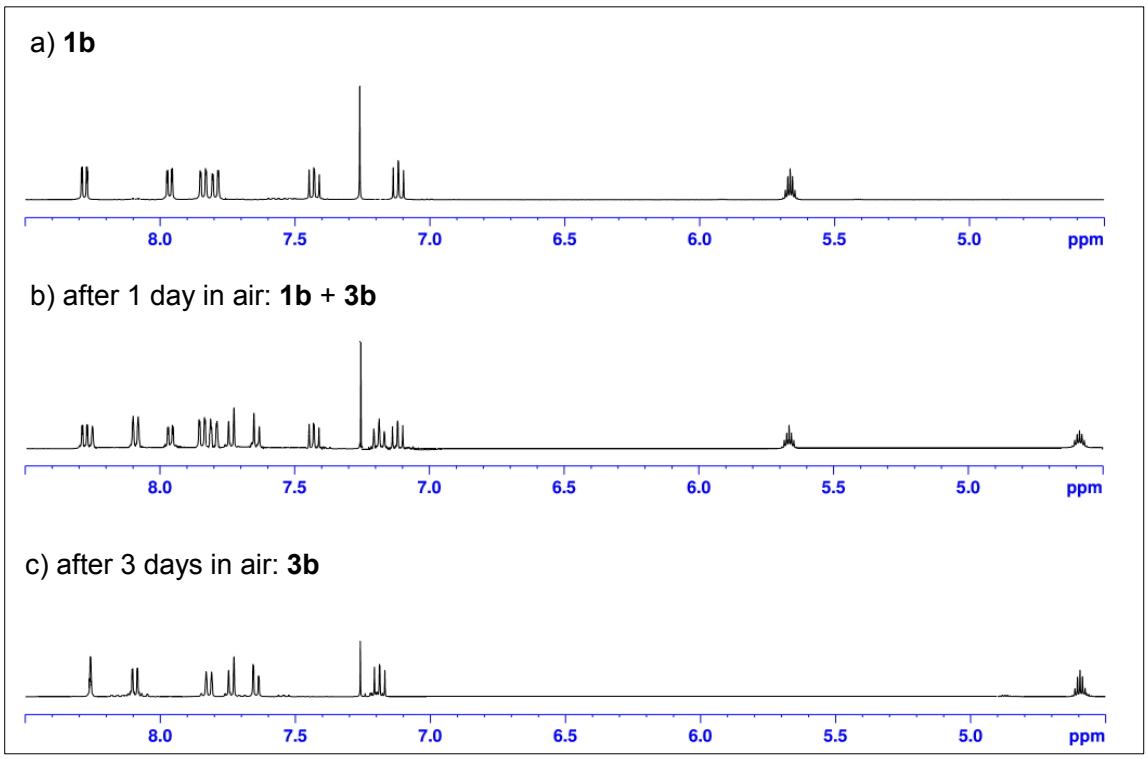

Figure 2. ^{1}H NMR spectra of **1b** and **3b** in $CDCl_3$.

The silyl migration was promoted by a catalytic amount of I_2 (Scheme 10). The silyl migration in 1-halo-8-silylnaphthalenes **1**, **2**, **18**, and **19** was monitored by ^{1}H NMR spectroscopy. A solution of the substrate in $CDCl_3$ or C_6D_6 was treated with I_2 (5 mol%) in an NMR tube for 5 min or less and the reaction mixture was directly subjected to ^{1}H NMR spectroscopy. The yields of the products were estimated by using cyclohexane as an internal standard.

Scheme 10. 1,2-Silyl migration in 1-halo-8-silylnaphthalene **1**, **2**, **18**, and **19** catalyzed by I_2.

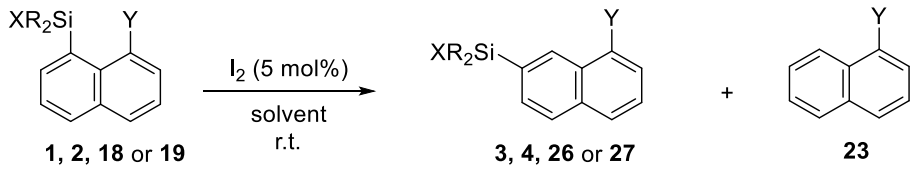

1, 2, 18 or **19** | **3, 4, 26** or **27** | **23**

1a: R = Me, X = H, Y = Br
1b: R = Me, X = H, Y = I
2a: R = Ph, X = H, Y = Br
2b: R = Ph, X = H, Y = I
18a: R = Me, X = Me, Y = Br
19a: R = Mes, X = H, Y = Br

3a: R = Me, X = H, Y = Br
3b: R = Me, X = H, Y = I
4a: R = Ph, X = H, Y = Br
4b: R = Ph, X = H, Y = I
26a: R = Me, X = Me, Y = Br
27a: R = Mes, X = H, Y = Br

23a: Y = Br
23b: Y = I

The results of these experiments are summarized in Table 1. Dimethylsilyl derivatives **1** produced the migrated products **3** in 33–81% yields in addition to protodesilylated products **21** in 19–64% yields and **18**, **19**, and **21** did not react in the presence of the same condition. Diphenylsilyl derivatives **2** afforded migrated products **4** in 10–21% yields with protodesilylated products **21** (34–56% yields) and **2** (30–45% yields). 1-Methoxy derivatives **22** afforded **23** in 20% yields. The amount of I_2 was also significant, as only protodesilylated products **21** were obtained from **1**, **2**, **18**, **19**, **21**, and **22** in the presence of 50 mol% I_2. The migrated products were obtained in higher yields in C_6D_6 than in $CDCl_3$. Dimethylsilyl derivatives **1** produced the migrated products in higher yields than diphenylsilyl derivatives **2**.

Table 1. 1,2-Silyl migration reactions in an NMR tube.

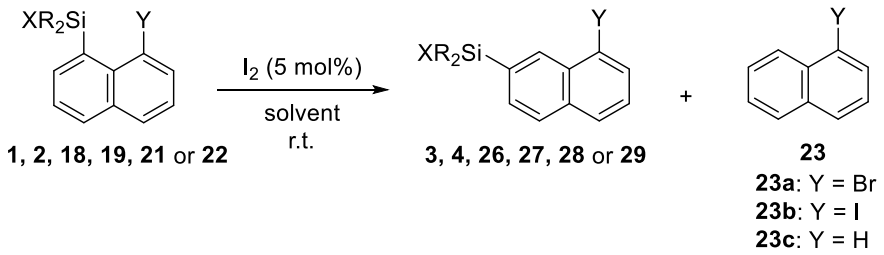

	R	X	Y	solvent	time (min)	products (yield (%))[a)]		
1a	Me	H	Br	$CDCl_3$	1	**1a** (0)	**3a** (33)	**23a** (64)
1a	Me	H	Br	C_6D_6	5	**1a** (0)	**3a** (41)	**23a** (56)
1b	Me	H	I	$CDCl_3$	1	**1b** (0)	**3b** (46)	**23b** (35)
1b	Me	H	I	C_6D_6	3	**1b** (0)	**3b** (81)	**23b** (19)
2a	Ph	H	Br	$CDCl_3$	1	**2a** (45)	**4a** (21)	**23a** (34)
2b	Ph	H	I	$CDCl_3$	1	**2b** (30)	**4b** (10)	**23b** (56)
18a	Mes	Me	Br	C_6D_6	5	**18a** (100)	**26a** (0)	**23a** (0)
19a	Me	Me	Br	C_6D_6	5	**19a** (100)	**27a** (0)	**23a** (0)
21	Me	Me	H	C_6D_6	5	**21** (100)	**28** (0)	**23c** (0)
22	Me	Me	OMe	C_6D_6	5	**22** (80)	**29** (0)	**23c** (20)

a) The yields were estimated from the ^{1}H NMR spectra using cyclohexane as an internal standard.

The migrated products were obtained in higher yields in hexane and C_6D_6 than in $CDCl_3$. Dimethylsilyl derivatives **1** produced the migrated products in higher yields than diphenylsilyl derivatives **2**. Thus, the migration reactions of **1** and **2** were also performed in a reaction flask in hexane or hexane-toluene, and migrated products **3** and **4** were isolated in 38%–83% yields, as summarized in Table 2.

Table 2. 1,2-Silyl migration reactions in a flask to isolate **3** and **4**.

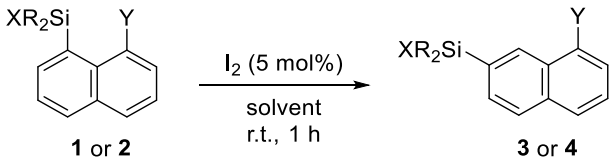

	R	X	Y	solvent	products	yield (%)[a]
1a	Me	H	Br	hexane	**3a**	43
1b	Me	H	I	hexane	**3b**	83
2a	Ph	H	Br	hexane-toluene	**4a**	40
2b	Ph	H	I	hexane-toluene	**4b**	38

[a] Isolated yields.

2.4 Structures of 1-halo-8-silylnaphthalenes

The driving force for silyl migration may be relief of steric compression, as discussed for the reactions of 1,2-disilylbenzenes, 1,2-disilylnaphthalene, and 1-silylnaphthalene.[2,3,12]

Steric repulsion in **1** was supported by the NMR spectra. The ^{1}H resonances of the proton on the silicon atom in **1** and **2** were deshielded, whereas the ^{29}Si resonances of the silicon atom of the hydrosilyl group were shielded compared with the corresponding values of silylnaphthalenes **21** and **30**, respectively, as shown in Table 3. This behavior can be explained in terms of the van der Waals effect[13]; the steric repulsion between the hydrosilyl group and the halogen atom causes a decrease in the electron density on the hydrogen atom and an increase in the electron density on the silicon atom. The van der Waals effect was also indicated by the IR spectra (Table 3); the ν(Si−H) absorptions in **1** and **2** appeared at higher frequencies than those in **23** and **30**, respectively.

Table 3. Selected ^{1}H and ^{29}Si resonances in **1**, **2**, **21**, and **30**

	R	X	Y	^{1}H (δ)	^{29}Si (δ)	ν(Si-H) (cm^{-1})
1a	Me	H	Br	5.19	−13.4	2164
1b	Me	H	I	5.66	−18.8	2158
2a	Ph	H	Br	6.43	−17.0	2162
2b	Ph	H	I	6.90	−17.8	2137
21	Me	H	H	4.96	−20.4	2123
30	Ph	H	H	5.92	−20.6	2108

The molecular structures of **2a** and **2b** were revealed by X-ray crystallographic analysis (Figure 3).[14,15] Each molecule is distorted owing to the steric repulsion between the halogen atom and the silyl group. The substituents are not coplanar with the naphthalene ring. The dihedral angles of Si−C8−C1−Y are 23.6° (Y = Br (**2a**)) and 27.5° (Y = I (**2b**)). The atomic distance between Si and Y (3.22 Å (Y = Br (**2a**)); 3.42 Å (Y = I (**2b**)) is longer than the mean distance between C1 and C8 on the naphthalene ring.

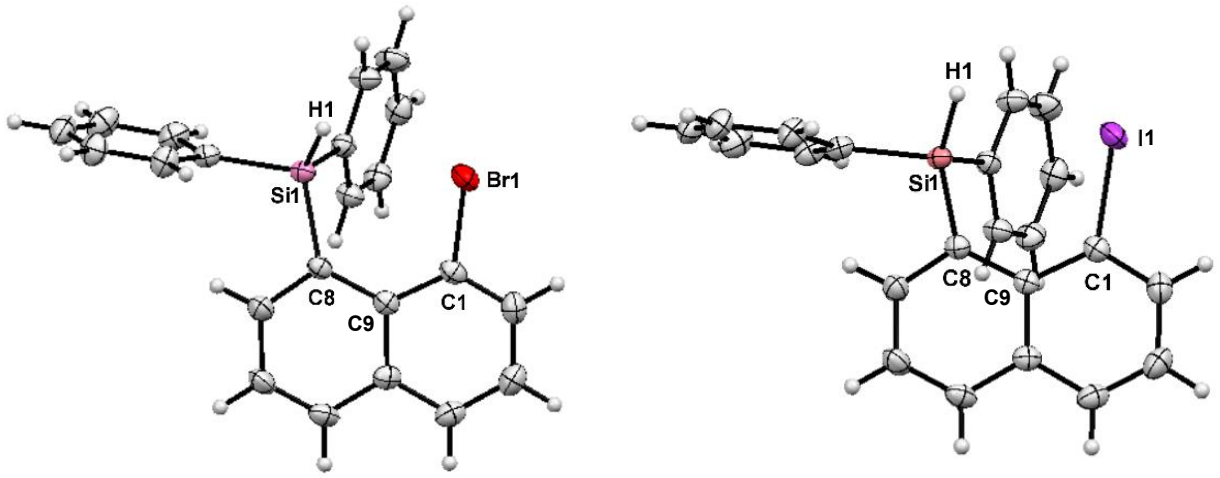

Figure 3. Crystal structure of **2a** (left) and **2b** (right) at the 30% probability level. Selected bond lengths (Å) and angles (deg): **2a**, Si1−H1, 1.256(2); Br1−C1, 1.9011(1); Si1−C8, 1.895(1); Si1−Br1, 3.22; Si1−C8−C9, 127.49(1); C9−C1−Br1, 121.54(1); Si1−C8−C1−Br1, 23.58. **2b**, Si−H1, 1.412(2); I1−C1, 2.104(1); Si1−C8, 1.900(1); Si1−I1, 3.42; Si1−C8−C9, 127.91(1); C9−C1−I1, 123.71(1); Si1−C8−C1−Br, 27.53.

DFT calculations also supported the existence of steric repulsion.[16] The structures of **1a**, **1b**, **3a** and **3b** were optimized at the B3LYP/6-31G(d)+LANL2DZ level of theory, as shown in Figure 4. 7-Silylnaphthalene **3** is more stable than 8-silylnaphthalene **1** by 15.6–56.3 kcal/mol. 8-Silylnaphthalene **1** was highly distorted, such extent that the dihedral angle of Si−C8−C1−I is 11.3° (Y = Br (**1a**)) and 24.4° (Y = I (**1b**)). In contrast, 7-silylnaphthalene **3** is almost planar, as the dihedral angle of Si−C7−C1−Y (Y = Br (**3a**) and Y = I (**3b**)) were 0°, respectively.

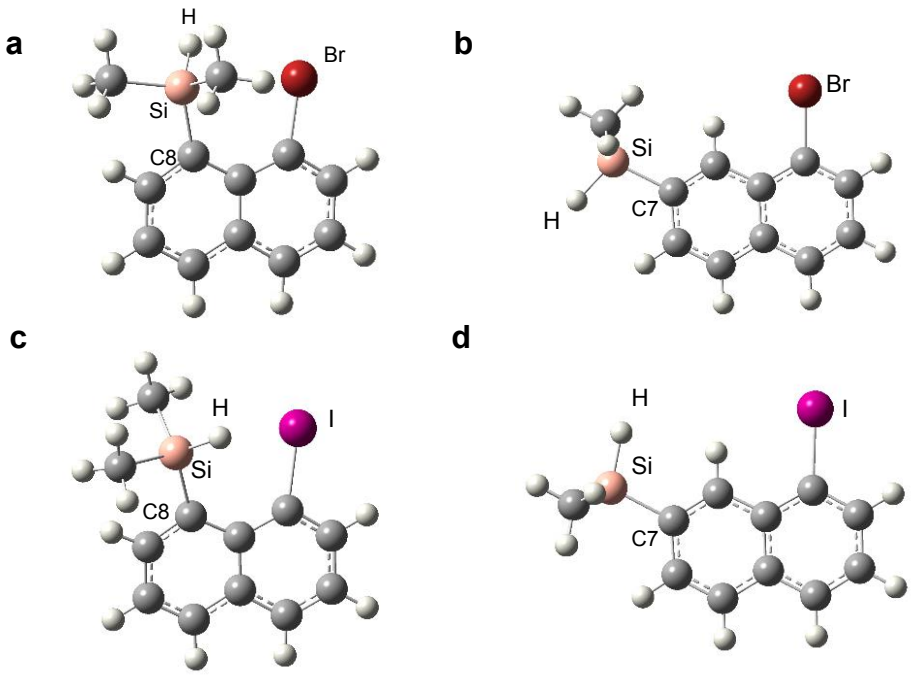

Figure 4. Optimized structures of (a) **1a**, (b) **3a**, (c) **1b** and (d) **3b**.

2.5 Reaction mechanism of silyl migration

To gain further insight into the reaction mechanism of silyl migration, D-labeling experiments were performed (Scheme 11). Deuterated silane **1a-D** was treated with I_2 under the conditions used for the nondeuterated compounds. In the presence of 4 mol% I_2, **3a-D** (56%), **23a-D** (5%), and **23a** (37% yield) were obtained. In contrast, when 50 mol% I_2 was used, **23a-D** (52%) and **23a** (43%) were obtained, but **3a-D** was not obtained.

Scheme 11. D-labeling experiment for 1,2-silyl migration in **1a-D**.

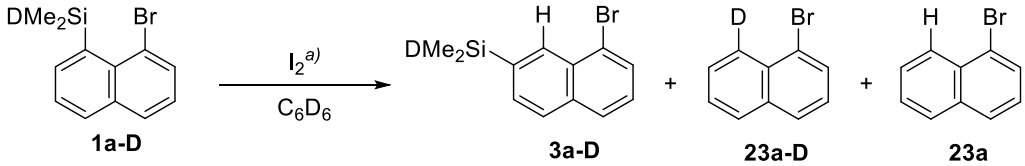

	3a-D	23a-D	23a
a) 4 mol%:	56%	5%	37%
a) 50 mol%:	0%	52%	43%

According to the literature[2,3,9] and the D-labeling experiments, the reaction mechanism is postulated as follows (Scheme 12). (i) Reaction of **1-D$_{Si}$** with catalytic amounts of I_2 affords iodosilylnaphthalene **1-I** and **DI**.[14] (ii) Reaction of **1-D$_{Si}$** with **DI** yields Wheland complex **IntA-D$_{Si}$D**.[16] (iii) A hydrosilyl group in **IntA-D$_{Si}$D** migrates to the cationic carbon at the 7-position to form **IntB-D$_{Si}$D**. (iv) Iodide (or another nucleophile) attacks the hydrogen at the 7-position in **IntB-D$_{Si}$D** to afford **3-D$_{Si}$D**. Alternatively, iodide (or another nucleophile) attacks the silyl group in **IntA-D$_{Si}$D** to produce desilylated naphthalene **23-D**. After **DI** is consumed, **1-D$_{Si}$** reacts with HI to form **IntA-D$_{Si}$H**, **IntB-D$_{Si}$H**, and finally **3-D$_{Si}$H** in manners similar to the reaction of **1-D$_{Si}$** with **DI**. D-

incorporation into the naphthalene ring is induced only by **DI**, which is generated by the reaction of **1-D**$_{Si}$ and I_2 in the initial step. Thus, the extent of D-incorporation depends on the amount of I_2.

Scheme 12. Plausible mechanism of 1,2-silyl migration in **1-D**.

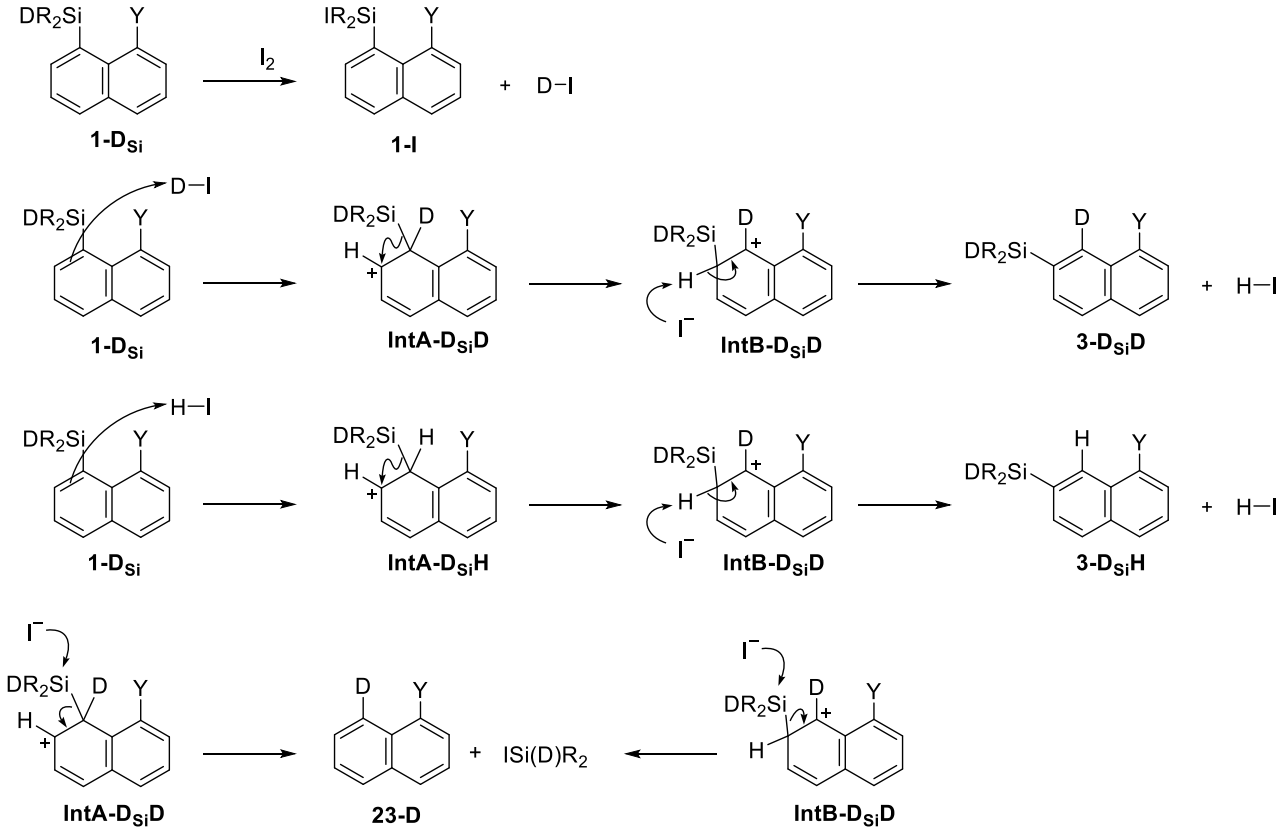

3. Conclusion

1-Halo-8-(hydrosilyl)naphthalenes **1** and **2** underwent 1,2-silyl migration to afford 1-halo-7-silylnaphthalenes **3** and **4**. The driving force for the silyl migration may be relief of steric compression, which was supported by the NMR spectra and DFT calculations. D-labeling experiments were also performed to obtain further insight into the reaction mechanism of silyl migration. It was postulated that the migration process may include four steps: (i) generation of acid (HI) by the reaction of the hydrosilane with I_2, (ii) protonation of the naphthalene ring, (iii) silyl group migration in the protonated intermediate, and (iv) deprotonation of the naphthalene ring.

4. Experimental section

4.1 General considerations

^{1}H (400 MHz), ^{13}C (100 MHz), and ^{29}Si (79.5 MHz) NMR spectra were recorded using a Bruker Avance III 400 spectrometer. ^{1}H and ^{13}C chemical shifts were referenced to the internal $CDCl_3$ (δ (^{1}H) = 7.26 ppm; δ(^{13}C) = 77.00 ppm). ^{29}Si chemical shifts were referenced to external tetramethylsilane (δ = 0 ppm). The mass spectra (EI) were recorded 70 eV using a JEOL JMS-Q1000GC Mk II mass spectrometer and the elemental analyses were performed using the JSL MICRO CORDER JM10 elemental analyzer. Column chromatography was performed using silica gel 60N (63–210 mesh, Kanto Chemical Co., Inc.). Thin layer chromatography (TLC) was performed on plates of silica gel 60 F_{254} (Merck).

4.2 Materials

1-Bromonaphthalene (Tokyo Chemical Industry Co., Ltd.), *n*-butyllithium in hexane (Kanto Chemical Co., Inc.), chlorodiphenylsilane (Shin-Etsu Chemical Co., Ltd.), lithium aluminum hydride (Wako Pure Chemical Industries, Ltd.), and TCCA (Wako Pure Chemical Industries, Ltd.) were used as received. Chlorodimethylsilane (Tokyo Chemical Industry Co., Ltd.) and dichlorodimethylsilane (Tokyo Chemical Industry Co., Ltd.) were distilled under a nitrogen atmosphere over calcium hydride. Chlorotrimethylsilane (Tokyo Chemical Industry Co., Ltd.) was treated with small pieces of sodium under a nitrogen atmosphere to remove dissolved HCl, and the supernatant was used. Triethylamine (Tokyo Chemical Industry Co., Ltd.) was distilled under a nitrogen atmosphere over calcium hydride.

Chlorodimesitylsilane and 1-iodo-8-methoxynaphthalene were prepared according to the literature method.[16,17] THF and Et_2O were distilled under a nitrogen atmosphere over sodium benzophenone ketyl. Hexane was distilled under a nitrogen atmosphere over sodium. All reactions were carried out under an inert gas atmosphere.

4.3 Experimental details

Chloromethoxydimethylsilane (10a)[18] (CAS No. 1825-68-9). To a mixture of MeOH (2.1 mL, 52.7 mmol) and dichlorodimethylsilane (6.0 mL, 50.2 mmol) in pentane (50 mL) was added dropwise Et_3N (8.0 mL, 57.7 mmol) in pentane (10 mL) at 0 °C. The mixture was stirred at room temperature for 2 h, and filtered. The filtrate was concentrated (350 mmHg) and the residue was distilled (55–58 °C) to obtain **10a** (4.2 g, 67% yield, 87% purity) as a colorless oil. ^{1}H NMR ($CDCl_3$, δ) 0.47 (s, 6H), 3.54 (s, 3H). ^{13}C{^{1}H} NMR (C_6D_6, δ) 2.91, 58.90. ^{29}Si{^{1}H} NMR (C_6D_6, δ) 16.24. MS(EI) *m/z* 126 ($M^+[^{37}Cl]$, 1), 124 ($M^+[^{35}Cl]$, 4), 111 ($M^+[^{37}Cl]$−Me, 37), 109 ($M^+[^{35}Cl]$−Me, 100), 81 ($M^+[^{37}Cl]$−Me−OMe, 38), 79 ($M^+[^{35}Cl]$−Me−OMe, 14).

Chloro(isopropoxy)dimethylsilane (10b)[18] (CAS No. 1825-71-4). To a mixture of *i*-PrOH (4.1 mL, 52.7mmol) and dichlorodimethylsilane (6.0 mL, 50.2 mmol) in THF (50 mL) was added dropwise Et_3N (8.0 mL, 57.7 mmol) in THF (20 mL) at 0 °C. The reaction mixture was stirred overnight at room temperature, diluted with hexane (60 mL) and filtered. The filtrate was concentrated (110 mmHg) and the residue was distilled (102–106 °C) to obtain **10b** (4.2 g, 55% yield)

as a colorless oil. ^{1}H NMR ($CDCl_3$, δ) 0.46 (s, 6H), 1.21 (d, J = 6 Hz, 6H), 4.18 (sept, J = 6 Hz, 1H). ^{13}C{^{1}H} NMR (C_6D_6, δ) 4.90, 25.54, 66.06. ^{29}Si{^{1}H} NMR (C_6D_6, δ) 3.26.

Chloro(*tert*-butoxy)dimethylsilane (10c)[18] (CAS No. 58566-07-7). To a mixture of *t*-BuOH (2.4 mL, 25.1 mmol), dichlorodimethylsilane (3.0 mL, 25.1 mmol) and DMAP (3.1 g, 2.5 mmol) in THF (25 mL) was added Et_3N (4.2 mL, 30.1 mmol) in THF (10 mL) at 0 °C. The reaction mixture was stirred overnight at room temperature, diluted with hexane (35 mL) and filtered. The filtrate was concentrated (110 mmHg) and the residue was distilled (104–106 °C) to obtain **10c** (1.6 g, 53% yield) as a colorless oil. ^{1}H NMR ($CDCl_3$, δ) 0.46 (s, 6H), 1.34 (s, 9H). ^{13}C{^{1}H} NMR (C_6D_6, δ) 4.80, 31.69, 75.09. ^{29}Si{^{1}H} NMR (C_6D_6, δ) 3.26.

Chloro(diethylamino)dimethylsilane (10d)[18] (CAS No. 6026-02-4). This compound was prepared in a manner similar to that used for **10b** and obtained as a colorless oil (4.7 g, 58% yield) after distillation (150–153 °C). ^{1}H NMR ($CDCl_3$, δ) 0.46 (s, 6H), 1.03 (t, J = 7 H, 6H), 2.88 (q, J = 7 H, 4H). ^{13}C{^{1}H} NMR (C_6D_6, δ) 1.92, 15.36, 40.07. ^{29}Si{^{1}H} NMR (C_6D_6, δ) 11.55.

2-Bromo-2'-[(methoxy)dimethylsilyl]biphenyl (11a). A solution of *n*-BuLi in hexane (1.60 mol/L, 1.40 mL, 2.20 mmol) was added dropwise to a solution of 2,2'-dibromobiphenyl (624 mg, 2.00 mmol) in THF (15 mL) and Et_2O (5 mL) at −78 °C. After the reaction mixture was stirred at this temperature for 1 h, **10a** (274 mg, 2.20 mmol) was added via a syringe. Then the mixture was warmed to room temperature. The solvent was removed in vacuo and the residue was subjected to column chromatography on silica gel eluted with hexane-AcOEt (20:1) (R_f = 0.12) to give **11a** (409 mg, 70% yield) as a colorless oil. ^{1}H NMR ($CDCl_3$, δ) −0.01 (s, 3H), 0.03 (s, 3H), 3.36 (s, 3H),

7.19–7.21 (m, 1H), 7.23–7.25 (m, 1H), 7.28 (dd, J = 8 Hz, J = 2 Hz, 1H), 7.34 (ddd, J = 8 Hz, J = 8 Hz, J = 1 Hz, 1H), 7.40–7.47(m, 2H), 7.64 (dd, J = 8 Hz, J = 1 Hz, 1H), 7.73–7.76 (m, 1H). $^{13}C\{^1H\}$ NMR ($CDCl_3$, δ) −1.91, −0.74, 50.46, 124.10, 126.56, 126.91, 128.99, 129.02, 129.85, 131.57, 132.36, 134.61, 136.17, 143.95, 147.20. $^{29}Si\{^1H\}$ NMR ($CDCl_3$, δ) 9.15. MS(EI) *m/z* 307 ($M^+[^{81}Br]$−Me, 100), 307 ($M^+[^{81}Br]$−Me, 98), 292 ($M^+[^{81}Br]$−2Me, 25), 290 ($M^+[^{79}Br]$−2Me, 23), 275 ($M^+[^{81}Br]$−OMe−Me, 55), 275 ($M^+[^{79}Br]$−OMe−Me, 52).

2-Bromo-2'-[(isopropoxy)dimethylsilyl]biphenyl (11b). This compound was prepared in a manner similar to that used for **11a** and obtained as a colorless oil (419 mg, 60% yield) after column chromatography on silica gel eluted with hexane-AcOEt (20:1) (R_f = 0.16). ^1H NMR ($CDCl_3$, δ) −0.08 (s, 3H), 0.06 (s, 3H), 1.11 (d, J = 4 Hz, 3H), 1.12 (d, J = 4 Hz, 3H), 3.96 (sept, J = 6 Hz, 1H), 7.17–7.24 (m, 2H), 7.30–7.32 (m, 2H), 7.39–7.44 (m, 2H), 7.61–7.64 (m, 1H), 7.80–7.82 (m, 1H). $^{13}C\{^1H\}$ NMR ($CDCl_3$, δ) −0.50, 0.13, 25.68, 25.71, 65.12, 124.18, 126.53, 126.81, 128.80, 128.92, 129.76, 131.81, 132.31, 134.86, 136.99, 144.15, 147.00. $^{29}Si\{^1H\}$ NMR ($CDCl_3$, δ) 4.38. MS(EI) *m/z* 337 (M^+ $[^{79}Br]$−Me, 98), 335 (M^+ $[^{81}Br]$−Me, 100), 275 ($M^+[^{81}Br]$−Me−O*i*-Pr, 54), 273 ($M^+[^{79}Br]$−Me−O*i*-Pr, 41).

2-Bromo-2'-[(*tert*-butoxy)dimethylsilyl]biphenyl (11c). This compound was prepared in a manner similar to that used for **11a** and obtained as a colorless oil (371 mg, 51% yield) after column chromatography on silica gel eluted with hexane-AcOEt (20:1) (R_f = 0.38). ^1H NMR ($CDCl_3$, δ) −0.04 (s, 3H), 0.12 (s, 3H), 1.21 (s, 9H), 7.14–7.16 (m, 1H), 7.19–7.23 (m, 1H), 7.29–7.35 (m, 2H), 7.38–7.41 (m, 2H), 7.62 (dd, J = 8 Hz, J = 1 Hz, 1H), 7.80–7.82 (m, 1H). $^{13}C\{^1H\}$ NMR ($CDCl_3$,

δ) 2.24, 2.66, 32.00, 72.77, 124.22, 126.37, 126.70, 128.44, 128.77, 129.77, 132.05, 132.24, 134.84, 138.58, 144.31, 146.68. $^{29}Si\{^{1}H\}$ NMR ($CDCl_3$, δ) −2.28. MS(EI) *m/z* 349 ($M^+[^{81}Br]$−Me, 91), 347 ($M^+[^{79}Br]$−Me, 86), 291 (M^+−Me−*t*-Bu, 100), 275 ($M^+[^{81}Br]$−Me−O*t*-Bu, 38), 273 ($M^+[^{79}Br]$−Me−O*t*-Bu, 36), 211 (M^+−O*t*-Bu−Br, 64). Anal. Calcd for $C_{18}H_{23}BrOSi$: C, 59.50; H, 6.38; Found: C, 59.47; H, 6.34.

2-Bromo-2'-[(diethylamino)dimethylsilyl]biphenyl (11d). This compound was prepared in a manner similar to that used for **11a** and obtained as a colorless oil (471g, 65% yield) after bulb to bulb distillation (140–150 °C/0.85 mmHg). ^{1}H NMR ($CDCl_3$, δ) −0.13 (s, 3H), 0.00 (s, 3H), 0.92 (t, *J* = 7 Hz, 6H), 2.72 (q, *J* = 7 Hz, 4H), 7.11–7.14 (m, 1H), 7.17–7.21 (m, 1H), 7.23–7.31 (m, 2H), 7.36–7.38 (m, 2H), 7.61 (dd, *J* = 8 Hz, *J* = 1 Hz, 1H), 7.70–7.72 (m, 1H). $^{13}C\{^{1}H\}$ NMR ($CDCl_3$, δ) −0.17, 0.40, 124.83, 126.56, 127.07, 128.87, 128.96, 130.45, 132.04, 132.67, 135.70, 138.52, 145.18, 147.76. $^{29}Si\{^{1}H\}$ NMR ($CDCl_3$, δ) −1.84. MS(EI) m/z 363 ($M^+[^{81}Br]$, 6), 361 ($M^+[^{79}Br]$, 7), 348 ($M^+[^{81}Br]$−Me, 44), 346 ($M^+[^{79}Br]$−Me, 43), 291 ($M^+[^{81}Br]$−NEt_2, 100), 289 ($M^+[^{79}Br]$−NEt_2, 98).

2-Bromo-2'-(dimethylsilyl)biphenyl (10e). This compound was prepared in a manner similar to that used for **11a** and obtained as a colorless oil (470 mg, 81% yield) after column chromatography on silica gel eluted with hexane (R_f = 0.55). ^{1}H NMR ($CDCl_3$, δ) 0.06 (d, *J* = 4 Hz, 3H), 0.07 (d, *J* = 4 Hz, 3H), 4.14 (sept, *J* = 4 Hz, 1H), 7.17–7.22 (m, 2H), 7.23 (dd, *J* = 8 Hz, *J* = 2 Hz, 1H), 7.31 (ddd, *J* = 8 Hz, *J* = 1 Hz, *J* = 1 Hz, 1H), 7.37 (ddd, *J* = 8 Hz, *J* = 8 Hz, *J* = 1 Hz, 1H), 7.41 (ddd, *J* = 8 Hz, *J* = 8 Hz, *J* = 1 Hz, 1H), 7.61–7.64 (m, 2H). $^{13}C\{^{1}H\}$ NMR ($CDCl_3$, δ) −3.39, −3.23, 124.09,

126.63, 126.99, 128.78, 128.95, 129.37, 131.45, 132.36, 134.75, 136.20, 143.61, 147.70. ^{29}Si NMR ($CDCl_3$, δ) −18.50 (d, $^1J_{Si\text{-}H}$ = 184 Hz). MS(EI) *m/z* 277 ($M^+[^{81}Br]$−Me, 5), 275 ($M^+[^{81}Br]$−Me, 7), 211 (M^+−Br, 80), 195 (M^+−Me−Br, 100).

2-Bromo-2'-[(isopropoxy)dimethylsilyl]binaphthyl (12b). A solution of *n*-BuLi in hexane (1.60 mol/L, 0.69 mL, 1.10 mmol) was added dropwise to a solution of 2,2'-dibromobinaphthyl (412 mg, 1.00 mmol) in THF (15 mL) at −78 °C. After the reaction mixture was stirred at this temperature for 1 h, **10b** (183 mg, 1.20 mmol) was added via a syringe. Then the mixture was warmed to room temperature. The solvent was removed in vacuo and the residue was subjected to column chromatography on silica gel eluted with hexane-AcOEt (20:1) (R_f = 0.60) to give **12b** (180 mg, 40% yield) as a pale yellow oil ^{1}H NMR ($CDCl_3$, δ) −0.41 (s, 3H), −0.16 (s, 3H), 1.03 (d, *J* = 6 Hz, 6H), 3.89 (sept, *J* = 6 Hz, 1H), 7.10 (dd, *J* = 8 Hz, *J* = 1 Hz, 2H), 7.23–7.28 (m, 2H), 7.45–7.50 (m, 2H), 7.77 (d, *J* = 8 Hz, 1H), 7.84 (d, *J* = 8 Hz, 1H), 7.91 (t, *J* = 8 Hz, 2H), 7.99 (d, *J* = 8 Hz, 1H), 8.01 (d, *J* = 8 Hz, 1H). ^{13}C{^{1}H} NMR ($CDCl_3$, δ) −0.43, −0.28, 25.58, 65.08, 123.48, 125.92, 126.13, 126.27, 126.49, 126.82, 127.02, 127.12, 127.86, 127.98, 129.33, 129.79, 131.00, 131.76, 132.13, 133.95, 135.03, 136.46, 138.81, 143.03. ^{29}Si{^{1}H} NMR ($CDCl_3$, δ) 4.79. MS(EI) *m/z* 450 ($M^+[^{81}Br]$, 30), 448 ($M^+[^{79}Br]$, 28), 435 ($M^+[^{81}Br]$−Me, 47), 433 ($M^+[^{79}Br]$−Me, 43), 311 (M^+−Me−*i*-Pr−Br, 49), 252 (M^+−Si−Br, 100).

2-Bromo-2'-(dimethylsilyl)binaphthyl (12e). A solution of *n*-BuLi in hexane (1.60 mol/L, 0.69 mL, 1.10 mmol) was added dropwise to a solution of 2,2'-dibromobinaphthyl (412 mg, 1.00 mmol) in THF (15 mL) at −78 °C. After the reaction mixture was stirred at this temperature for 1

h, chlorodimethylsilane (0.13 mL, 1.20 mmol) was added via a syringe. Then the mixture was warmed to room temperature. The solvent was removed in vacuo and the residue was subjected to column chromatography on silica gel eluted with hexane (R_f = 0.20) to give **12e** (352 mg, 90% yield) as a colorless crystal. ^{1}H NMR ($CDCl_3$, δ) −0.10 (d, *J* = 4 Hz, 3H), −0.01 (d, *J* = 4 Hz, 3H), 3.82 (sept, *J* = 4 Hz, 1H), 7.07 (dd, *J* = 8 Hz, *J* = 1 Hz, 1H), 7.13 (dd, *J* = 8 Hz, *J* = 1 Hz, 1H), 7.25 (ddd, *J* = 8 Hz, *J* = 7 Hz, *J* = 1 Hz, 1H), 7.27 (ddd, *J* = 8 Hz, *J* = 7 Hz, *J* = 1 Hz, 1H), 7.45–7.50 (m, 2H), 7.78 (d, *J* = 8 Hz, 2H), 7.84 (d, *J* = 8 Hz, 1H), 7.91 (t, *J* = 8 Hz, 2H), 7.98 (d, *J* = 8 Hz, 1H). ^{13}C{^{1}H} NMR ($CDCl_3$, δ) −3.45, −3.44, 123.47, 125.78, 126.13, 126.42, 126.47, 126.88, 126.89, 127.32, 127.95, 128.07, 129.35, 129.79, 130.75, 131.79, 132.12, 133.91, 134.76, 135.18, 138.41, 144.05. ^{29}Si NMR ($CDCl_3$, δ) −18.35 (d, $^1J_{Si\text{-}H}$ = 193 Hz). MS(EI) *m/z* 392 (M^+[^{81}Br], 5), 390 (M^+[^{79}Br], 4), 311 (M^+−Br, 100), 295 (M^+−Br−2Me−H, 52).

A Typical Procedure for Preparation of 11 and reaction with Mes_2BF: Generation of 12. A solution of *tert*-BuLi in pentane (1.56 mol/L, 1.28 mL, 2.00 mmol) was added to a solution of **11** (1.00 mmol) in Et_2O (2 mL) at −78 °C over 1 min. After the reaction mixture was stirred at this temperature for 2 h, Mes_2BF (268 mg, 1.00 mmol) in Et_2O (2 mL) was added over 3 min. The reaction mixture was stirred at the same temperature for 1 h and then allowed to warm to room temperature. The solvent was removed in vacuo and the residue was subjected to column chromatography on silica gel eluted with hexane (R_f = 0.40) to give **12** as a colorless crystal. ^{1}H NMR ($CDCl_3$, δ) 0.42 (s, 6H), 7.28 (dd, *J* = 7 Hz, *J* = 1 Hz, 2H), 7.43 (ddd, *J* = 7 Hz, *J* = 1 Hz, *J* = 1 Hz, 2H), 7.63 (ddd, *J* = 7 Hz, *J* = 2 Hz, *J* = 1 Hz, 2H), 7.82 (d, *J* = 8 Hz, 2H). ^{13}C{^{1}H} NMR ($CDCl_3$,

δ) −3.28, 120.79, 127.31, 130.14, 132.69, 138.89, 147.77. $^{29}Si\{^{1}H\}$ NMR ($CDCl_3$, δ) 0.44. MS(EI) *m/z* 210 (M^+, 50), 195 (M^+−Me, 100).

A Typical Procedure for Preparation of 14 and reaction with Mes_2BF: Generation of 15. A solution of *tert*-BuLi in pentane (1.56 mol/L, 1.28 mL, 2.00 mmol) was added to a solution of **14** (1.00 mmol) in Et_2O (2 mL) at −78 °C over 1 min. After the reaction mixture was stirred at this temperature for 2 h, Mes_2BF (268 mg, 1.00 mmol) in Et_2O (2 mL) was added over 3 min. The reaction mixture was stirred at the same temperature for 1 h and then allowed to warm to room temperature. The solvent was removed in vacuo and the residue was subjected to column chromatography on silica gel eluted with hexane (R_f = 0.30) to give **0** as a colorless crystal. ^{1}H NMR ($CDCl_3$, δ) 0.47 (s, 6H), 7.38 (ddd, *J* = 8 Hz, *J* = 1 Hz, *J* = 1 Hz, 2H), 7.51 (ddd, *J* = 8 Hz, *J* = 1 Hz, *J* = 1 Hz, 2H), 7.81 (d, *J* = 8 Hz, 2H), 7.89 (d, *J* = 8 Hz, 2H), 7.94 (d, *J* = 8 Hz, 2H), 7.99 (d, *J* = 8 Hz, 2H). $^{13}C\{^{1}H\}$ NMR ($CDCl_3$, δ) −3.33, 124.26, 125.73, 127.81, 127.89, 128.26, 128.48, 129.71, 135.71, 139.86, 147.11. $^{29}Si\{^{1}H\}$ NMR ($CDCl_3$, δ) 3.07. MS(EI) *m/z* 310 (M^+, 100), 295 (M^+−Me, 31), 252 (M^+−$SiMe_2$, 19).

1,8-Dibromonaphthalene (16a)[6] (CAS No. 17135-74-9). To 1,8-diaminonaphthalene (4.75 g, 30.0 mmol) in 7 mol/L H_2SO_4 (60 mL) at −10 °C with stirring, $NaNO_2$ (6.62 g, 96.0 mmol) in H_2O (24 mL) was added, and the temperature was maintained at −10 °C. As soon as the addition was completed, CuBr (12.9 g, 90.0 mmol) in HBr (20 mL) solution was added dropwise over 15 min. The solution was stirred at 80 ºC for 30 min, and allowed to cool to room temperature. The reaction mixture was neutralized with saturated NaOH solution at 0 °C. The reaction mixture was filtered

and the residue stirred with CH_2Cl_2 (50 mL) at room temperature overnight. The resulting solution was filtered and the filtrate was washed with H_2O (20 mL×3). After drying (Na_2SO_4), the solvent was removed in vacuo, and the residue was subjected to column chromatography on silica gel eluted with hexane (R_f = 0.45) to give **16a** (4.00 g, 23% yield) as a pale yellow crystal. ^{1}H NMR ($CDCl_3$, δ) 7.27 (t, J = 8 Hz, 2H), 7.82 (dd, J = 8 Hz, J = 1 Hz, 2H), 7.94 (dd, J = 8 Hz, J = 1 Hz, 2H). ^{13}C{^{1}H} NMR (C6D6, δ) 119.32, 126.21, 128.64, 129.48, 135.12, 136.83. MS(EI) *m/z* 288 ($M^+[^{81}Br][^{81}Br]$, 48), 286 ($M^+[^{81}Br][^{79}Br]$, 100), 284 ($M^+[^{79}Br][^{79}Br]$, 52), 207 ($M^+[^{81}Br]-Br[^{79}Br]$, 21), 205 ($M^+[^{79}Br]-Br[^{81}Br]$, 22), 126 (M^+-2Br, 54).

1,8-Diiodonaphthalene (16b)[7] (CAS No. 1730-04-7). To 1,8-diaminonaphthalene (4.75 g, 30.0 mmol) in 7 mol/L H_2SO_4 (60 mL) at −10 °C with stirring, $NaNO_2$ (6.62 g, 96.0 mmol) in H_2O (24 mL) was added, and the temperature was maintained at −10 °C. As soon as the addition was completed, KI (31.9 g, 192.0 mmol) in H_2O (30 mL) was added dropwise over 5 min. Afterwards it was quickly heated to 80 °C for a short time. Subsequently, the reaction mixture was cooled to room temperature, and neutralized with saturated NaOH solution at 0 °C. The reaction mixture was filtered and the residue stirred with Et_2O (50 mL) at room temperature overnight. The resulting solution was filtered and the filtrate was washed with saturated $Na_2S_2O_3$ solution (20 mL×3). After drying (Na_2SO_4), the solvent was removed in vacuo to afford a brown solid that was filtered over silica gel with hexane-Et_2O (5:1) to obtain pale yellow solution. The solvent was removed in vacuo, and the residue was subjected to column chromatography on silica gel eluted with hexane (R_f = 0.43) to give **16b** (3.06 g, 27% yield) as a pale yellow crystal. ^{1}H NMR ($CDCl_3$, δ) 7.08 (dd, J = 8 Hz, J

= 8 Hz, 2H), 7.85 (dd, J = 8 Hz, J = 1 Hz, 2H), 8.43 (dd, J = 8 Hz, J = 1 Hz, 2H). $^{13}C\{^1H\}$ NMR ($CDCl_3$, δ) 95.62, 126.93, 131.00, 132.36, 135.90, 144.03. MS(EI) *m/z* 380 (M^+, 100), 253 (M^+−I, 61), 341 (M^+−2I, 51).

1-Bromo-8-(dimethylsilyl)naphthalene (1a) (CAS No. 1313372-01-8). A solution of n-BuLi in hexane (1.64 mol/L, 2.68 mL, 4.40 mmol) was added dropwise to a solution of **7a** (1.14 g, 4.00 mmol) in Et_2O (40 mL) at −78 °C. After the reaction mixture was stirred at this temperature for 1 h, chlorodimethylsilane (0.50 mL, 4.50 mmol) was added via a syringe. Then the mixture was warmed to room temperature. The solvent was removed in vacuo and the residue (1161 mg) was subjected to column chromatography on silica gel eluted with hexane (R_f = 0.52) to give **1a** (891 mg, 84% yield) as a colorless oil. ^1H NMR ($CDCl_3$, δ) 0.60 (d, J = 4 Hz, 6H), 5.19 (sept, J = 4 Hz, 1H), 7.30 (dd, J = 8 Hz, J = 7 Hz, 1H), 7.46 (dd, J = 7 Hz, J = 1 Hz, 1H), 7.84 (dd, J = 8 Hz, J = 1 Hz, 1H), 7.87 (dd, J = 8 Hz, J = 1 Hz, 1H), 7.88 (dd, J = 7 Hz, J = 1 Hz, 1H), 8.02 (dd, J = 7 Hz, J = 1 Hz, 1H). $^{13}C\{^1H\}$ NMR ($CDCl_3$, δ) 0.94, 123.16, 125.43, 125.83, 129.43, 131.25, 132.26, 136.00, 136.63, 136.76, 138.49. ^{29}Si NMR ($CDCl_3$, δ) −13.43 (d, $^1J_{Si\text{-}H}$ = 199 Hz). MS(EI) m/z: 266 ($M^+[^{81}Br]$, 28), 264 ($M^+[^{79}Br]$, 28), 251 ($M^+[^{79}Br]$−Me, 98), 249 ($M^+[^{81}Br]$−Me, 100), 169 (M^+−Me−Br, 71). IR (Nujol) (cm^{-1}) 3025, 2723, 2164 (ν(Si-H)), 1597, 1377, 1250, 1149, 980, 918, 772, 723.

1-Iodo-8-(dimethylsilyl)naphthalene (1b) (CAS No. 105090-68-4). A solution of *n*-BuLi in hexane (1.60 mol/L, 2.06 mL, 3.30 mmol) was added dropwise to a solution of **7b** (1.14 g, 3.00 mmol) in THF-Et_2O (20 mL/20 mL) at −78 °C. After the reaction mixture was stirred at this temperature

for 1 h, chlorodimethylsilane (0.39 mL, 3.60 mmol) was added via a syringe. Then the mixture was warmed to room temperature. The reaction mixture was washed with brine, dried over Na_2SO_4, and concentrated in vacuo to give **1b** (850 mg, 91% yield) as a yellow oil. ^{1}H NMR ($CDCl_3$, δ) 0.60 (d, J = 4 Hz, 6H), 5.66 (sept, J = 4Hz, 1H), 7.12 (dd, J = 8 Hz, J = 7 Hz, 1H), 7.43 (dd, J = 8 Hz, J = 7 Hz, 1H), 7.79 (dd, J = 8 Hz, J = 1 Hz, 1H), 7.84 (dd, J = 7 Hz, J = 1 Hz, 1H), 7.96 (dd, J = 7 Hz, J = 1 Hz, 1H), 8.28 (dd, J = 7 Hz, J = 1 Hz, 1H). ^{13}C{^{1}H} NMR ($CDCl_3$, δ) 1.22, 96.96, 125.07, 126.33, 130.29, 131.43, 135.77, 138.37, 138.73, 139.80, 141.02. ^{29}Si NMR ($CDCl_3$, δ) −18.78 (d, $^1J_{Si\text{-}H}$ = 201 Hz). MS(EI) m/z: 312 (M^+, 27), 311 (M^+−H, 27), 297 (M^+−Me, 100), 169 (M^+−I, 46). IR (Nujol) (cm^{-1}) 3053, 2158 (ν(Si-H)), 1594, 1540, 1304, 1248, 1142, 1047, 974, 893, 783, 652.

1-(Dimesitylboryl)-7-(dimethylsilyl)naphthalene (17). A solution of *tert*-BuLi in pentane (1.56 mol/L, 3.8 mL, 6.00 mmol) was added to a solution of **1b** (645 mg, 3.00 mmol) in Et_2O (6 mL) at −78 °C over 4 min. After the reaction mixture was stirred at this temperature for 2 h, Mes_2BF (903 mg, 3.00 mmol) in Et_2O (6 mL) was added over 3 min. The reaction mixture was stirred at the same temperature for 1 h and then allowed to warm to room temperature. After the solvents were removed in vacuo, the residue was dissolved in hexane (10 mL) and filtered. The solvent was removed in vacuo, and the residue was subjected to column chromatography on silica gel eluted with hexane (R_f = 0.35) to give **17** (1.40 g, 54% yield) as a colorless crystal. ^{1}H NMR ($CDCl_3$, δ) 0.12 (d, J = 4 Hz, 6H), 2.00 (br, 12H), 2.32 (s, 6H), 4.33 (sept, J = 4 Hz, 1H), 6.82 (br, 4H), 7.43 (dd, J = 8 Hz, J = 7 Hz, 1H), 7.56 (ddd, J = 8 Hz, J = 8 Hz, J = 1 Hz, 2H), 7.82 (d, J = 8 Hz, 1H), 7.91 (d, J = 8 Hz, 1H), 8.03 (d, J = 1 Hz, 1H). ^{13}C{^{1}H} NMR ($CDCl_3$, δ) −4.33, 21.19, 23.06 (br), 125.97,

127.51, 128.39, 130.25, 131.68, 133.54, 134.52, 134.60, 134.87, 135.28, 138.94, 140.45 (br), 143.64 (br). ^{11}B NMR ($CDCl_3$, δ) 74 (br). ^{29}Si NMR ($CDCl_3$, δ) −17.43 (d, $^1J_{Si\text{-}H}$ = 194 Hz). MS(EI) *m/z* 434 (M^+, 7), 314 (M^+−Mes, 100), 299 (M^+−Mes−Me, 21), 255 (M^+−Mes−Si2MeH, 21). Anal. Calcd for $C_{30}H_{35}BSi$: C, 82.93; H, 8.12; Found: C, 82.85; H, 8.17.

1-Bromo-8-(diphenylsilyl)naphthalene (2a). This compound was prepared in a manner similar to that used for **1a** and obtained as a pale yellow solid after column chromatography on silica gel eluted with hexane (R_f = 0.25). The solid was recrystallized from hexane to give **2a** (1.28 g) as a pale yellow crystal in 82% yield. ^{1}H NMR ($CDCl_3$, δ) 6.43 (s, 1H), 7.30–7.42 (m, 8H), 7.49–7.52 (m, 4H), 7.78 (dd, *J* = 7 Hz, *J* = 1 Hz, 1H), 7.82 (dd, *J* = 7 Hz, *J* = 1 Hz, 1H), 7.86 (dd, *J* = 8 Hz, *J* = 1 Hz, 1H), 7.91 (dd, *J* = 8 Hz, *J* = 1 Hz, 1H). ^{13}C{^{1}H} NMR ($CDCl_3$, δ) 123.70, 125.43, 126.09, 127.88, 129.14, 129.43, 131.86, 132.45, 134.30, 135.63, 136.09, 137.05, 141.82 (signals corresponding to the two ipso carbons in the phenyl groups were not observed). ^{29}Si NMR ($CDCl_3$, δ) −16.98 (d, $^1J_{Si\text{-}H}$ = 213 Hz). MS(EI) m/z: 389 (M^+[^{81}Br], 4), 387 (M^+[^{79}Br], 4), 311 (M^+−Br, 100), 231 (M^+−Br−Ph, 81). IR (Nujol) (cm^{-1}) 2725, 2162 (ν(Si-H)), 1585, 1309, 1190, 1115, 974, 868, 818, 731, 696. Anal. Calcd for $C_{22}H_{17}BrSi$: C, 67.86; H, 4.40; Found: C, 67.73; H, 4.42.

1-Iodo-8-(diphenylsilyl)naphthalene (2b). This compound was prepared in a manner similar to that used for **1b** and obtained as a pale yellow solid after column chromatography on silica gel eluted with hexane (R_f = 0.30). The solid was recrystallized from hexane to give **2b** (1.27 g) as a pale yellow crystal in 73% yield. ^{1}H NMR ($CDCl_3$, δ) 6.90 (s, 1H), 7.15 (t, *J* = 8 Hz, 1H), 7.31–7.41 (m, 7H), 7.47–7.49 (m, 4H), 7.76 (d, *J* = 7 Hz, 1H), 7.84 (dd, *J* = 8 Hz, *J* = 1 Hz, 1H), 7.88 (dd,

J = 8 Hz, J = 1 Hz, 1H), 8.24 (dd, J = 7 Hz, J = 1 Hz, 1H). $^{13}C\{^1H\}$ NMR ($CDCl_3$, δ) 97.58, 125.08, 126.60, 127.91, 129.15, 130.33, 132.21, 134.30, 135.77, 137.23, 140.21, 141.21, 142.23 (signals corresponding to the two *ipso* carbons in the phenyl groups were not observed). ^{29}Si NMR ($CDCl_3$, δ) −17.83 (d, $^1J_{Si\text{-}H}$ = 215 Hz). MS(EI) m/z 435 (M^+−H, 4), 358 (M^+−Ph, 23), 307 (M^+−I, 11), 231 (M^+−Ph−I, 100). IR (Nujol) (cm^{-1}) 2727, 2137 (ν(Si-H)), 1604, 1300, 985, 857, 777, 729, 687. Anal. Calcd for $C_{22}H_{17}ISi$: C, 60.55; H, 3.93; Found: C, 60.36; H, 4.01.

1-Bromo-8-[(methoxy)dimethylsilyl]naphthalene (20a).[19] A solution of **1a** (248 mg, 0.94 mmol) in hexane (1.5 mL) was added dropwise to a suspension of TCCA (217 mg, 0.94 mmol) in hexane (0.5 mL) at 0 °C and the reaction mixture was stirred at room temperature for 6 h. After filtering the reaction mixture, the solvent was removed in vacuo to afford 1-bromo-8-[(chloro)dimethylsilyl]naphthalene (**25**) as a colorless oil. THF (2 mL), MeOH (0.04 mL, 1.06 mmol), and Et_3N (0.15 mL, 1.16 mmol) were added to the oil, which was then stirred for 1 h at room temperature. The solvent was removed in vacuo and the residue (389 mg) was subjected to column chromatography on silica gel eluted with hexane-AcOEt (20:1) (R_f = 0.50) to give **20a** (180 mg, 65% yield) as a colorless oil. ^1H NMR ($CDCl_3$, δ) 0.71 (s, 6H), 3.47 (s, 3H), 7.30 (dd, J = 8 Hz, J = 7 Hz, 1H), 7.51 (dd, J = 8 Hz, J = 7 Hz, 1H), 7.81–7.85 (m, 2H), 7.87 (dd, J = 7 Hz, J = 1 Hz, 1H), 8.20 (dd, J = 7 Hz, J = 1 Hz, 1H). $^{13}C\{^1H\}$ NMR ($CDCl_3$, δ) 2.69, 50.55, 122.09, 125.40, 125.70, 129.40, 131.15, 132.03, 136.11, 136.21, 136.90, 137.64. $^{29}Si\{^1H\}$ NMR ($CDCl_3$, δ) 6.73. MS(EI) m/z: 296 ($M^+[^{81}Br]$, 8), 294 ($M^+[^{79}Br]$, 7), 281 ($M^+[^{81}Br]$−Me, 100), 279 ($M^+[^{79}Br]$−Me, 98), 266 ($M^+[^{81}Br]$−2Me, 73), 264 ($M^+[^{79}Br]$−2Me, 71), 215 (M^+−Br, 91). IR (Nujol) (cm^{-1}) 3055, 1547,

1306, 1254, 1095, 978, 868, 814, 787. Anal. Calcd for $C_{13}H_{15}BrOSi$: C, 52.88; H, 5.12; Found: C, 52.64; H, 5.13.

1-Bromo-8-(trimethylsilyl)naphthalene (18a) (CAS No. 124153-82-8). A solution of *n*-BuLi in hexane (1.64 mol/L, 0.67 mL, 1.10 mmol) was added dropwise to a solution of **16a** (286 mg, 1.00 mmol) in THF (10 mL) at −78 °C. After the reaction mixture was stirred at this temperature for 1 h, chlorotrimethylsilane (0.15 mL, 1.20 mmol) was added via a syringe. Then, the mixture was warmed to room temperature. The solvent was removed in vacuo and the residue (343 mg) was subjected to column chromatography on silica gel eluted with hexane (R_f = 0.63) to give **18a** (217 mg, 78% yield) as a colorless oil. ^{1}H NMR ($CDCl_3$, δ) 0.60 (s, 9H), 7.30 (dd, *J* = 8 Hz, *J* = 7 Hz, 1H), 7.45 (dd, *J* = 8 Hz, *J* = 7 Hz, 1H), 7.82 (dd, *J* = 7 Hz, *J* = 1 Hz, 1H), 7.84 (dd, *J* = 7 Hz, *J* = 1 Hz, 1H), 7.89 (dd, *J* = 7 Hz, *J* = 1 Hz, 1H), 8.01 (dd, *J* = 7 Hz, *J* = 1 Hz, 1H). ^{13}C{^{1}H} NMR ($CDCl_3$, δ) 4.57, 122.35, 125.13, 125.61, 129.46, 130.83, 132.30, 136.06, 137.02, 137.65, 138.62. ^{29}Si{^{1}H} NMR ($CDCl_3$, δ) −2.70. MS(EI) m/z: 280 (M^+[^{81}Br], 12), 278 (M^+[^{79}Br], 11), 265 (M^+[^{81}Br]−Me, 100), 263 (M^+[^{79}Br]−Me, 98), 183 (M^+−Me−Br, 87). IR (Nujol) (cm^{-1}) 3055, 1547, 1493, 1304, 1250, 1192, 978, 870, 834, 766, 702.

1-Bromo-8-(dimesitylsilyl)naphthalene (19a). This compound was prepared in a manner similar to that used for **1a** and obtained as a pale yellow solid after column chromatography on silica gel eluted with hexane (R_f = 0.10). The solid was recrystallized from hexane to give **19a** (592 mg) as a pale yellow crystal in 49% yield. ^{1}H NMR ($CDCl_3$, δ) 2.12 (s, 12H), 2.82 (s, 6H), 6.63 (s, 1H), 6.80 (s, 4H), 7.30 (dd, *J* = 8 Hz, *J* = 7 Hz, 3H), 7.31 (dd, *J* = 8 Hz, *J* = 7 Hz, 1H), 7.84 (dd, *J* = 8 Hz,

J = 1 Hz, 1H), 7.85 (dd, J = 8 Hz, J = 1 Hz, 1H), 7.87 (dd, J = 7 Hz, J = 1 Hz, 1H), 7.88 (dd, J = 7 Hz, J = 1 Hz, 1H). $^{13}C\{^1H\}$ NMR ($CDCl_3$, δ) 21.13, 23.80, 124.09, 125.77, 125.91, 128.83, 129.51, 131.38, 132.52, 133.26, 135.97, 136.29, 137.00, 138.61, 139.86, 144.39. ^{29}Si NMR ($CDCl_3$, δ) −35.47 (d, $^1J_{Si\text{-}H}$ = 214 Hz). MS(EI) *m/z* (M^+, 100), 157 (M^+−Me, 36), 128 (M^+−$SiMeH_2$).

1-methoxy-8-(dimethylsilyl)naphthalene (22). This compound was prepared in a manner similar to that used for **1a** and obtained after column chromatography on silica gel eluted with hexane (R_f = 0.38) to give **22** (504 mg, 58% yield) as a colorless oil. ^1H NMR ($CDCl_3$, δ) 0.47 (d, J = 4 Hz, 6H), 4.00 (s, 3H), 4.74 (sept, J = 4 Hz, 1H), 6.87 (dd, J = 7 Hz, J = 1 Hz, 1H), 7.43 (t, J = 8 Hz, 1H), 7.48–7.52 (m, 2H), 7.87 (dd, J = 8 Hz, J = 1 Hz, 1H), 7.91 (dd, J = 7 Hz, J = 1 Hz, 1H). $^{13}C\{^1H\}$ NMR ($CDCl_3$, δ) −1.18, 54.09, 104.18, 121.25, 125.58, 125.81, 129.41, 129.61, 132.97, 134.68, 135.48, 156.00. ^{29}Si NMR ($CDCl_3$, δ) −12.55 (d, $^1J_{Si\text{-}H}$ =184 Hz). MS(EI) *m/z* 216 (M^+, 60), 201 (M^+−Me, 95), 186 (M^+−2Me, 100).

1-Bromo-8-[(deuterio)dimethylsilyl]naphthalene (1a-D). A solution of **20a** (480 mg, 1.60 mmol) in THF (4 mL) was added dropwise to a suspension of $LiAlD_4$ (68 mg, 1.60 mmol) in THF (2 mL) at 0 °C, and the reaction mixture was stirred at room temperature for 4 h. Chlorotrimethylsilane (0.20 mL, 1.60 mmol) was added dropwise to the reaction mixture at 0 °C, and the reaction mixture was stirred at room temperature for 2 h. After the solvents were removed in vacuo, the residue was diluted with hexane (10 mL) and filtered. The filtrate was subjected to bulb-to-bulb distillation (110–120 °C/1.5 mm Hg) to give **1a-D** (128 mg, 30% yield) as a colorless oil. The D-labeling was evidenced by comparsion to the spectra of **1a**. ^1H NMR ($CDCl_3$) δ 0.62 (s, 6H), 7.31 (t, J = 8 Hz,

1H), 7.47 (dd, J = 8 Hz, J = 7 Hz, 1H), 7.84 (dd, J = 8 Hz, J = 1 Hz, 1H), 7.87 (dd, J = 7 Hz, J = 1 Hz, 1H), 7.89 (dd, J = 8 Hz, J = 1 Hz, 1H), 8.05 (dd, J = 7 Hz, J = 1 Hz, 1H). $^{13}C\{^1H\}$ NMR ($CDCl_3$, δ) 0.86, 123.16, 125.42, 125.81, 129.42, 131.24, 132.23, 135.98, 136.62, 136.71, 138.50. ^{29}Si NMR ($CDCl_3$, δ) −13.62 (t, $^1J_{Si\text{-}D}$ = 152 Hz). MS(EI) m/z: 267 ($M^+[^{81}Br]$, 22), 265 ($M^+[^{79}Br]$, $M^+[^{81}Br]$−H, 38), 263 ($M^+[^{79}Br]$−H, 18), 252 ($M^+[^{89}Br]$−H, 98), 250 ($M^+[^{79}Br]$−Me, 100), 186 (M^+−Me−Br, 75). IR (Nujol) (cm^{-1}) 3055, 2898, 1564 (ν(Si-D)), 1493, 1417, 1358, 1306, 1248, 1192, 1051, 978, 866, 823, 795, 768, 706.

1-Bromo-7-(dimethylsilyl)naphthalene (3a). A solution of **1a** (106 mg, 0.40 mmol) and iodine (4 mg, 0.02 mmol, 5 mol%) in hexane (1.0 mL) was stirred at room temperature for 1 h. The reaction mixture was washed with saturated $Na_2S_2O_3$ solution (0.5 mL) and dried over Na_2SO_4. The solvent was removed in vacuo. The residue (91 mg) was subjected to column chromatography on silica gel eluted with hexane (R_f = 0.58) to give **3a** (46 mg, 43% yield) as colorless oil. ^1H NMR ($CDCl_3$, δ) 0.47 (d, J = 4 Hz, 6H), 4.60 (sept, J = 4 Hz, 1H), 7.33 (dd, J = 8 Hz, J = 7 Hz, 1H), 7.67 (dd, J = 8 Hz, J = 1 Hz, 1H), 7.78–7.83 (m, 3H), 8.44 (d, J = 1 Hz, 1H). $^{13}C\{^1H\}$ NMR ($CDCl_3$, δ) −3.75, 123.06, 126.67, 127.37, 127.81, 130.04, 131.06, 131.24, 133.52, 135.03, 137.04. ^{29}Si NMR ($CDCl_3$, δ) −16.04 (d, $^1J_{Si\text{-}H}$ = 190 Hz). MS(EI) m/z: 266 ($M^+[^{81}Br]$, 31), 264 ($M^+[^{79}Br]$, 30), 251 ($M^+[^{81}Br]$−Me, 100), 249 ($M^+[^{79}Br]$−Me, 99), 169 (M^+−Me−Br, 33). IR (Nujol) (cm^{-1}) 3053, 2958, 2900, 2723, 2121 (ν(Si-H)), 1545, 1415, 1354, 1306, 1250, 1150, 881, 825, 761. Anal. Calcd for $C_{12}H_{13}BrSi$: C, 54.34; H, 4.94; Found: C, 54.22; H, 4.80.

1-Iodo-7-(dimethylsilyl)naphthalene (3b). A solution of **1b** (125 mg, 0.40 mmol) and iodine

(4 mg, 0.02 mmol, 5 mol%) in hexane (1.0 mL) was stirred at room temperature for 1 h. The reaction mixture was washed with saturated $Na_2S_2O_3$ solution (0.5 mL) and dried over Na_2SO_4. The solvent was removed in vacuo. The residue (123 mg) was subjected to column chromatography on silica gel eluted with hexane (R_f = 0.48) to give **3b** (106 mg, 83% yield) as a yellow oil. ^{1}H NMR ($CDCl_3$, δ) 0.46 (d, J = 4 Hz, 6H), 4.59 (sept, J = 4 Hz, 1H), 7.19 (dd, J = 8 Hz, J = 7 Hz, 1H), 7.64 (dd, J = 8 Hz, J = 1 Hz, 1H), 7.73 (d, J = 8 Hz, 1H), 7.82 (d, J = 8 Hz, 1H), 8.09 (dd, J = 7 Hz, J = 1 Hz, 1H), 8.26 (d, J = 1 Hz, 1H). ^{13}C{^{1}H} NMR ($CDCl_3$, δ) −3.76, 100.00, 127.33, 127.58, 128.87, 131.09, 133.44, 134.57, 137.45, 137.56, 138.67. ^{29}Si NMR ($CDCl_3$, δ) −16.21 (d, $^1J_{Si\text{-}H}$ = 190 Hz). MS(EI) m/z: 312 (M^+, 51), 297 (M^+−Me, 25), 185 (M^+−I, 100). IR (Nujol) (cm^{-1}) 3051, 2119 (ν(Si-H)), 1925, 1585, 1303, 1252, 1200, 1093, 879, 788, 642. Anal. Calcd for $C_{12}H_{13}ISi$: C, 46.16; H, 4.20; Found: C, 45.87; H, 3.98.

1-Bromo-7-(diphenylsilyl)naphthalene (4a). A solution of **2a** (156 mg, 0.4 mmol) and iodine (4 mg, 0.02 mmol, 5 mol%) in hexane–toluene (1.0 mL/1.0 mL) was stirred at room temperature for 1 h. The reaction mixture was washed with saturated $Na_2S_2O_3$ solution (0.5 mL) and dried over Na_2SO_4. The solvents were removed in vacuo. The residue (110 mg) was subjected to column chromatography on silica gel eluted with hexane (R_f = 0.20) to give **4a** (59 mg, 38% yield) as a yellow solid. ^{1}H NMR ($CDCl_3$, δ) 5.67 (s, 1H), 7.36 (t, J = 8 Hz, 1H), 7.40–7.49 (m, 6H), 7.64–7.67 (m, 4H), 7.70 (d, J = 8 Hz, 1H), 7.79–7.84 (m, 3H), 8.57 (s, 1H). ^{13}C{^{1}H} NMR ($CDCl_3$, δ) 123.24, 127.08, 127.64, 127.81, 128.14, 129.97, 130.16, 131.36, 132.14, 132.92, 133.01, 135.28, 135.84, 135.98. ^{29}Si NMR ($CDCl_3$, δ) –17.60 (d, $^1J_{Si\text{-}H}$ = 203 Hz). MS(EI) m/z: 390 (M^+[^{81}Br], 29), 388

($M^+[^{79}Br]$, 28), 309 (M^+−Br, 100). IR (Nujol) (cm^{-1}) 2723, 2671, 2127 (ν(Si-H)), 1587, 1377, 1109, 968, 802, 729. Anal. Calcd for $C_{22}H_{17}BrSi$: C, 67.86; H, 4.40; Found: C, 67.85; H, 4.43.

1-Iodo-7-(diphenylsilyl)naphthalene (4b). This compound was prepared in a manner similar to the used for **4a** and obtained as a yellow solid (70 mg, 40% yield) after column chromatography on silica gel eluted with hexane (R_f = 0.18). ^{1}H NMR ($CDCl_3$, δ) 5.64 (s, 1H), 7.21 (t, J = 8 Hz, 1H), 7.39–7.48 (m, 6H), 7.60–7.68 (m, 5H), 7.74 (d, J = 8 Hz, 1H), 7.82 (d, J = 8 Hz, 1H), 8.10 (dd, J = 7 Hz, J = 1 Hz, 1H), 8.36 (s, 1H). $^{13}C\{^1H\}$ NMR ($CDCl_3$, δ) 100.15, 127.73, 127.82, 128.14, 128.86, 129.97, 132.17, 132.91, 133.42, 133.62, 134.85, 135.86, 137.67, 141.15. ^{29}Si NMR ($CDCl_3$, δ) −17.83 (d, $^1J_{Si\text{-}H}$ = 201 Hz). MS(EI) m/z: 436 (M^+, 36), 358 (M^+−Ph, 26), 309 (M^+−I, 100), 231 (M^+−I−Ph, 57). IR (Nujol) (cm^{-1}) 2725, 2669, 2129 (ν(Si-H)), 1589, 1377, 1109, 802, 729. Anal. Calcd for $C_{22}H_{17}ISi$: C, 60.55; H, 3.93; Found: C, 60.44; H, 3.96.

1-(Dimethylsilyl)naphthalene (21) (CAS No. 30274-80-5). A solution of *n*-BuLi in hexane (1.64 mol/L, 2.59 mL, 4.24 mmol) was added dropwise to a solution of 1-bromonaphthalene (800 mg, 3.86 mmol) in Et_2O (10 mL) at 0 °C. After the reaction mixture was stirred at this temperature for 1 h, chlorodimethylsilane (0.50 mL, 4.59 mmol) was added via a syringe. Then the mixture was warmed to room temperature. The solvent was removed in vacuo and the residue (1157 mg) was subjected to column chromatography on silica gel eluted with hexane (R_f = 0.53) to give **21** (811 mg, 79% yield) as a colorless oil. ^{1}H NMR ($CDCl_3$, δ) 0.57 (d, J = 4 Hz, 6H), 4.96 (sept, J = 4 Hz, 1H), 7.51–7.61 (m, 3H), 7.80 (dd, J = 7 Hz, J = 1 Hz, 1H), 7.91–7.95 (m, 2H), 8.20 (dd, J = 8 Hz, J = 1 Hz, 1H). $^{13}C\{^1H\}$ NMR ($CDCl_3$, δ) −3.26, 125.15, 125.51, 125.90, 127.58, 128.94, 129.99, 133.20,

133.61, 135.60, 136.96. ^{29}Si NMR ($CDCl_3$, δ) −20.41 (d, $^1J_{Si\text{-}H}$ = 204 Hz). MS(EI) m/z: 186 (M^+, 66), 171 (M^+−Me, 100). IR (Nujol) (cm^{-1}) 3048, 2123 (ν(Si-H)), 1506, 1376, 1250, 1146, 985, 883, 839, 779.

1-(Diphenylsilyl)naphthalene (30) (CAS No. 100447-84-5). This compound was prepared in a manner similar to that used for **21** and obtained as a colorless solid after column chromatography on silica gel eluted with hexane (R_f = 0.33). The solid was recrystallized from hexane to give **30** (969 mg) as a pale yellow crystal in 81% yield. ^{1}H NMR ($CDCl_3$, δ) 5.92 (s, 1H), 7.41–7.50 (m, 9H), 7.59–7.64 (m, 5H), 7.89 (d, *J* = 8 Hz, 1H), 7.94 (d, *J* = 8 Hz, 1H), 8.07 (d, *J* = 8 Hz, 1H). ^{13}C{^{1}H} NMR ($CDCl_3$, δ) 125.24, 125.72, 126.16, 128.09, 128.25, 128.81, 129.80, 130.79, 131.42, 133.23, 133.27, 135.98, 136.83, 137.37. ^{29}Si NMR ($CDCl_3$, δ) −20.57 (d, $^1J_{Si\text{-}H}$ = 200 Hz). MS(EI) m/z: 310 (M^+, 82), 231 (M^+−Ph, 100). IR (Nujol) (cm^{-1}) 2727, 2663, 2108 (ν(Si-H)), 1587, 1305, 1109, 982, 787, 771, 731, 698.

Typical Procedure for NMR experiments: Reaction of 1-halo-8-silylnaphthalenes with I_2 in $CDCl_3$. To a solution of a 1-halo-8-silylnaphthalene (0.040 mmol) and cyclohexane (20 μL) in $CDCl_3$ (0.60 mL) in a J. Young NMR tube was added I_2 (0.5 mg, 2.0 μmol) in one portion at room temperature. The reaction mixture was shaken at room temperature for 1 min, and the sample was directly subjected to ^{1}H NMR spectroscopy. The yields of the products were estimated from the integral ratios using cyclohexane as an internal standard.

4.4 X-ray crystallographic data

X-ray crystallographic data for **2a**, **2b**, and **17** were collected using a SMART APEX-II CCD diffractometer with graphite-monochromated Mo-K_α radiation (λ= 0.71073 Å) at 173 K at the Department of Chemistry, Graduate School of Science, Hiroshima University. The structures were solved by direct methods using SIR 97[13] and refined by a full-matrix least-squares procedure based on F^2 with SHELX-97.[14] All non-hydrogen atoms were refined anisotropically. Hydrogen atoms were located at the expected positions by a geometrical calculation and refined isotropically or found on the difference Fourier map and refined isotropically.

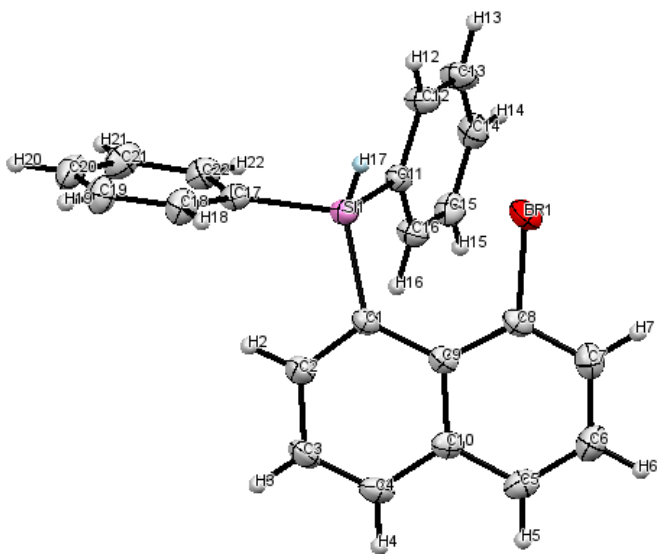

Figure 5. Crystal structure of **2a** at the 30% probability level.

Table 4. Crystal data and structure refinement for **2a**.

Identification code	787_0m_a	
Empirical formula	C22 H17 Br Si	
Formula weight	389.35	
Temperature	173(2) K	
Wavelength	0.71073 Å	
Crystal system	Monoclinic	
Space group	$P2_1/c$	
Unit cell dimensions	a = 10.1994(7) Å	α = 90°.
	b = 16.3064(12) Å	β = 107.9380(10)°.
	c = 11.1616(8) Å	γ = 90°.
Volume	1766.1(2) Å3	
Z	4	
Density (calculated)	1.464 Mg/m3	
Absorption coefficient	2.395 mm-1	
F(000)	792	
Crystal size	0.215 x 0.133 x 0.088 mm3	
Theta range for data collection	2.289 to 27.871°.	
Index ranges	-13<=h<=11, -16<=k<=21, -12<=l<=14	

Reflections collected	10208
Independent reflections	4177 [R(int) = 0.0127]
Completeness to theta = 25.242°	99.8 %
Absorption correction	Semi-empirical from equivalents
Max. and min. transmission	0.817 and 0.742
Refinement method	Full-matrix least-squares on F2
Data / restraints / parameters	4177 / 0 / 221
Goodness-of-fit on F2	1.033
Final R indices [I>2sigma(I)]	R1 = 0.0221, wR2 = 0.0590
R indices (all data)	R1 = 0.0252, wR2 = 0.0608
Extinction coefficient	n/a
Largest diff. peak and hole	0.338 and -0.314 e.Å-3

All hydrogen atoms were located at the expected positions by a geometrical calculation and refined isotropically.

Table 5. Atomic coordinates (x 10^4) and equivalent isotropic displacement parameters ($Å^2$x 10^3) for **2a**. U(eq) is defined as one third of the trace of the orthogonalized U^{ij} tensor.

	x	y	z	U(eq)
Br(1)	4566(1)	6002(1)	2051(1)	35(1)
Si(1)	6738(1)	4647(1)	3583(1)	23(1)
C(1)	6822(1)	5476(1)	4795(1)	22(1)
C(2)	7573(2)	5259(1)	6014(1)	29(1)
C(3)	7980(2)	5825(1)	7018(1)	32(1)
C(4)	7676(2)	6631(1)	6798(1)	29(1)
C(5)	6631(2)	7756(1)	5376(2)	31(1)
C(7)	5349(2)	7498(1)	3226(2)	32(1)
C(6)	5903(2)	8050(1)	4218(2)	35(1)
C(8)	5585(1)	6673(1)	3412(1)	25(1)
C(9)	6425(1)	6327(1)	4565(1)	21(1)
C(10)	6906(1)	6908(1)	5578(1)	25(1)
C(11)	7650(1)	5042(1)	2474(1)	24(1)
C(12)	7346(2)	4769(1)	1235(1)	31(1)
C(13)	8086(2)	5047(1)	459(2)	37(1)

C(14)	9136(2)	5611(1)	904(2)	32(1)
C(17)	7678(1)	3705(1)	4383(1)	24(1)
C(16)	8723(2)	5608(1)	2905(1)	28(1)
C(15)	9458(2)	5893(1)	2124(1)	30(1)
C(18)	7097(2)	3221(1)	5126(2)	31(1)
C(19)	7739(2)	2516(1)	5714(2)	35(1)
C(20)	8975(2)	2268(1)	5561(2)	36(1)
C(21)	9561(2)	2727(1)	4816(2)	38(1)
C(22)	8924(2)	3441(1)	4239(2)	30(1)

Table 6. Bond lengths [Å] and angles [°] for **2a**.

Br(1)-C(8)	1.9011(14)	C(2)-C(3)	1.412(2)
Si(1)-C(11)	1.8757(14)	C(2)-H(2)	0.9500
Si(1)-C(17)	1.8838(14)	C(3)-C(4)	1.355(2)
Si(1)-C(1)	1.8958(14)	C(3)-H(3)	0.9500
Si(1)-H(17)	1.365(16)	C(4)-C(10)	1.420(2)
C(1)-C(2)	1.3850(19)	C(4)-H(4)	0.9500
C(1)-C(9)	1.4474(19)	C(5)-C(6)	1.364(2)

C(5)-C(10)	1.414(2)	C(15)-H(15)	0.9500
C(5)-H(5)	0.9500	C(18)-C(19)	1.385(2)
C(7)-C(8)	1.371(2)	C(18)-H(18)	0.9500
C(7)-C(6)	1.404(2)	C(19)-C(20)	1.383(2)
C(7)-H(7)	0.9500	C(19)-H(19)	0.9500
C(6)-H(6)	0.9500	C(20)-C(21)	1.384(2)
C(8)-C(9)	1.4241(18)	C(20)-H(20)	0.9500
C(9)-C(10)	1.4402(18)	C(21)-C(22)	1.390(2)
C(11)-C(12)	1.3946(19)	C(21)-H(21)	0.9500
C(11)-C(16)	1.3983(19)	C(22)-H(22)	0.9500
C(12)-C(13)	1.388(2)		
C(12)-H(12)	0.9500	C(11)-Si(1)-C(17)	108.04(6)
C(13)-C(14)	1.383(2)	C(11)-Si(1)-C(1)	107.65(6)
C(13)-H(13)	0.9500	C(17)-Si(1)-C(1)	109.78(6)
C(14)-C(15)	1.378(2)	C(11)-Si(1)-H(17)	111.5(7)
C(14)-H(14)	0.9500	C(17)-Si(1)-H(17)	103.8(8)
C(17)-C(22)	1.3967(19)	C(1)-Si(1)-H(17)	115.8(7)
C(17)-C(18)	1.4015(19)	C(2)-C(1)-C(9)	117.31(12)
C(16)-C(15)	1.393(2)	C(2)-C(1)-Si(1)	114.14(10)
C(16)-H(16)	0.9500	C(9)-C(1)-Si(1)	127.49(10)

C(1)-C(2)-C(3)	123.46(14)	C(9)-C(8)-Br(1)	121.54(10)
C(1)-C(2)-H(2)	118.3	C(8)-C(9)-C(10)	114.44(12)
C(3)-C(2)-H(2)	118.3	C(8)-C(9)-C(1)	126.72(12)
C(4)-C(3)-C(2)	119.66(14)	C(10)-C(9)-C(1)	118.84(12)
C(4)-C(3)-H(3)	120.2	C(5)-C(10)-C(4)	119.21(13)
C(2)-C(3)-H(3)	120.2	C(5)-C(10)-C(9)	120.95(13)
C(3)-C(4)-C(10)	120.70(13)	C(4)-C(10)-C(9)	119.84(13)
C(3)-C(4)-H(4)	119.6	C(12)-C(11)-C(16)	117.56(13)
C(10)-C(4)-H(4)	119.6	C(12)-C(11)-Si(1)	122.73(11)
C(6)-C(5)-C(10)	121.19(14)	C(16)-C(11)-Si(1)	119.64(10)
C(6)-C(5)-H(5)	119.4	C(13)-C(12)-C(11)	121.15(14)
C(10)-C(5)-H(5)	119.4	C(13)-C(12)-H(12)	119.4
C(8)-C(7)-C(6)	119.99(14)	C(11)-C(12)-H(12)	119.4
C(8)-C(7)-H(7)	120.0	C(14)-C(13)-C(12)	120.19(14)
C(6)-C(7)-H(7)	120.0	C(14)-C(13)-H(13)	119.9
C(5)-C(6)-C(7)	119.46(14)	C(12)-C(13)-H(13)	119.9
C(5)-C(6)-H(6)	120.3	C(15)-C(14)-C(13)	119.94(14)
C(7)-C(6)-H(6)	120.3	C(15)-C(14)-H(14)	120.0
C(7)-C(8)-C(9)	123.66(13)	C(13)-C(14)-H(14)	120.0
C(7)-C(8)-Br(1)	114.59(11)	C(22)-C(17)-C(18)	117.36(13)

C(22)-C(17)-Si(1)	123.01(11)	C(20)-C(19)-H(19)	120.0
C(18)-C(17)-Si(1)	119.59(10)	C(18)-C(19)-H(19)	120.0
C(15)-C(16)-C(11)	121.37(13)	C(19)-C(20)-C(21)	119.63(15)
C(15)-C(16)-H(16)	119.3	C(19)-C(20)-H(20)	120.2
C(11)-C(16)-H(16)	119.3	C(21)-C(20)-H(20)	120.2
C(14)-C(15)-C(16)	119.78(14)	C(20)-C(21)-C(22)	120.33(14)
C(14)-C(15)-H(15)	120.1	C(20)-C(21)-H(21)	119.8
C(16)-C(15)-H(15)	120.1	C(22)-C(21)-H(21)	119.8
C(19)-C(18)-C(17)	121.61(14)	C(21)-C(22)-C(17)	121.09(14)
C(19)-C(18)-H(18)	119.2	C(21)-C(22)-H(22)	119.5
C(17)-C(18)-H(18)	119.2	C(17)-C(22)-H(22)	119.5
C(20)-C(19)-C(18)	119.97(14)		

Symmetry transformations used to generate equivalent atoms: #1 -x+1,-y,-z+1

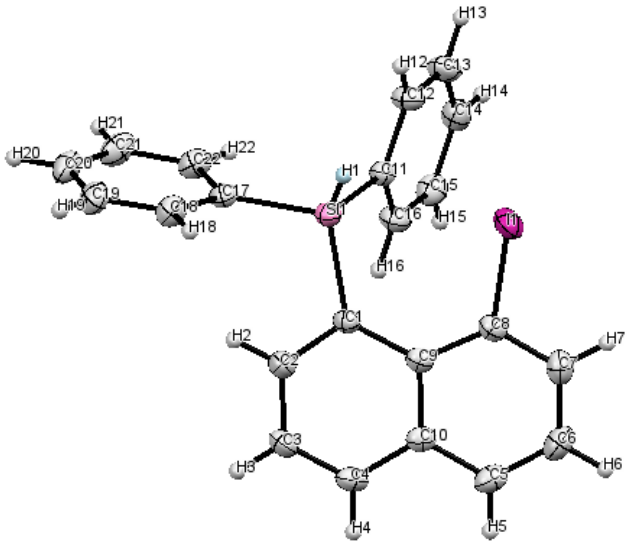

Figure 6. Crystal structure of **2b** at the 30% probability level.

Table 7. Crystal data and structure refinement for **2b**.

Identification code	788_0m_a	
Empirical formula	C22 H17 I Si	
Formula weight	436.34	
Temperature	173(2) K	
Wavelength	0.71073 Å	
Crystal system	Monoclinic	
Space group	$P2_1/c$	
Unit cell dimensions	a = 10.2281(9) Å	a= 90°.
	b = 16.1277(14) Å	b= 106.6440(10)°.

	c = 11.3827(10) Å g = 90°.
Volume	1799.0(3) $Å^3$
Z	4
Density (calculated)	1.611 Mg/m^3
Absorption coefficient	1.846 mm^{-1}
F(000)	864
Crystal size	0.234 x 0.221 x 0.197 mm^3
Theta range for data collection	2.254 to 27.896°.
Index ranges	-12<=h<=13, -21<=k<=20, -13<=l<=14
Reflections collected	10388
Independent reflections	4268 [R(int) = 0.0146]
Completeness to theta = 25.242°	99.8 %
Absorption correction	Semi-empirical from equivalents
Max. and min. transmission	0.712 and 0.665
Refinement method	Full-matrix least-squares on F^2
Data / restraints / parameters	4268 / 0 / 221
Goodness-of-fit on F^2	1.087
Final R indices [I>2sigma(I)]	R1 = 0.0182, wR2 = 0.0479
R indices (all data)	R1 = 0.0194, wR2 = 0.0485
Extinction coefficient	n/a

Largest diff. peak and hole	0.353 and -0.487 e.Å^{-3}

All hydrogen atoms were located at the expected positions by a geometrical calculation and refined isotropically.

Table 8. Atomic coordinates (x 10^4) and equivalent isotropic displacement parameters (Å^{2}x 10^3) for **2b**. U(eq) is defined as one third of the trace of the orthogonalized U^{ij} tensor.

	x	y	z	U(eq)
I(1)	5619(1)	6004(1)	8023(1)	32(1)
C(1)	3187(1)	5497(1)	5213(1)	21(1)
Si(1)	3225(1)	4646(1)	6376(1)	22(1)
C(4)	2347(2)	6672(1)	3277(1)	28(1)
C(3)	2073(2)	5853(1)	3052(1)	31(1)
C(2)	2472(2)	5280(1)	4027(1)	27(1)
C(5)	3319(2)	7808(1)	4663(2)	30(1)
C(6)	4018(2)	8107(1)	5785(2)	34(1)
C(7)	4581(2)	7551(1)	6743(2)	30(1)

C(8)	4387(1)	6710(1)	6568(1)	23(1)
C(9)	3570(1)	6359(1)	5447(1)	20(1)
C(10)	3084(1)	6948(1)	4468(1)	23(1)
C(11)	2294(2)	5048(1)	7459(1)	23(1)
C(12)	2560(2)	4772(1)	8667(1)	29(1)
C(13)	1792(2)	5051(1)	9416(2)	34(1)
C(14)	750(2)	5617(1)	8980(2)	31(1)
C(15)	466(2)	5902(1)	7789(2)	31(1)
C(16)	1232(2)	5619(1)	7038(1)	28(1)
C(17)	2292(2)	3703(1)	5581(1)	23(1)
C(18)	2889(2)	3220(1)	4848(2)	28(1)
C(19)	2251(2)	2517(1)	4248(2)	32(1)
C(20)	1008(2)	2268(1)	4392(2)	34(1)
C(21)	415(2)	2722(1)	5136(2)	36(1)
C(22)	1049(2)	3435(1)	5720(2)	30(1)

Table 9. Bond lengths [Å] and angles [°] for **2b**.

I(1)-C(8)	2.1044(14)	C(1)-C(2)	1.384(2)

C(1)-C(9)	1.448(2)	C(11)-C(12)	1.397(2)
C(1)-Si(1)	1.8995(14)	C(11)-C(16)	1.400(2)
Si(1)-C(11)	1.8752(15)	C(12)-C(13)	1.388(2)
Si(1)-C(17)	1.8842(15)	C(12)-H(12)	0.9500
Si(1)-H(1)	1.412(18)	C(13)-C(14)	1.383(2)
C(4)-C(3)	1.358(2)	C(13)-H(13)	0.9500
C(4)-C(10)	1.421(2)	C(14)-C(15)	1.382(2)
C(4)-H(4)	0.9500	C(14)-H(14)	0.9500
C(3)-C(2)	1.411(2)	C(15)-C(16)	1.393(2)
C(3)-H(3)	0.9500	C(15)-H(15)	0.9500
C(2)-H(2)	0.9500	C(16)-H(16)	0.9500
C(5)-C(6)	1.361(2)	C(17)-C(22)	1.394(2)
C(5)-C(10)	1.416(2)	C(17)-C(18)	1.403(2)
C(5)-H(5)	0.9500	C(18)-C(19)	1.386(2)
C(6)-C(7)	1.403(2)	C(18)-H(18)	0.9500
C(6)-H(6)	0.9500	C(19)-C(20)	1.387(2)
C(7)-C(8)	1.377(2)	C(19)-H(19)	0.9500
C(7)-H(7)	0.9500	C(20)-C(21)	1.385(3)
C(8)-C(9)	1.4273(19)	C(20)-H(20)	0.9500
C(9)-C(10)	1.4399(19)	C(21)-C(22)	1.392(2)

C(21)-H(21)	0.9500	C(3)-C(2)-H(2)	118.2
C(22)-H(22)	0.9500	C(6)-C(5)-C(10)	120.95(14)
		C(6)-C(5)-H(5)	119.5
C(2)-C(1)-C(9)	117.51(13)	C(10)-C(5)-H(5)	119.5
C(2)-C(1)-Si(1)	113.40(11)	C(5)-C(6)-C(7)	119.44(15)
C(9)-C(1)-Si(1)	127.91(10)	C(5)-C(6)-H(6)	120.3
C(11)-Si(1)-C(17)	108.21(7)	C(7)-C(6)-H(6)	120.3
C(11)-Si(1)-C(1)	107.20(6)	C(8)-C(7)-C(6)	120.53(15)
C(17)-Si(1)-C(1)	110.02(6)	C(8)-C(7)-H(7)	119.7
C(11)-Si(1)-H(1)	112.0(7)	C(6)-C(7)-H(7)	119.7
C(17)-Si(1)-H(1)	103.5(9)	C(7)-C(8)-C(9)	122.89(14)
C(1)-Si(1)-H(1)	115.7(8)	C(7)-C(8)-I(1)	112.93(11)
C(3)-C(4)-C(10)	120.57(14)	C(9)-C(8)-I(1)	123.70(10)
C(3)-C(4)-H(4)	119.7	C(8)-C(9)-C(10)	114.48(13)
C(10)-C(4)-H(4)	119.7	C(8)-C(9)-C(1)	127.13(13)
C(4)-C(3)-C(2)	119.39(14)	C(10)-C(9)-C(1)	118.39(12)
C(4)-C(3)-H(3)	120.3	C(5)-C(10)-C(4)	118.46(13)
C(2)-C(3)-H(3)	120.3	C(5)-C(10)-C(9)	121.35(14)
C(1)-C(2)-C(3)	123.67(14)	C(4)-C(10)-C(9)	120.19(13)
C(1)-C(2)-H(2)	118.2	C(12)-C(11)-C(16)	117.39(13)

C(12)-C(11)-Si(1)	123.02(11)	C(22)-C(17)-Si(1)	123.24(11)
C(16)-C(11)-Si(1)	119.50(11)	C(18)-C(17)-Si(1)	119.17(11)
C(13)-C(12)-C(11)	121.10(14)	C(19)-C(18)-C(17)	121.50(14)
C(13)-C(12)-H(12)	119.4	C(19)-C(18)-H(18)	119.3
C(11)-C(12)-H(12)	119.4	C(17)-C(18)-H(18)	119.3
C(14)-C(13)-C(12)	120.48(14)	C(18)-C(19)-C(20)	119.86(15)
C(14)-C(13)-H(13)	119.8	C(18)-C(19)-H(19)	120.1
C(12)-C(13)-H(13)	119.8	C(20)-C(19)-H(19)	120.1
C(15)-C(14)-C(13)	119.71(15)	C(21)-C(20)-C(19)	119.70(15)
C(15)-C(14)-H(14)	120.1	C(21)-C(20)-H(20)	120.2
C(13)-C(14)-H(14)	120.1	C(19)-C(20)-H(20)	120.2
C(14)-C(15)-C(16)	119.73(15)	C(20)-C(21)-C(22)	120.26(15)
C(14)-C(15)-H(15)	120.1	C(20)-C(21)-H(21)	119.9
C(16)-C(15)-H(15)	120.1	C(22)-C(21)-H(21)	119.9
C(15)-C(16)-C(11)	121.58(14)	C(21)-C(22)-C(17)	121.11(15)
C(15)-C(16)-H(16)	119.2	C(21)-C(22)-H(22)	119.4
C(11)-C(16)-H(16)	119.2	C(17)-C(22)-H(22)	119.4
C(22)-C(17)-C(18)	117.55(14)		

Symmetry transformations used to generate equivalent atoms: #1 -x+1,-y,-z+1

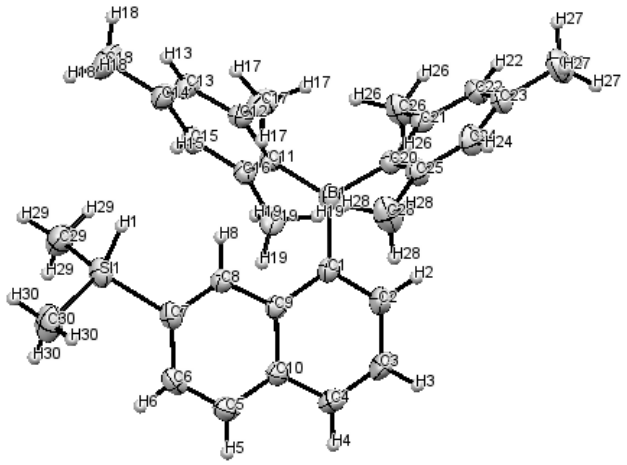

Figure 7. Crystal structure of **17** at the 30% probability level.

Table 10. Crystal data and structure refinement for **17**.

Identification code	785_0m_a
Empirical formula	C30 H34.97 B Si
Formula weight	434.45
Temperature	173(2) K
Wavelength	0.71073 Å
Crystal system	Monoclinic
Space group	C2/c
Unit cell dimensions	a = 41.91(2) Å α= 90°.

	b = 12.024(7) Å β= 96.496(7)°.
	c = 10.723(6) Å γ = 90°.
Volume 5369(5) Å3	
Z	8
Density (calculated)	1.075 Mg/m3
Absorption coefficient	0.102 mm-1
F(000)	1872
Crystal size	0.106 x 0.078 x 0.017 mm3
Theta range for data collection	1.763 to 25.407°.
Index ranges	-44<=h<=50, -9<=k<=14, -12<=l<=12
Reflections collected	11234
Independent reflections	4904 [R(int) = 0.0846]
Completeness to theta = 25.242°	99.1 %
Absorption correction	Semi-empirical from equivalents
Max. and min. transmission	0.998 and 0.676
Refinement method	Full-matrix least-squares on F2
Data / restraints / parameters	4904 / 145 / 352
Goodness-of-fit on F2	1.132

Final R indices [I>2sigma(I)]	R1 = 0.1291, wR2 = 0.2483
R indices (all data)	R1 = 0.2088, wR2 = 0.2759
Extinction coefficient	n/a
Largest diff. peak and hole	0.580 and -0.378 e.Å-3

All hydrogen atoms were located at the expected positions by a geometrical calculation and refined isotropically.

Table 11. Atomic coordinates (x 10^4) and equivalent isotropic displacement parameters (Å^{2}x 10^3) for **17**. U(eq) is defined as one third of the trace of the orthogonalized U^{ij} tensor.

	x	y	z	U(eq)
C(11)	3748(2)	2008(5)	7399(5)	36(2)
C(10)	3579(2)	2509(5)	3009(5)	40(2)
C(9)	3646(2)	2673(4)	4332(5)	36(2)
C(8)	3960(2)	3027(5)	4793(5)	40(2)
C(7)	4200(2)	3221(5)	4041(5)	45(2)
C(6)	4122(2)	3043(5)	2714(6)	52(2)
C(5)	3823(2)	2717(5)	2241(5)	46(2)

C(4)	3266(2)	2171(5)	2527(5)	48(2)
C(3)	3032(2)	2033(5)	3281(6)	52(2)
C(2)	3098(2)	2248(5)	4587(6)	44(2)
B(1)	3455(2)	2591(5)	6619(6)	35(2)
C(1)	3401(2)	2514(4)	5132(5)	34(1)
C(12)	3830(2)	895(5)	7163(6)	44(2)
C(13)	4070(2)	368(6)	7940(6)	58(2)
C(14)	4247(2)	891(6)	8942(6)	56(2)
C(15)	4176(2)	1998(6)	9143(6)	51(2)
C(16)	3929(2)	2565(5)	8427(5)	36(2)
C(17)	3652(2)	221(5)	6085(6)	59(2)
C(18)	4506(2)	290(8)	9774(9)	98(3)
C(19)	3874(2)	3780(5)	8717(6)	49(2)
C(20)	3188(1)	3219(5)	7268(5)	37(2)
C(21)	3021(2)	2713(5)	8188(5)	41(2)
C(22)	2788(2)	3293(6)	8736(6)	50(2)
C(23)	2716(2)	4409(6)	8434(6)	49(2)
C(24)	2881(2)	4897(6)	7544(5)	46(2)

C(25)	3113(2)	4343(5)	6948(5)	37(2)
C(26)	3091(2)	1519(6)	8589(6)	60(2)
C(27)	2472(2)	5053(8)	9084(7)	72(2)
C(28)	3294(2)	4970(5)	6011(5)	43(2)
Si(1)	4603(1)	3725(2)	4730(2)	68(1)
C(29A)	4562(4)	4360(20)	6307(15)	71(6)
C(30A)	4907(5)	2782(18)	4840(30)	96(7)
C(29B)	4663(16)	3640(80)	6340(50)	79(14)
C(30B)	4906(14)	2740(50)	4050(70)	64(12)
C(29C)	4715(8)	2870(40)	6310(30)	80(9)
C(30C)	4924(10)	3170(40)	3660(30)	90(12)

Table 6. Bond lengths [Å] and angles [°] for **17**.

C(11)-C(12)	1.412(8)	C(10)-C(9)	1.428(7)
C(11)-C(16)	1.431(8)	C(9)-C(8)	1.420(8)
C(11)-B(1)	1.572(9)	C(9)-C(1)	1.423(8)
C(10)-C(5)	1.408(9)	C(8)-C(7)	1.378(8)
C(10)-C(4)	1.412(9)	C(8)-H(8)	0.9500

C(7)-C(6)	1.440(9)	C(14)-C(18)	1.510(10)
C(7)-Si(1)	1.867(7)	C(15)-C(16)	1.394(8)
C(6)-C(5)	1.355(9)	C(15)-H(15)	0.9500
C(6)-H(6)	0.9500	C(16)-C(19)	1.517(8)
C(5)-H(5)	0.9500	C(17)-H(17A)	0.9800
C(4)-C(3)	1.350(9)	C(17)-H(17B)	0.9800
C(4)-H(4)	0.9500	C(17)-H(17C)	0.9800
C(3)-C(2)	1.420(8)	C(18)-H(18A)	0.9800
C(3)-H(3)	0.9500	C(18)-H(18B)	0.9800
C(2)-C(1)	1.374(8)	C(18)-H(18C)	0.9800
C(2)-H(2)	0.9500	C(19)-H(19A)	0.9800
B(1)-C(20)	1.575(9)	C(19)-H(19B)	0.9800
B(1)-C(1)	1.588(8)	C(19)-H(19C)	0.9800
C(12)-C(13)	1.385(9)	C(20)-C(21)	1.410(8)
C(12)-C(17)	1.534(9)	C(20)-C(25)	1.421(8)
C(13)-C(14)	1.385(9)	C(21)-C(22)	1.384(9)
C(13)-H(13)	0.9500	C(21)-C(26)	1.517(9)
C(14)-C(15)	1.387(10)	C(22)-C(23)	1.406(10)

C(22)-H(22)	0.9500	Si(1)-C(30B)	1.94(6)
C(23)-C(24)	1.371(9)	Si(1)-C(30C)	1.98(3)
C(23)-C(27)	1.514(9)	Si(1)-C(29C)	1.99(3)
C(24)-C(25)	1.391(8)	Si(1)-H(31A)	1.65(8)
C(24)-H(24)	0.9500	Si(1)-H(31B)	1.65(8)
C(25)-C(28)	1.527(8)	Si(1)-H(31C)	1.64(8)
C(26)-H(26A)	0.9800	C(29A)-H(29A)	0.9800
C(26)-H(26B)	0.9800	C(29A)-H(29B)	0.9800
C(26)-H(26C)	0.9800	C(29A)-H(29C)	0.9800
C(27)-H(27A)	0.9800	C(30A)-H(30A)	0.9800
C(27)-H(27B)	0.9800	C(30A)-H(30B)	0.9800
C(27)-H(27C)	0.9800	C(30A)-H(30C)	0.9800
C(28)-H(28A)	0.9800	C(29B)-H(29D)	0.9800
C(28)-H(28B)	0.9800	C(29B)-H(29E)	0.9800
C(28)-H(28C)	0.9800	C(29B)-H(29F)	0.9800
Si(1)-C(30A)	1.699(19)	C(30B)-H(30D)	0.9800
Si(1)-C(29B)	1.71(5)	C(30B)-H(30E)	0.9800
Si(1)-C(29A)	1.880(16)	C(30B)-H(30F)	0.9800

C(29C)-H(29G)	0.9800	C(9)-C(8)-H(8)	118.1
C(29C)-H(29H)	0.9800	C(8)-C(7)-C(6)	117.0(6)
C(29C)-H(29I)	0.9800	C(8)-C(7)-Si(1)	120.7(5)
C(30C)-H(30G)	0.9800	C(6)-C(7)-Si(1)	122.2(5)
C(30C)-H(30H)	0.9800	C(5)-C(6)-C(7)	120.7(6)
C(30C)-H(30I)	0.9800	C(5)-C(6)-H(6)	119.7
		C(7)-C(6)-H(6)	119.7
C(12)-C(11)-C(16)	117.7(6)	C(6)-C(5)-C(10)	122.3(6)
C(12)-C(11)-B(1)	121.2(5)	C(6)-C(5)-H(5)	118.8
C(16)-C(11)-B(1)	121.0(5)	C(10)-C(5)-H(5)	118.8
C(5)-C(10)-C(4)	122.9(6)	C(3)-C(4)-C(10)	121.5(6)
C(5)-C(10)-C(9)	118.9(6)	C(3)-C(4)-H(4)	119.2
C(4)-C(10)-C(9)	118.2(6)	C(10)-C(4)-H(4)	119.2
C(8)-C(9)-C(1)	122.3(5)	C(4)-C(3)-C(2)	119.6(6)
C(8)-C(9)-C(10)	117.2(5)	C(4)-C(3)-H(3)	120.2
C(1)-C(9)-C(10)	120.4(6)	C(2)-C(3)-H(3)	120.2
C(7)-C(8)-C(9)	123.8(5)	C(1)-C(2)-C(3)	121.9(6)
C(7)-C(8)-H(8)	118.1	C(1)-C(2)-H(2)	119.0

C(3)-C(2)-H(2)	119.0	C(16)-C(15)-H(15)	118.6
C(11)-B(1)-C(20)	122.0(5)	C(15)-C(16)-C(11)	119.4(6)
C(11)-B(1)-C(1)	121.5(5)	C(15)-C(16)-C(19)	118.7(5)
C(20)-B(1)-C(1)	116.4(5)	C(11)-C(16)-C(19)	121.9(5)
C(2)-C(1)-C(9)	118.0(5)	C(12)-C(17)-H(17A)	109.5
C(2)-C(1)-B(1)	117.5(5)	C(12)-C(17)-H(17B)	109.5
C(9)-C(1)-B(1)	124.5(5)	H(17A)-C(17)-H(17B)	109.5
C(13)-C(12)-C(11)	120.0(6)	C(12)-C(17)-H(17C)	109.5
C(13)-C(12)-C(17)	118.1(6)	H(17A)-C(17)-H(17C)	109.5
C(11)-C(12)-C(17)	121.9(6)	H(17B)-C(17)-H(17C)	109.5
C(12)-C(13)-C(14)	123.3(6)	C(14)-C(18)-H(18A)	109.5
C(12)-C(13)-H(13)	118.4	C(14)-C(18)-H(18B)	109.5
C(14)-C(13)-H(13)	118.4	H(18A)-C(18)-H(18B)	109.5
C(13)-C(14)-C(15)	116.8(7)	C(14)-C(18)-H(18C)	109.5
C(13)-C(14)-C(18)	121.9(7)	H(18A)-C(18)-H(18C)	109.5
C(15)-C(14)-C(18)	121.3(7)	H(18B)-C(18)-H(18C)	109.5
C(14)-C(15)-C(16)	122.9(6)	C(16)-C(19)-H(19A)	109.5
C(14)-C(15)-H(15)	118.6	C(16)-C(19)-H(19B)	109.5

H(19A)-C(19)-H(19B)	109.5	C(25)-C(24)-H(24)	118.4
C(16)-C(19)-H(19C)	109.5	C(24)-C(25)-C(20)	119.5(5)
H(19A)-C(19)-H(19C)	109.5	C(24)-C(25)-C(28)	119.5(6)
H(19B)-C(19)-H(19C)	109.5	C(20)-C(25)-C(28)	120.9(5)
C(21)-C(20)-C(25)	117.7(6)	C(21)-C(26)-H(26A)	109.5
C(21)-C(20)-B(1)	122.4(5)	C(21)-C(26)-H(26B)	109.5
C(25)-C(20)-B(1)	119.9(5)	H(26A)-C(26)-H(26B)	109.5
C(22)-C(21)-C(20)	120.6(6)	C(21)-C(26)-H(26C)	109.5
C(22)-C(21)-C(26)	118.6(5)	H(26A)-C(26)-H(26C)	109.5
C(20)-C(21)-C(26)	120.8(6)	H(26B)-C(26)-H(26C)	109.5
C(21)-C(22)-C(23)	121.7(6)	C(23)-C(27)-H(27A)	109.5
C(21)-C(22)-H(22)	119.1	C(23)-C(27)-H(27B)	109.5
C(23)-C(22)-H(22)	119.1	H(27A)-C(27)-H(27B)	109.5
C(24)-C(23)-C(22)	117.2(6)	C(23)-C(27)-H(27C)	109.5
C(24)-C(23)-C(27)	121.4(7)	H(27A)-C(27)-H(27C)	109.5
C(22)-C(23)-C(27)	121.4(6)	H(27B)-C(27)-H(27C)	109.5
C(23)-C(24)-C(25)	123.2(6)	C(25)-C(28)-H(28A)	109.5
C(23)-C(24)-H(24)	118.4	C(25)-C(28)-H(28B)	109.5

H(28A)-C(28)-H(28B)	109.5	C(30B)-Si(1)-H(31B)	103(3)
C(25)-C(28)-H(28C)	109.5	C(7)-Si(1)-H(31C)	134(3)
H(28A)-C(28)-H(28C)	109.5	C(30C)-Si(1)-H(31C)	101(2)
H(28B)-C(28)-H(28C)	109.5	C(29C)-Si(1)-H(31C)	101(2)
C(30A)-Si(1)-C(7)	116.7(8)	Si(1)-C(29A)-H(29A)	109.5
C(29B)-Si(1)-C(7)	114(2)	Si(1)-C(29A)-H(29B)	109.5
C(30A)-Si(1)-C(29A)	110.5(9)	H(29A)-C(29A)-H(29B)	109.5
C(7)-Si(1)-C(29A)	108.5(6)	Si(1)-C(29A)-H(29C)	109.5
C(29B)-Si(1)-C(30B)	108(3)	H(29A)-C(29A)-H(29C)	109.5
C(7)-Si(1)-C(30B)	105(2)	H(29B)-C(29A)-H(29C)	109.5
C(7)-Si(1)-C(30C)	107.7(13)	Si(1)-C(30A)-H(30A)	109.5
C(7)-Si(1)-C(29C)	106.6(10)	Si(1)-C(30A)-H(30B)	109.5
C(30C)-Si(1)-C(29C)	102.2(14)	H(30A)-C(30A)-H(30B)	109.5
C(30A)-Si(1)-H(31A)	114(2)	Si(1)-C(30A)-H(30C)	109.5
C(7)-Si(1)-H(31A)	101(3)	H(30A)-C(30A)-H(30C)	109.5
C(29A)-Si(1)-H(31A)	105.1(18)	H(30B)-C(30A)-H(30C)	109.5
C(29B)-Si(1)-H(31B)	113(3)	Si(1)-C(29B)-H(29D)	109.5
C(7)-Si(1)-H(31B)	113(5)	Si(1)-C(29B)-H(29E)	109.5

H(29D)-C(29B)-H(29E)	109.5	Si(1)-C(29C)-H(29H)	109.5
Si(1)-C(29B)-H(29F)	109.5	H(29G)-C(29C)-H(29H)	109.5
H(29D)-C(29B)-H(29F)	109.5	Si(1)-C(29C)-H(29I)	109.5
H(29E)-C(29B)-H(29F)	109.5	H(29G)-C(29C)-H(29I)	109.5
Si(1)-C(30B)-H(30D)	109.5	H(29H)-C(29C)-H(29I)	109.5
Si(1)-C(30B)-H(30E)	109.5	Si(1)-C(30C)-H(30G)	109.5
H(30D)-C(30B)-H(30E)	109.5	Si(1)-C(30C)-H(30H)	109.5
Si(1)-C(30B)-H(30F)	109.5	H(30G)-C(30C)-H(30H)	109.5
H(30D)-C(30B)-H(30F)	109.5	Si(1)-C(30C)-H(30I)	109.5
H(30E)-C(30B)-H(30F)	109.5	H(30G)-C(30C)-H(30I)	109.5
Si(1)-C(29C)-H(29G)	109.5	H(30H)-C(30C)-H(30I)	109.5

Symmetry transformations used to generate equivalent atoms:

4.6 Computational methods

Computations were executed with the Gaussian 09 program package[15] at Research Center for Computing and Multimedia Studies, Hosei University. The structures of **1a**, **1b**, **3a**, and **3b** were

optimized at the B3LYP/(6-31G(d) for H, C, and Si; LANL2DZ for Br and I) level of theory. The frequency calculations were carried out for each compounds at the same level as in the structure optimization to confirm the absence of any imaginary frequencies.

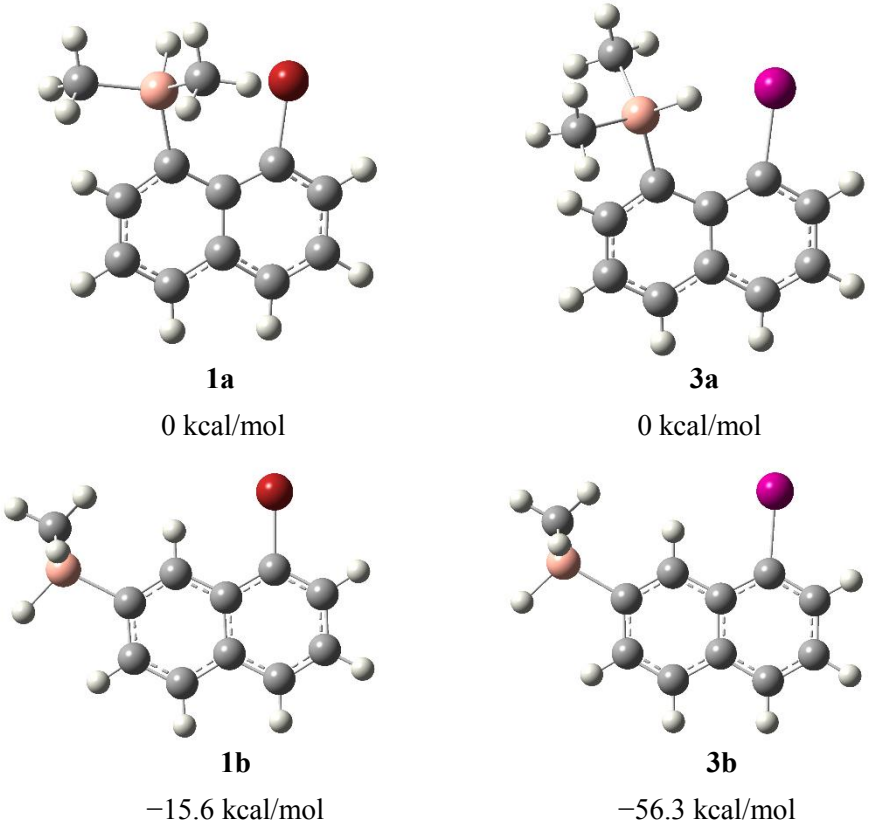

Figure 6. Optimized structures of **1a**, **1b**, **3a**, and **3b**.

References

(1) (a) Reviews: "Silyl Migration", Kira, M.; Iwamoto, T. The Chemistry of Organic Silicon Compounds; Rappoport, Z.; Apeloig, Y. Eds; Wiley; 2001; Vol. 3, Chapter 16. (b) "Molecular Rearrangements of Organosilicon Compounds", Brook, A. G.; Bassindale, A. R. Rearrangements in Ground and Excited States; Academic Press; 1980; Vol. 2, Essay 9. (c) "Rearrangement Reactions with Migration of Silicon", Colvin, E. W. Silicon in Organic Synthesis; Butterworths; 1981; Chapter 5.

(2) Seyferth, D.; White, D. L. Acid-catalyzed isomerization of 1,2-bis(trimethylsilyl)benzene and related compounds. *J. Am. Chem. Soc*. **1972**, *94*, 3132–3138.

(3) Becker, B.; Herman, A.; Wojnowski, W. The rearrangement of 1-naphthyllphenylmethylsilane. *J. Organomet. Chem*. **1980**, *193*, 293–297.

(4) Emsley, J. *The Elements, 2nd Edition*; Clarendon, Oxford, UK, 1991.

(5) (a) Moriarty, R. M.; Khosrowshahi, J. S.; Dalecki, T. M. Hypervalent iodine iodinative decarboxylation of cubyl and homocubyl carboxylic acids. *J. Chem. Soc. Chem. Commun.* **1987**, 675–676. (b) Hu, J. Y.; Pu, Y. J.; Nakata, G.; Kawata, S.; Sasabe, H.; Kido, J. A single-molecule excimer-emitting compound for highly efficient fluorescent organic light-emitting devices. *Chem. Commun*. **2012**, *48*, 8434–8436.

(6) (a) Weimar, M.; Dürner, G.; Bats, J. W.; Göbel, M. W. Enantioselective Synthesis of (+)-Estrone Exploiting a Hydrogen Bond-Promoted Diels−Alder Reaction. *J. Org. Chem.* **2010**, *75,* 2718–2721. (b) House, H. O.; Koepsell, D. G.; Campbell, W. J. Synthesis of some diphenyl and

triphenyl derivatives of anthracene and naphthalene. *J. Org. Chem.* **1972**, *37*, 1003–1011.

(7) (a) Lühmann, N.; Hirano, H.; Sason, S.; Müller, T. Disilylfluoronium Ions-Synthesis, Structure, and Bonding. *Organometallics* **2011**, *30*, 4087–4096. (b) Kordts, N.; Künzler, S.; Rathjen, S.; Sieling, T.; Großekappenberg, H.; Schmidtmann, M.; Müller, T. Silyl Chalconium Ions: Synthesis, Structure and Application in Hydrodefluorination Reactions. *Chem. Eur. J.* **2017**, *23*, 10068–10079.

(8) Wipf, P.; Jung, J.-K. Formal Total Synthesis of (+)-Diepoxin σ. *J. Org. Chem.* **2000**, *65*, 6319–6337.

(9) Kisukuri, C. M.; Palmeira, D. J.; Rodrigues, T. S.; Camargo, P. H. C.; Andrade, L. H. Bimetallic Nanoshells as Platforms for Metallo−and Biometallo−Catalytic Applications. C*hemCatChem.* **2016**, *8*, 171–179.

(10) Gevorgyan, V. N.; Ignatovich, L. M.; Lukevics, E. Reduction of alkoxysilanes, halo-silanes and -Germanes with lithium aluminium hydride under phase-transfer conditions. *J. Organomet. Chem*. **1985**, *284*, C31–C32.

(11) Seyferth, D.; Vick, S. C. Synthesis of 1,8-bis(trimethylsilyl)- and 1,8-bis(trimethylstannyl)-naphthalene. The relative steric effects of carbon, silicon and tin in the 1,8-bis(trimethylelement)-naphthalenes. *J. Organomet. Chem*. **1977**, *141*, 173–187.

(12) Günter, H. in NMR Spectroscopy: Basic Principles, Concepts, and Applications in Chemistry, 2nd ed., Chichester, UK 1995, 94–97.

(13) SIR97: Altomare, A.; Burla, M. C.; Camalli, M.; Cascarano, G.; Giacovazzo, C.; Guagliardi,

A.; Moliterni, A. G. G.; Polidori, G.; Spagna, R. *J. Appl. Crystallogr.* **1999**, *32*, 115–119.

(14) SHELX-97: Sheldrick, G. University of Göttingen, Göttingen, Germany, 1997.

(15) Gaussian 09, rev. B.01: Frisch, M. J.; Trucks, G. W.; Schlegel, H. B.; Scuseria, G. E.; Robb, M. A.; Cheeseman, J. R.; Scalmani, G.; Barone, V.; Mennucci, B.; Petersson, G. A.; Nakatsuji, H.; Caricato, M.; Hratchian, X.; Li, H. P.; Izmaylov, A. F.; Bloino, J.; Zheng, G.; Sonnenberg, J. L.; Hada, M.; Ehara, M.; Toyota, K.; Fukuda, R.; Hasegawa, J.; Ishida, M.; Nakajima, T.; Honda, Y.; Kitao, O.; Nakai, H.; Vreven, T.; Montgomery, Jr. J. A.; Peralta, J. E.; Ogliaro, F.; Bearpark, M.; Heyd, J. J.; Brothers, E.; Kudin, K. N.; Staroverov, V. N.; Kobayashi, R.; Normand, J.; Raghavachari, K.; Rendell, A.; Burant, J. C.; Iyengar, S. S.; Tomasi, J.; Cossi, M.; Rega, N.; Millam, J. M.; Klene, M.; Knox, J. E.; Cross, J. B.; Bakken, V.; Adamo, C.; Jaramillo, J.; Gomperts, R.; Stratmann, R. E.; Yazyev, O.; Austin, A. J.; Cammi, R.; Pomelli, C.; Ochterski, J. W.; Martin, R. L.; Morokuma, K.; Zakrzewski, V. G.; Voth, G. A.; Salvador, P.; Dannenberg, J. J.; Dapprich, S.; Daniels, A. D.; Farkas, Ö.; Foresman, J. B.; Ortiz, J. V.; Cioslowski, J.; and Fox, D. J. Gaussian, Inc., Wallingford CT, 2010.

(16) Semin, G. K.; Bryukhova, E. V.; Kadina, M. A.; Frolova, G. V. Investigation of the electronic effects in a series of halo derivatives of organosilicon compounds by the method of nuclear quadrupole resonance of ^{79}Br, ^{81}Br, and ^{127}I. *Bull. Acad. Sci. USSR, Div. Chem. Sci. (Engl. Transl.)* **1971**, *20*, 1090–1092.

(17) Bähr, S.; Ostreich, M. Electrophilic Aromatic Substitution with Silicon Electrophiles: Catalytic Friedel–Crafts C−H Silylation. *Angew. Chem. Int. Ed.* **2017**, *56*, 52–59.

(18) Delpon-Lacaze, G.; Battisti, C.; Couret, C. Le dimésitylnéopentylsilène, un silène stable et facile à préparer synthèse et aspects de sa réactivité. *J. Organomet.Chem.* **1996**, *514*, 59–66.

(19) Betz, J.; Bauer, W. NMR and Calculational Studies on the Regioselective Lithiation of 1-Methoxynaphthalene. *J. Am. Chem. Soc*. **2002**, *124*, 8699–8706.

Conclusion and Outlook

In summary, the author discloses in this article the synthesis and properties of (silyl)(boryl)benzene, where the B···O interaction activates the C−O bond, and the details of the 1,2-silyl migration reaction in silylnaphthalene.

Chapter 2 described the synthesis and properties of **1** and **2** bearing a *p*-tolyl or *p*-*t*-butylphenyl group on the boron atom. Thus the C−O bond in **1** and **2** was activated by intramolecular interaction between the oxygen atom and the boron atomand underwent conversion reactions: (i) exchange of alkoxy group by alcohols, and (ii) siloxyborate formation by tertiary amines.

Chapter 2

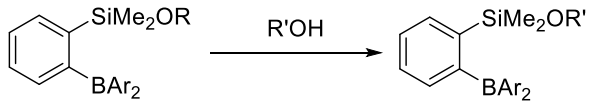

1: Ar = *p*-MeC_6H_4,
2: Ar = *p*-*t*-BuC_6H_4

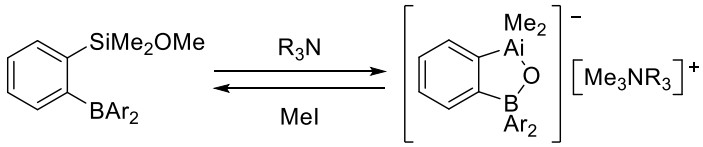

Chapter 3 described the synthesis and photophysical properties of **3** bearing a borafluorenyl group. The C−O bond in **3** was activated by B···O interaction. The large Stokes shift was due to the BICT transition caused by the four-coordinate ground state (coordination of the boron to the oxygen) and the three-coordinate (non-coordinated) excited state.

Chapter 3

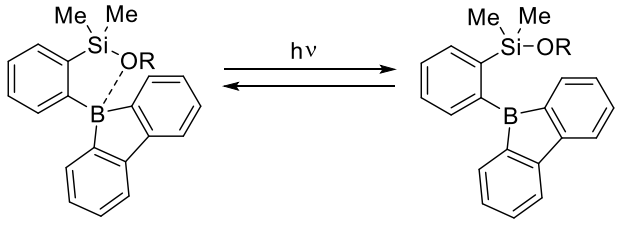

3

coordinated non-coordinated

Chapter 4 described the details of the acid-catalyzed silyl migration of 1-halo-8-(hydrosilyl)naphthalenes **4**. The scope, limitations, and reaction mechanism were elucidated through the effects of substituents on silicon atoms, solvent effects, and D-labeling experiments.

Chapter 4

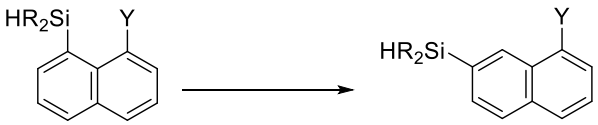

4

The potentials of this study deserve a comment. The intramolecular B···O interaction in the arylsilanes may be useful for preparations of various cationic species of such as silyloxoniums and carbocations. The coordination environment can be monitored through the photophysical properties of the borafluorenyl moiety. The 1,2-silyl migration on the aromatic ring may provide new access to silicon-substituted aromatic compounds.

Acknowledgment

The studies described in this dissertation have been carried out under the direction of Professor Atsushi Kawachi at the Faculty of Bioscience and Applied Chemistry, Hosei University.

The author sincerely wishes to express his heartfelt gratitude to Professor Atsushi Kawachi for his continuing guidance and valuable discussions and encouragement throughout the course of studies. The author is also indebted to Professor Naokazu Kano at Gakushuin University, and Professor Kenji Sugiyama, for their valuable suggestion and comments.

The author wishes to thank Prof. Yohsuke Yamamoto and Dr. Shogo Morisako at Hiroshima University, for their work of X-ray crystallographic analysis. The author wishes to thank Ms. Naoko Koiso and Ms. Yumiko Ashihara, Center of Instrumental Analysis, for their work of NMR spectroscopy. The author wishes to thank Dr. Satomi Hosokawa and Ms. Momoko Iwai, for their work of elemental analysis, mass spectra.

The author is also thankful to all members of Kawachi's research group for their kind cooperation.

Finally, the author wishes to express his deep appreciation to his parents, Mr. Michio Shimizu and Mrs. Teiko Shimizu for their constant financial assistance and their affectionate encouragement.

February, 2020

Tomomi SHIMIZU

Major in Applied Chemistry, Graduate School of Science and Engineering

Hosei University